

Applications and Novel Syntheses of Arborescent Graft Copolymers

By

Abderrahim Khadir

A thesis

presented to the University of Waterloo

in fulfilment of the

thesis requirement for the degree of

Doctor of Philosophy

in Chemistry

Waterloo, Ontario, Canada, 1999

© Abderrahim Khadir 1999



**National Library
of Canada**

**Acquisitions and
Bibliographic Services**

**395 Wellington Street
Ottawa ON K1A 0N4
Canada**

**Bibliothèque nationale
du Canada**

**Acquisitions et
services bibliographiques**

**395, rue Wellington
Ottawa ON K1A 0N4
Canada**

Your file Votre référence

Our file Notre référence

The author has granted a non-exclusive licence allowing the National Library of Canada to reproduce, loan, distribute or sell copies of this thesis in microform, paper or electronic formats.

The author retains ownership of the copyright in this thesis. Neither the thesis nor substantial extracts from it may be printed or otherwise reproduced without the author's permission.

L'auteur a accordé une licence non exclusive permettant à la Bibliothèque nationale du Canada de reproduire, prêter, distribuer ou vendre des copies de cette thèse sous la forme de microfiche/film, de reproduction sur papier ou sur format électronique.

L'auteur conserve la propriété du droit d'auteur qui protège cette thèse. Ni la thèse ni des extraits substantiels de celle-ci ne doivent être imprimés ou autrement reproduits sans son autorisation.

0-612-44768-5

The University of Waterloo requires the signatures of all persons using or photocopying this thesis. Please sign below, and give address and date.

Abstract

Arborescent polymers were investigated as melt processing additives for commercial polymers. The branched polymers were blended with linear polystyrene (PS) or poly(methyl methacrylate) (PMMA), and the melt viscosity of the blends was monitored as a function of temperature. Arborescent polystyrene with a low branching functionality, when blended with PS, yielded an increase in melt viscosity at high temperatures. The enhancement was proportional to the amount of branched polymer added. For a PMMA matrix, however, the arborescent polystyrene additive led to a 2- to 3-fold decrease in melt viscosity in the temperature range studied. Arborescent copolymers containing polyisoprene segments of different lengths were also investigated. Blends of PMMA and the polyisoprene copolymers (1-10% w/w) with short branches displayed a decrease in melt viscosity up to 10-fold over the temperature range examined.

The second goal of the research concerned the synthesis of arborescent graft copolymers using anionic ring opening polymerization techniques. These copolymers incorporated a polystyrene core and either polydimethylsiloxane (PDMS) or polycaprolactone side chains. The graft copolymers were obtained by a *grafting from* method using hydroxyl-functionalized polystyrene cores to initiate the polymerization of hexamethylcyclotrisiloxane (D_3) or ϵ -caprolactone.

Acknowledgements

I would like to thank my supervisor, Professor Mario Gauthier, for giving me the opportunity to join his group, and I am grateful for his guidance and his support throughout this research project.

I would also like to thank Professor Costas Tzoganakis from the Chemical Engineering Department for his insightful discussions on the polymer blending aspects of this project.

I am thankful to Dr. Kent Nielsen and Dr. Claude Lavallée from 3M Canada (London, Ontario) for their suggestions and I would also like to thank Mr. Greg Snell, who reproduced some of the measurements at 3M Canada.

I am indebted to Dr. Henk Blom and Dr. J. W. Teh for their help with the rheological measurements. I am very grateful to my laboratory colleagues Tony Carrozzella, Randy Frank and Andy Kee, who provided me support throughout the project.

Finally, I would like to thank the Natural Sciences and Engineering Research Council (NSERC), the Ontario Centre for Materials Research (OCMR) and the University of Waterloo for their financial assistance

Table of Contents

Abstract	iv
Acknowledgements	v
Table of Contents	vi
List of Tables	xiv
List of Figures	xv
List of Acronyms and Symbols	xx
Chapter 1: General Introduction	1
1.1. Research Objectives	1
1.2. Thesis Outline	2
Chapter 2: Literature Review	4
2.1. Introduction to Branched Polymers	4
2.1.1. Star Polymers	6
2.1.1.1. Preparation	6
2.1.1.2. Transport Properties	7
2.1.1.3. Viscoelastic Properties	11
2.1.2. Dendrimers and Hyperbranched Polymers	13
2.1.2.1. Structural Characteristics	14
2.1.2.2. Physical Properties	16
2.1.2.2.1. Solution Viscosity	16
2.1.2.2.2. Glass Transition Temperature	16
2.1.2.2.3. Viscoelastic Properties	18

2.1.3. Arborescent polymers	19
2.1.3.1. Synthesis.....	20
2.1.3.2. Physical Properties.....	24
2.2. Polymer Blends	27
2.2.1. Thermodynamics of Polymer Blends	29
2.2.2. Blending Methods.....	33
2.2.3. Linear and Branched Polymer Blends	33
2.2.4. Polymeric Processing Additives.....	36
2.3. Synthesis and Properties of Polysiloxanes.....	38
2.3.1. General Features of Siloxane Polymerization.....	38
2.3.1.1. Synthesis from Chlorosilane Compounds	40
2.3.1.2. Ionic Ring-Opening Polymerization	
Under Equilibrium Conditions.....	41
2.3.1.3. Ionic Ring-Opening Polymerization Under	
Kinetic Control.....	43
2.3.1.4. Cationic Ring Opening Polymerization	43
2.3.1.5. Anionic Ring-Opening Polymerization Techniques	44
2.3.1.5.1. Cryptands in Ring Opening Polymerization.....	46
2.3.1.6. Termination of the Polymerization	46
2.3.2. Branched Polymers with Well-Defined Architectures	
Based on Polysiloxanes.....	47
2.3.2.1. Graft Copolymers.....	48
2.3.2.1.1. Copolymerization of Macromers	48

2.3.2.1.2. Grafting Reactions.....	49
2.3.2.2. Star-Branched Telechelic Polymers.....	51
2.3.2.3. Networks Based on PDMS Segments.....	53
2.3.2.4. Dendritic Polysiloxanes.....	53
2.4. Physical Characteristics of Polysiloxanes	56
2.4.1. Surface Properties	57
2.5. Synthesis and Properties of Poly(ϵ -caprolactones).....	57
2.5.1. Synthesis of Linear Poly(ϵ -caprolactone).....	57
2.5.2. Star-Branched Poly(ϵ -caprolactone)s	59
2.6. References.....	60
Chapter 3: Arborescent Polystyrenes as Melt Viscosity Modifiers	
for Linear Polymers.....	68
3.1. Introduction.....	68
3.2. Experimental Procedures.....	70
3.2.1. Preparation of Blends.....	70
3.2.2. Characterization.....	70
3.3. Results and Discussion	71
3.3.1. Polystyrene Matrix	72
3.3.1.1. Effect of Branched Polymer Content.....	73
3.3.1.2. Effect of Branch Length.....	74
3.3.1.3. Effect of Branching Functionality	75
3.3.2. Poly(methyl methacrylate) Matrix	77
3.3.2.1. Effect of Branched Polymer Content.....	80

3.3.2.2. Effect of Branching Functionality.....	80
3.4. Conclusions.....	82
3.5. References.....	84
Chapter 4: Polyisoprene Arborescent Copolymers as Melt Viscosity Modifiers for	
Linear Polymers	86
4.1. Introduction	86
4.2. Experimental Procedures.....	88
4.2.1. Preparation of Blends.....	88
4.2.2. Characterization.....	89
4.3. Results and Discussion.....	91
4.3.1. Effect of Copolymer Branch Length.....	92
4.3.2. Effect of Copolymer Concentration on the Melt Viscosity of PMMA.....	95
4.3.3. Tensile Measurements.....	99
4.4. Conclusions.....	99
4.5. References.....	100
Chapter 5: Arborescent Polydimethylsiloxane Graft Copolymers	102
5.1. Introduction.....	102
5.2. Experimental Procedures.....	103
5.2.1. Reagent and Solvent Purification Procedures.....	103
5.2.1.1. Reagents	103
5.2.1.2. Purification of Solvents.....	104
5.2.1.3. Monomer Purification	104
5.2.1.4. Azeotropic Purification of 1,1-Diphenylethylene	

and Core Polymers.....	106
5.2.2. Synthesis of Linear Polydimethylsiloxane.....	107
5.2.2.1. Anionic Polymerization of D ₃ Initiated with <i>n</i> -Butyllithium	107
5.2.2.2. Anionic Polymerization of D ₃ Initiated with Lithium <i>n</i> -Butoxide.....	108
5.2.3. Synthesis of Polystyrene Grafting Substrates.....	109
5.2.3.1. Linear Polystyrene	109
5.2.3.2. Chloromethylation of Linear Polystyrene	110
5.2.3.3. Living Free Radical Polymerization	111
5.2.3.4. Preparation of 6-Lithiohexyl Acetaldehyde Acetal.....	111
5.2.3.5. Synthesis of Linear Polystyrene with Acetal Pendant Groups.....	112
5.2.3.6. Synthesis of Acetal-Terminated Comb-Branched Polystyrene.....	113
5.2.3.7. Fractionation and Acetal Group Hydrolysis.....	114
5.2.4. Polydimethylsiloxane Graft Copolymers.....	115
5.2.4.1. Metal-Halogen Exchange Reaction.....	115
5.2.4.2. Copolymer Based on Linear Polystyrene with Pendant Hydroxyl Groups.....	116
5.2.4.3. Copolymer Based on Hydroxyl-Terminated Comb-Branched Polystyrene	117
5.2.4.4. Copolymer Based on Hydroxyl-Terminated G1 Arborescent Polystyrene	118
5.2.5. Characterization.....	118

5.2.5.1. Size Exclusion Chromatography	118
5.2.5.2. Infra-Red Spectroscopy.....	119
5.2.5.3. ¹ H-NMR Spectroscopy.....	119
5.3. Results and Discussion	119
5.3.1. Synthesis of Linear Polydimethylsiloxane.....	120
5.3.1.1. <i>n</i> -Butyllithium-Initiated Anionic polymerization.....	120
5.3.1.2. Lithium <i>n</i> -Butoxide-Initiated Anionic Polymerization	121
5.3.2. Synthesis of Chloromethylated Polystyrene Cores.....	121
5.3.2.1. Chloromethylation of Linear Polystyrene	121
5.3.2.2. Living Free Radical Polymerization	123
5.3.3. Preparation of Hydroxyl-Functionalized Core Polymers	123
5.3.3.1. Synthesis of Bifunctional Initiator	123
5.3.3.2. Synthesis of Acetal-Functionalized Linear Polystyrene	124
5.3.3.3. Synthesis of Acetal-Terminated Comb Polystyrene	126
5.3.3.4. Fractionation and Hydrolysis of Acetal-Terminated Comb Polystyrene	127
5.3.3.5. Metal-Halogen Exchange Reaction	129
5.3.3.6. Synthesis of G1 Hydroxyl-Terminated Polystyrene	130
5.3.4. Synthesis of Arborescent PDMS Graft Copolymers	130
5.3.4.1. PDMS Copolymers Based on G1 Hydroxyl-Terminated Core Polymer	131
5.3.4.2. PDMS Copolymer Based on Comb Polystyrene Core.....	136
5.3.4.3. PDMS Copolymer Based on Hydroxyl-Functionalized	

Linear Polystyrene Core	138
5.4. Conclusions	139
5.5. References	139
Chapter 6: Arborescent Poly(ϵ-caprolactone) Graft Copolymers	141
6.1. Introduction	141
6.2. Experimental Procedures	142
6.2.1. Monomer and Reagent Purification	142
6.2.2. Anionic Polymerization of ϵ-Caprolactone Initiated with Lithium <i>n</i>-Butoxide	143
6.2.3. Synthesis of Copolymers	144
6.2.3.1. Copolymer Based on Linear Polystyrene with Hydroxyl Pendant Groups	144
6.2.3.2. Copolymer based on Hydroxyl-Terminated G1 Polystyrene	145
6.2.4. Characterization	145
6.3. Results and Discussion	146
6.3.1. Synthesis of Linear Poly(ϵ-caprolactone)	146
6.3.2. Arborescent Poly(ϵ-caprolactone) Graft Copolymers	146
6.3.2.1. Poly(ϵ-caprolactone) Copolymer Based on Linear Polystyrene With Pendant Hydroxyl Groups	147
6.3.2.3. Poly(ϵ-caprolactone) Copolymer based on Hydroxyl G1 Core	149
6.4. Conclusions	150
6.5. References	151
Chapter 7: Conclusions and Suggestions for Future Work	153

List of Tables

Table 2.1. Characteristics of arborescent polystyrenes with 5 000 g.mol⁻¹ branches	25
Table 3.1. Characteristics of the arborescent polystyrene used	71
Table 4.1. Characteristics of the arborescent polyisoprene copolymers used	89
Table 4.2. Interaction parameters for PIP/PMMA, PIP/PS and PS/PMMA.....	91
Table 4.3. Surface energy of linear polymers	92
Table 5.1. SEC Characterization results for linear PDMS samples prepared using lithium <i>n</i>-butoxide.....	121

List of Figures

Figure 2.1. Well-defined branched polymers	5
Figure 2.2. Comparison of intrinsic viscosity of star and linear polymers	8
Figure 2.3. Diffusion coefficients for (a) linear and (b) three-arm star deuterated polybutadiene molecules in a high-density polyethylene melt as a function of the degree of polymerization N	9
Figure 2.4. Reptation model: linear chain contained in a virtual tube	10
Figure 2.5. The motion of a three-arm star polymer in a tube.....	11
Figure 2.6. Synthesis of polyamidoamine (PAMAM) dendrimer	15
Figure 2.7.a. Viscosity of dendritic polyethers of successive generations for low molecular weight range	19
Figure 2.7.b. Viscosity of dendritic polyethers of successive generations in the high molecular weight range	20
Figure 2.8. Synthetic scheme for the preparation of arborescent polystyrenes	22
Figure 2.9. Arborescent poly(ethylene oxide) copolymer synthesis.....	23
Figure 2.10. Intrinsic viscosity of arborescent polystyrenes of successive generations.....	25
Figure 2.11. Atomic force microscopy pictures of monomolecular films of generation G1(left) and G3 (right) arborescent polystyrenes	26
Figure 2.12. Zero-shear melt viscosity (η_0) of arborescent polystyrenes at 170°C	27
Figure 2.13. Cyclic siloxane monomers.....	39
Figure 2.14. Nomenclature for methyl-substituted siloxane compounds.....	40
Figure 2.15. Hydrolysis of a dichlorosilane	41

Figure 2.16. Preparation of linear PDMS by a two-step anionic polymerization	
reaction.....	45
Figure 2.17. Structure of Kryptofix 2.2.2, a cryptand.....	47
Figure 2.18. Preparation of poly(methyl methacrylate)-g-polydimethylsiloxane	49
Figure 2.19. Preparation of polysulfone-g-polydimethylsiloxane	50
Figure 2.20. Preparation of poly(1-phenyl-1-propyne)-g-polydimethylsiloxane	51
Figure 2.21. Preparation of amino-terminated three-arm star-branched PDMS.....	52
Figure 2.22. Preparation of networks based on PDMS segments.....	54
Figure 2.23. Preparation of a dendritic polysiloxane	55
Figure 2.24. Intermolecular (A) and intramolecular (B) transesterification in	
ϵ-caprolactone polymerization.....	58
Figure 2.25. Synthesis of hyperbranched polyesters.....	60
Figure 3.1. Effect of concentration of arborescent polystyrene on the melt viscosity	
of linear polystyrene.....	74
Figure 3.2. Effect of branch length of arborescent polystyrene on the melt viscosity	
of polystyrene	75
Figure 3.3. Effect of branching functionality of arborescent polystyrene	
with long branches on the melt viscosity of polystyrene	76
Figure 3.4. Effect of branching functionality of arborescent polystyrene	
with short branches on the melt viscosity of polystyrene	77
Figure 3.5. Effect of concentration of arborescent polystyrene on the melt viscosity	
of PMMA.....	81
Figure 3.6. Effect of branching functionality of arborescent polystyrene	

with long branches on the melt viscosity of PMMA	82
Figure 3.7. Effect of branching functionality of arborescent polystyrene	
with long branches on the melt viscosity of PMMA	83
Figure 4.1. Synthetic scheme for the preparation of arborescent polyisoprene	
copolymers.....	88
Figure 4.2. Effect of branch length of arborescent polyisoprene copolymers	
on the melt viscosity of PMMA.....	93
Figure 4.3. Effect of branch length of polyisoprene copolymers	
on the melt viscosity of polystyrene.....	96
Figure 4.4. Effect of polyisoprene copolymer concentration	
on the melt viscosity of PMMA.....	97
Figure 5.1. Apparatus for monomer purification	106
Figure 5.2. Apparatus for purification by azeotropic distillation	107
Figure 5.3. Polymerization reactor	110
Figure 5.4. Apparatus for the metal-halogen exchange reaction	116
Figure 5.5. SEC trace for linear PDMS prepared using <i>n</i>-butyllithium	120
Figure 5.6. ¹H-NMR spectrum of linear Partially	
chloromethylated polystyrene.....	122
Figure 5.7. Synthesis of the bifunctional initiator 6-lithiohexyl acetaldehyde acetal ...	124
Figure 5.8. Synthesis of linear polystyrene with acetal pendant groups and comb	
polystyrene with acetal end groups.....	125
Figure 5.9. ¹H-NMR spectrum of acetal-functionalized linear polystyrene	125
Figure 5.10. ¹H-NMR spectrum of hydroxyl-functionalized linear polystyrene	126

Figure 5.11. SEC trace for the crude acetal-terminated comb polystyrene synthesized.....	127
Figure 5.12. FT-IR spectra for the acetal-terminated comb polystyrene before and after hydrolysis.....	128
Figure 5.13. Intermolecular cross-linking reactions involving metal-halogen exchange.....	129
Figure 5.14. Arborescent PDMS graft copolymer synthesis by a <i>grafting from</i> method.....	131
Figure 5.15. SEC traces for G1 hydroxyl-terminated core polymer and arborescent PDMS graft copolymer obtained without cryptand.....	132
Figure 5.16. SEC traces for G1 hydroxyl-terminated core polymer and arborescent PDMS graft copolymer obtained with cryptand, first attempt.....	133
Figure 5.17. SEC traces for G1 hydroxyl-terminated core polymer and arborescent PDMS graft copolymer obtained with cryptand, second attempt.....	134
Figure 5.18. ¹H-NMR spectrum of fractionated arborescent PDMS graft copolymers.....	135
Figure 5.19. FT-IR spectra for the G1 core polymer, linear PDMS and arborescent graft copolymer.....	137
Figure 5.20. SEC traces for G0 core polymer and arborescent PDMS graft copolymer.....	138
Figure 6.1. Synthetic scheme for the preparation of poly(ϵ-caprolactone)-<i>b</i>-poly(ethylene glycol)-<i>b</i>-poly(ϵ-caprolactone).....	142
Figure 6.2. SEC trace for linear poly(ϵ-caprolactone) obtained from	

lithium <i>n</i>-butoxide	146
Figure 6.3. Arborescent poly(ϵ-caprolactone) prepared from linear polystyrene with hydroxyl pendant groups	148
Figure 6.4. Arborescent poly(ϵ-caprolactone) prepared from a hydroxyl-terminated G1 core polymer	150

List of Symbols and Acronyms

ABS: Acrylonitrile-butadiene-styrene copolymer

AFM: Atomic force microscopy

BHT: 2,6-di-*tert*-butyl-4-methylphenol

BuLi: Butyllithium

***c*:** Concentration

***D*:** Diffusion coefficient

***d*:** Hydrodynamic diameter

DPE: 1,1-diphenylethylene

DSC: Dynamic scanning calorimetry

EPDM: Ethylene-propylene-diene copolymer

***f*:** Branching functionality of star-branched polymers

FT-IR: Fourier transform-infrared

***f_w*:** Weight-average branching functionality of arborescent polymers

***G*:** Dendrimer generation

***g*:** Ratio of squared radius of gyration of star-branched and linear polymers

G0, G1, G2, ...: Generations of arborescent polymers

HDPE: High-density polyethylene

HDT: Heat distortion temperature

HIPS: High-impact polystyrene

***J_e⁰*:** Recoverable shear compliance

LCST: Lower critical solution temperature

LLDPE: Linear low density polyethylene

M_a : Molecular weight of the arms in a star-branched polymer

M_c : Core unit molecular weight in dendrimers

M_c : Critical molecular weight for entanglement formation

M'_c : Characteristic molecular weight

M_i : Molecular weight of component i

M_n : Number-average molecular weight

M_{RU} : Repeating unit molecular weight

M_T : Terminal unit molecular weight

M_w : Weight-average molecular weight

N : Degree of polymerization

N_A : Avogadro's number

N_b : Number of reactive sites introduced by a repeat unit in a dendrimer

N_c : Initiator core multiplicity in a dendrimer

NMR: Nuclear magnetic resonance (spectroscopy)

n_e : Number of end groups in a dendrimer

n_x : Refractive index of component X

PDI: Polydispersity index ($=M_w/M_n$)

PDMS: Polydimethylsiloxane

PE: Polyethylene

PEE: Poly(ethylene) or poly(1-butene)

PEP: Ethylene-propylene copolymer

PMMA: Poly(methyl methacrylate)

PPO: Poly(2,6-dimethyl-1,4-phenylene oxide)

PS: Polystyrene

PVC: Poly(vinyl chloride)

PVME: Poly(vinyl methyl ether)

R_G : Radius of gyration

R_H : Hydrodynamic radius

$\langle S^2 \rangle$: Squared radius of gyration

SBR: Styrene-butadiene rubber

SEC: Size exclusion chromatography

T_g : Glass transition temperature

THF: Tetrahydrofuran

USCT: Upper critical solution temperature

V_i : Molecular volume of component i

w_i : Weight fraction of component i

Z: Number of terminal groups in a dendrimer

γ : Surface energy

Γ : Viscosity enhancement factor

ΔG_{mix} : Free energy of mixing

ΔH_{mix} : Enthalpy of mixing

ΔS_{mix} : Entropy of mixing

$[\eta]$: Intrinsic viscosity

η_0 : Zero-shear viscosity

η_B : Viscosity of star-branched polymer

η_L : Viscosity of linear polymer

Θ : Free volume per chain per chain end

ρ : Density

ϕ_i : Volume fraction of component i

χ : Interaction parameter

Chapter 1: General Introduction

Branching affects the physical properties of polymers in various ways, depending on the overall structure of the molecules. In order to assess the influence of branching on physical properties, branched polymers with a well-defined structure should ideally be investigated.

Arborescent polymers are highly branched macromolecules with a tree-like dendritic architecture. Their structure is well-defined in terms of branching functionality, branch length, and molecular weight distribution. Arborescent polymers display unusual properties such as a very low melt viscosity relative to linear polymers of similar molecular weight. This and other unusual characteristics make arborescent polymers interesting as model branched polymers. This thesis is concerned with mixtures of arborescent polymers with linear polymers aimed at achieving certain performance modifications. Additionally, the synthesis of new types of polymers with an arborescent structure is reported.

1.1. Research Objectives

One main objective of this research was to investigate the effect of arborescent polymers on the melt viscosity of two commercial linear polymers, namely polystyrene and poly(methyl methacrylate). Two types of arborescent polymers were used in the study. One series of branched polymers contained only polystyrene side chains, and the second series were copolymers obtained by grafting polyisoprene side chains onto branched

polystyrene substrates. The effects of branched polymer content and structure on the properties of the polymer mixtures were examined in each case.

Polysiloxanes are interesting due to their unique properties. They are chemically inert, thermally stable, highly permeable to gases and have extremely low glass transition temperatures. One way to further benefit from the special characteristics of polysiloxanes may be by the incorporation of polysiloxane segments in arborescent copolymers. These polymers may find applications as surface modifiers, additives for other polymers or as elastomeric network components. A second main objective of this research program was to develop methods for the synthesis and characterization of arborescent polydimethylsiloxane graft copolymers.

Poly(ϵ -caprolactone) is also interesting because of its biocompatibility and biodegradability, among others. The polymer is characterized by a low glass transition temperature and has been investigated for use in drug delivery systems. Another characteristic of poly(ϵ -caprolactone) is its compatibility with a variety of polymers, which may again be interesting in the preparation of polymer blends. The last goal of the research program was the development of methods for the synthesis of arborescent poly(ϵ -caprolactone) graft copolymers.

1.2. Thesis Outline

Background information on the synthesis and physical properties of different types of branched polymers is provided in Chapter 2. This includes a section discussing polymer blends incorporating branched polymers. The synthesis and properties of polysiloxanes and

of poly(ϵ -caprolactone) with well-defined architectures (both linear and branched) are also discussed in Chapter 2, to provide additional information directly relevant to this project. Chapter 3 describes the investigation of arborescent polystyrenes as melt viscosity modifiers for linear polymers. In Chapter 4, arborescent copolymers with polyisoprene segments are investigated for the same type of application. The experimental procedures developed for the synthesis of arborescent copolymers with polydimethylsiloxane side chains are described Chapter 5. Exploratory work on the synthesis of arborescent graft copolymers with poly(ϵ -caprolactone) segments is presented in Chapter 6. The main conclusions drawn from the work and suggestions for future work are discussed in Chapter 7.

Chapter 2: Literature Review

2.1. Introduction to Branched Polymers

Branched polymers are characterized by the presence of more than two chain ends. For example, in the case of a star-branched polymer, three or more chains are linked to a single branching point. Branched polymers have a finite molecular weight and are in general soluble in the same solvents as their linear homologues. Branching affects the physical properties of polymers in various ways, depending on the branch length, the branching functionality (number of side chains or branches) and the overall structure of the molecules. Therefore by controlling these parameters, one can design materials with desired characteristics.

Many groups have investigated the synthesis of branched polymers, and established methods for the preparation of materials having a well-defined branched structure (1). However, physical characterization studies have been mainly limited to star-branched polymers. In order to assess the effect of branching on physical properties, the structure of the branched polymer should be well-defined, at least in terms of branch length and branching functionality. Well-defined branched polymers fall into three main categories, as outlined in Figure 2.1, namely the star-branched, comb and dendritic polymers.

The living anionic polymerization and grafting technique is a very powerful method for the preparation of branched polymers with well-defined architectures. The branched polymers obtained by this process typically have a narrow molecular weight distribution, a uniform branch length and a known branching functionality. There are two methods based

on anionic polymerization that can be used to synthesize branched polymers.

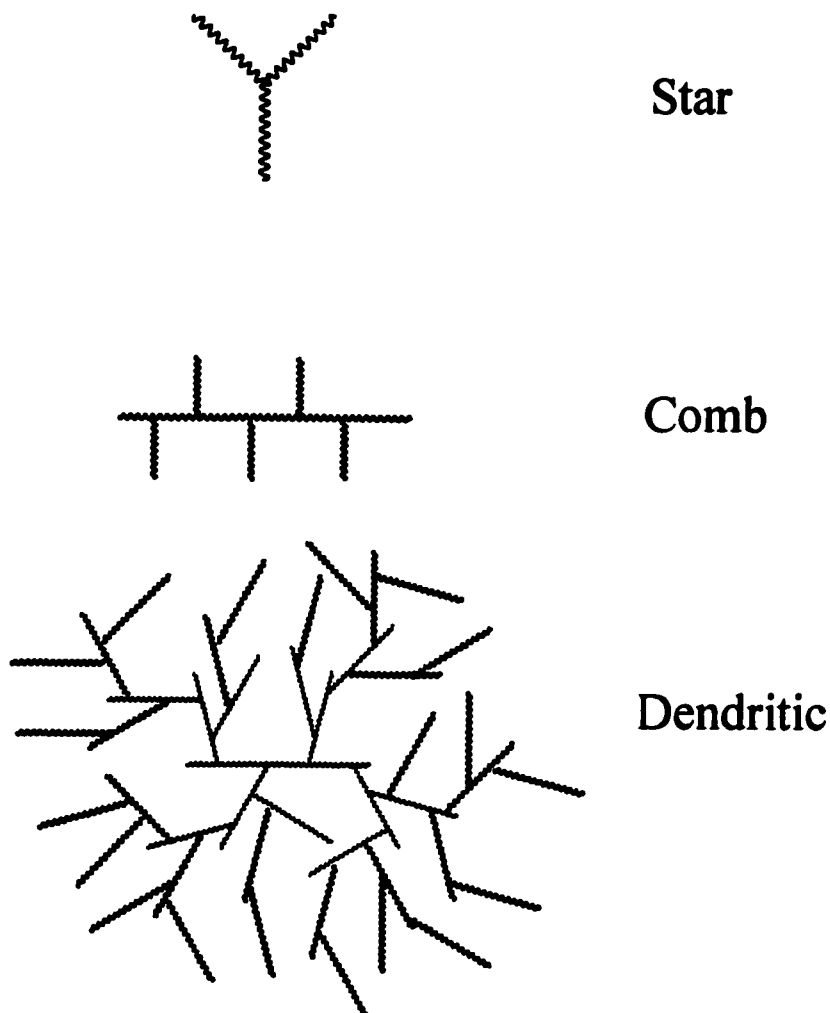


Figure 2.1. Well-defined branched polymers

The *grafting onto* method uses a coupling reaction between a ‘living’ linear polymer (prepared by anionic polymerization) and reactive groups on the grafting substrate under appropriate conditions. The *grafting from* method involves the preparation of a substrate carrying multiple anionic centers able to initiate the polymerization of monomers.

The ability to combine a backbone and side chains of different chemical compositions is a significant advantage of these techniques. The properties of the resulting copolymers can thus be varied not only through the structure, but also through the types of polymers used in the grafting process. For example, grafting polyisoprene or polybutadiene side chains onto a polystyrene backbone can help enhance heat resistance, while improving impact resistance as well as processability.

2.1.1. Star Polymers

Star polymers are considered to be the simplest kind of branched polymer. They consist of three or more branches (arms) linked at one branching point. Well-defined star polymers with a narrow molecular weight distribution are prepared by anionic polymerization and coupling. This method is of great significance, since the effect of branching (e.g., arm length and branching functionality) on the physical properties can be examined in a quantitative manner. Theories for branched polymers have been developed mainly for star polymers.

2.1.1.1. Preparation

The synthesis of styrene, butadiene and isoprene star polymers relies on the preparation of linear 'living' polymers via anionic polymerization, followed by the addition of a coupling agent. The coupling agents most commonly used are chlorosilane compounds with three or more reactive sites such as 1,2-bis(dichloromethylsilyl)ethane or 1,2-bis(trichlorosilyl)ethane (2-4).

2.1.1.2. Transport Properties

Two examples were selected to illustrate the effect of branching on the physical properties of star polymers, namely the intrinsic viscosity and the diffusion properties. The intrinsic viscosity of a series of star polymers of identical arm molecular weight is compared to the intrinsic viscosity of the arms as a function of the branching functionality f (number of arms) in Figure 2.2 (5). The intrinsic viscosity measurements were performed in both good and theta solvents, and a linear polymer was considered equivalent to a star polymer with two arms in the analysis (leftmost point on each curve). For branching functionalities below 5, the intrinsic viscosity ratio increases to a maximum, and then decreases as f increases. This behavior is ascribed to the rapid increase in molecular weight of star polymer molecules relative to their increase in hydrodynamic volume. The intrinsic viscosity $[\eta]$ of the star polymers is related to f and the molecular weight of the arms, M_a , by the equation

$$[\eta] = k \langle R_G^2 \rangle \langle R_H \rangle (f M_a)^{-1} \quad (2.1)$$

where R_G is the radius of gyration of the star polymer, R_H is the hydrodynamic radius, and k is a constant.

In another investigation of the effect of branching, the diffusion coefficients for three-arm star deuterated (saturated) polybutadiene molecules in a high-density polyethylene melt were compared to those for linear deuterated polybutadienes as a function of the overall degree of polymerization (N), as shown in Figure 2.3 (6). For three-arm star polymers, the diffusion coefficients are always lower than for linear polymers. Furthermore, the diffusion coefficient of star polymers initially decreases exponentially as a function of N , but the decrease becomes less pronounced for longer side chains. In

contrast, the diffusion coefficient for linear polymers is a power law ($D \propto N^{-2}$) of the degree of polymerization over the whole molecular weight range.

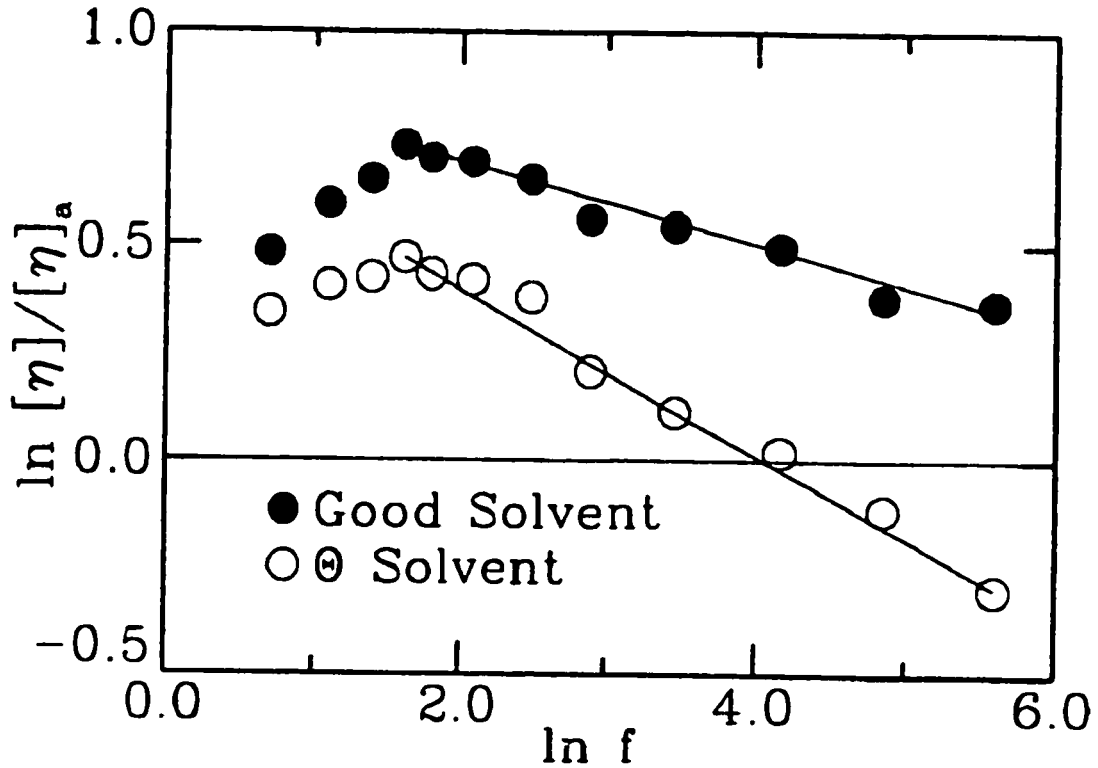


Figure 2.2. Comparison of intrinsic viscosity of star and linear polymers (From reference 5)

The lower diffusion coefficients for star polymers relative to linear polymers in the molten state were related to the dynamic properties of the macromolecules. In entangled linear polymers (with a molecular weight above the critical molecular weight for entanglement formation M_c), a chain diffuses by reptation or snakelike motions (7). In the reptation model the linear chains are contained in a virtual tube formed by the other surrounding chains, as pictured in Figure 2.4. The chain winds out or slides out of the tube

by constantly adopting new conformations.

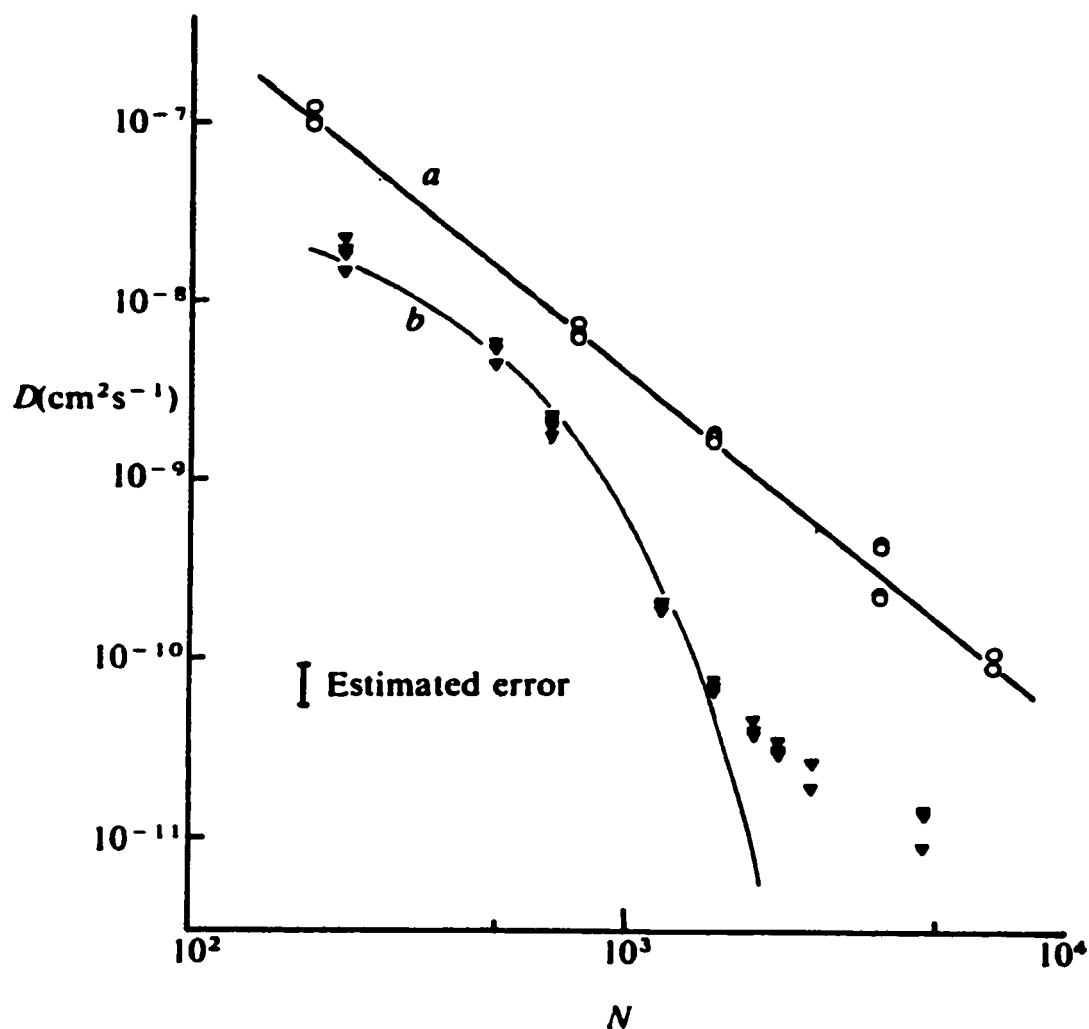


Figure 2.3. Diffusion coefficients for (a) linear and (b) three-arm star deuterated polybutadiene molecules in a high-density polyethylene melt as a function of the degree of polymerization N (From reference 6)

The dynamic behavior of branched polymer chains is not as well understood as that of linear chains. It was suggested that the virtual tube model used to confine the motions of linear polymers is still applicable in this case, however the reptation motions are

strongly hindered by the branches.

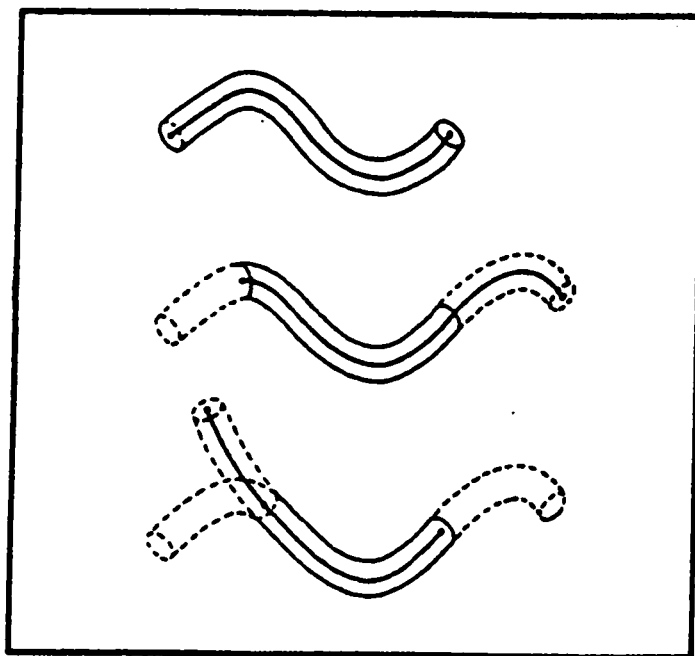


Figure 2.4. Reptation model: linear chain contained in a virtual tube (From reference 7)

Klein (8) has described the dynamic properties of star polymers confined in a tube. Diffusion of a three-arm star polymer begins by the retraction of an arm towards the branch point, followed by reexpansion of the arm in a new configuration. This mechanism is illustrated in Figure 2.5. The diffusion coefficient for a three-arm star polymer following this diffusion mechanism is given by the equation

$$D = K' N^{-2} \exp(-\alpha N) \quad (2.2)$$

where N is the degree of polymerization, and K' and α are constants, whereas D is simply proportional to N^{-2} for linear polymers. Thus the diffusion coefficient should be higher for a linear polymer than for a three-arm star polymer at a constant degree of polymerization (if α is assumed to be positive).

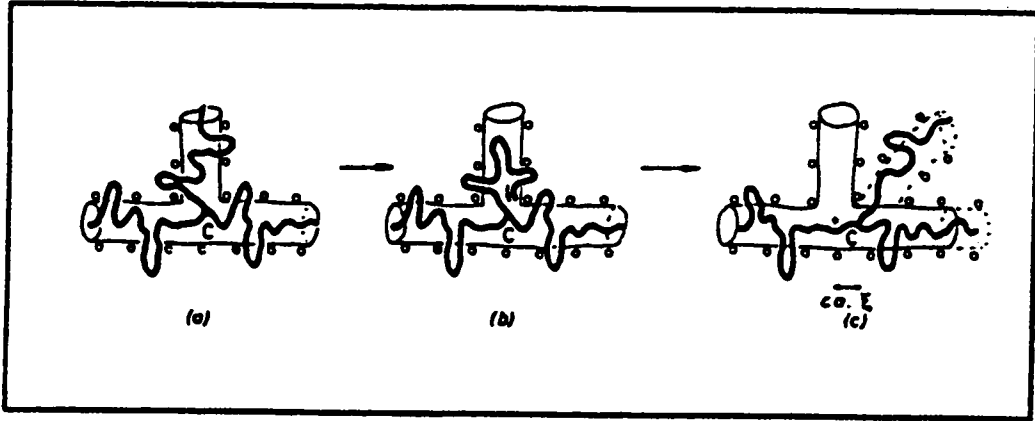


Figure 2.5. The motion of a three-arm star polymer in a tube (From reference 8)

2.1.1.3. Viscoelastic Properties

Star-branched polymers have a smaller radius of gyration than linear polymers with the same composition and molecular weight. For short side chains (below M_c), the viscosity η_B of star-branched polymers at a concentration c can be related to the viscosity η_L of linear polymers of identical molecular weight M (9) by Equations 2.3 and 2.4

$$\eta_B(c, M) = \eta_L(c, gM) \quad (2.3)$$

$$g = \frac{\langle S^2 \rangle_B}{\langle S^2 \rangle_L} \quad (2.4)$$

where $\langle S^2 \rangle$ is the squared radius of gyration, and subscripts B and L refer to branched and linear polymers, respectively. When the branches are sufficiently long (above M_c) the viscosity increases rapidly, due to enhanced molecular entanglement formation. This viscosity enhancement Γ is expressed by the equation

$$\Gamma = \frac{\eta_B(c, M)}{\eta_L(c, gM)} \quad (2.5)$$

The zero-shear viscosity for a linear polymer depends upon the molecular weight and temperature. For polymers with a narrow molecular weight distribution at a temperature above the glass transition temperature, the zero shear viscosity can be expressed as

$$\eta_0 = K(T)\rho M \left(\frac{M}{M_c} \right)^a \quad (2.6)$$

where $K(T)$ is a temperature-dependent parameter proportional to the local friction coefficient and ρ is the density. The parameter a is equal to zero for molecular weights (M) below a critical molecular weight (M_c) for entanglement formation and varies between 2.4 and 2.6 above M_c .

The zero-shear viscosity of star polymers is related to the molecular weight of the arms by the equation

$$\eta_0 = K_b(T) \exp\left(\gamma \frac{M_a}{M_c} \right) \quad (2.7)$$

where γ is a constant and $K_b(T)$ is a temperature-dependent parameter that varies with the molecular weight of the arms (M_a), the branching functionality, the temperature and the nature of the polymer (9,10).

The recoverable shear compliance of a linear polymer, a measure of the ability of the polymer chains to recoil after an elastic deformation, is given by the equation

$$J_e^0 = \frac{2M}{5\rho RT} \left(\frac{M}{M_c'} \right)^{a'} \quad (2.8)$$

where $a' = 0$ for $M < M_c'$, $a' = -1$ for $M > M_c'$, ρ is the density and the parameter M_c' represents a critical molecular weight characteristic for the polymer. For linear polymers,

the recoverable shear compliance initially increases with molecular weight and then becomes constant above the characteristic molecular weight M_c' .

For low branch molecular weights, the recoverable shear compliance is smaller for star-branched polymers than for linear polymers. In contrast, at high branch molecular weights (above the characteristic molecular weight M_c'), the shear compliance of branched polymers still increases with the molecular weight and becomes larger than the shear compliance for linear polymers (9-12). The recoverable shear compliance is related to the total molecular weight of star-branched polymers by the equation

$$J_e^0 = A \frac{M}{\rho RT} \quad (2.9)$$

where the constant A is a function of the branching functionality f of the polymer given by the equation

$$A = \frac{2}{5}(15f - 14)(3f - 2)^2 \quad (2.10)$$

2.1.2. Dendrimers and Hyperbranched Polymers

Dendritic polymers are highly branched molecules comprising dendrimers, hyperbranched and arborescent polymers. Dendrimers have a strictly controlled molecular weight, shape and topology. The well-defined structure of dendrimers is due to the series of protection-condensation-deprotection reaction sequences used in their preparation (13). Dendrimers are characterized by a relatively low molecular weight in most cases. In contrast, hyperbranched polymers are prepared in one-pot procedures based on random condensation reactions of AB_n monomers (14,15). This method yields high molecular weight products, albeit with a broad molecular weight distribution. Hyperbranched

polymers can be prepared with a number of chain ends per molecule comparable to dendrimers, but do not have a regularly branched structure.

Recently there has been considerable interest in the physical characterization of dendrimers and hyperbranched polymers. The physical properties of both families of compounds present many similarities. In the following sections, the characteristics of dendrimers will be discussed in terms of molecular weight, solution viscosity, hydrodynamic radii, glass transition temperature and viscoelastic properties.

2.1.2.1. Structural Characteristics

The synthesis of a typical dendrimer is represented in Figure 2.6. The molecular weight of a dendrimer as well as the number of terminal groups are dependent upon the initiator core multiplicity, N_c , and the number of reactive sites introduced by each repeat unit, N_b . Equations 2.11-2.13 predict the number of terminal groups, the degree of polymerization and the molecular weight, respectively, for a dendrimer of generation G (16).

Number of terminal groups:

$$Z = N_c N_b^G \quad (2.11)$$

Degree of polymerization:

$$N_{RU} = N_c \left(\frac{N_b^{G+1} - 1}{N_b - 1} \right) \quad (2.12)$$

Molecular weight:

$$M = M_c + N_c \left(M_{RU} \left(\frac{N_b^{G+1} - 1}{N_b - 1} \right) + M_T N_b^G \right) \quad (2.13)$$

where M_C , M_{RU} and M_T are the core, repeating unit and terminal unit molecular weights, respectively.

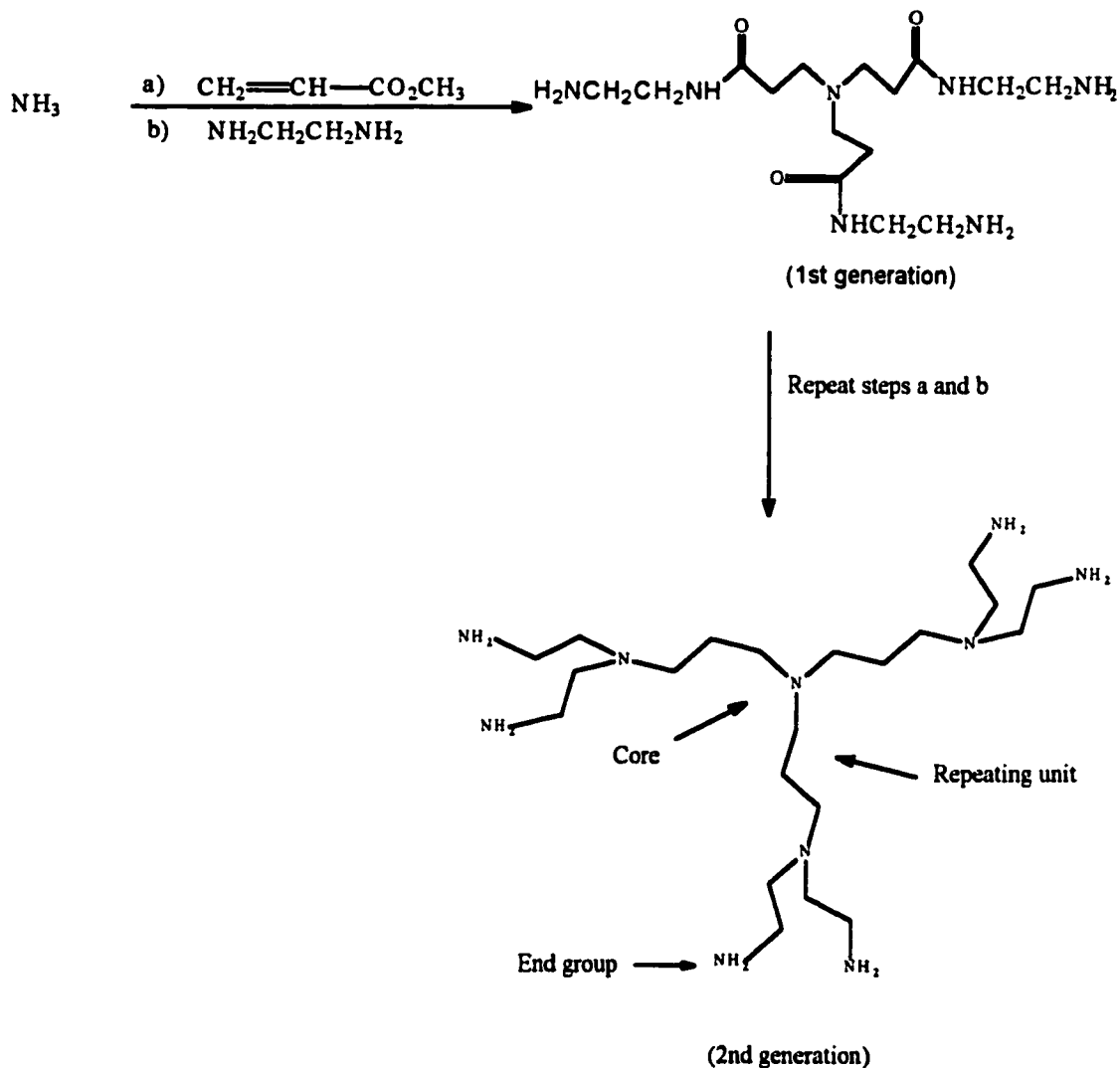


Figure 2.6. Synthesis of a polyamidoamine (PAMAM) dendrimer

There is growing interest in the use of Matrix Assisted Laser Desorption and Ionization-Time Of Flight (MALDI-TOF) mass spectrometry for the characterization of dendrimers (17). Comparison of the MALDI-TOF results with the calculated molecular weights and those obtained by SEC analysis showed that MALDI yields the most accurate

information on the molecular weight distribution of dendrimers. Errors of up to 20% in the molecular weight were observed when dendrimers were analyzed by the SEC-LALLS technique, in particular for molecular weights below 2 000 g/mol (18). The MALDI-TOF method, in contrast, yielded the expected molecular weights and showed that these materials are characterized by an extremely narrow molecular weight distribution.

2.1.2.2. Physical Properties

2.1.2.2.1. Solution Viscosity

The intrinsic viscosity of dendrimers is not related to molecular weight in the same way as in linear systems, and the Mark-Houwink-Sakurada equation is not obeyed. The intrinsic viscosity-molecular weight curve displays a maximum, in analogy to star polymers (18). This effect is explained by a transition in the structure of dendrimers from an open structure at low molecular weights to a globular structure for higher molecular weights.

The hydrodynamic diameter d can be calculated from the intrinsic viscosity $[\eta]$ and the molecular weight M of a dendrimer (19) according to the equation

$$d = \left(\frac{240}{\pi N_A} \right)^{1/3} (M[\eta])^{1/3} \quad (2.14)$$

where N_A is Avogadro's number. The hydrodynamic radius was found to increase linearly as a function of generation number for dendrimers based on 3,5-dihydroxybenzyl alcohol, as well as for PAMAM dendrimers (16,20).

2.1.2.2.2. Glass Transition Temperature

Dendrimers are essentially monodisperse materials with a precise number of chain ends, repeat units and a well-defined molecular weight. Because of these characteristics, it has been possible to correlate the glass transition temperature of dendrimers to their molecular weight, chain-end composition and bulk chemical composition (21,22) using theories similar to those developed for linear and star-branched polymers.

The effect of molecular weight on the glass transition temperature of dendrimers has been explored in a few studies (21,22). The model describing the effect of molecular weight on the glass transition temperature of linear polymers must take into account the non-linear increase in the number of chain ends with increasing molecular weight. Application of the free volume theory to dendritic macromolecules with n_e end groups, a molecular weight M and a density ρ yielded the equation

$$T_g = T_g^\infty - \Theta \left(\frac{\rho N_A n_e}{M} \right) \quad (2.15)$$

where Θ is the free volume per chain end and N_A is Avogadro's number. This equation can be rewritten as

$$T_g = T_g^\infty - K' \left(\frac{n_e}{M} \right) \quad (2.16)$$

to indicate a linear relation between the measured T_g and the ratio n_e/M , if K' is considered constant. A linear relation between T_g and n_e/M is observed experimentally, suggesting that if terms such as the density ρ or the chain end free volume Θ vary with molecular weight, this variation is not important. It was shown that for dendrimers, n_e/M does not tend towards zero at high molecular weights like in linear polymers, but rather approaches a constant value which is dependent upon the composition of the polymer and its end

groups (21).

In dendrimers, the number of chain ends increases geometrically with the generation number. Consequently, their glass transition temperature should also depend on the chemical nature of the chain ends. An increase in end group polarity was found to lead to an increased glass transition temperature (22). The introduction of more polar groups such as -Br or -CN at the chain ends resulted in considerably higher glass transition temperatures ($\Delta T_g=20-100^\circ\text{C}$) than those for the unsubstituted dendrimer (-H).

2.1.2.2.3. Viscoelastic Properties

Dendritic polyether macromolecules based on 3,5-dihydroxybenzyl alcohol of various generations were subjected to melt viscosity measurements (23). A logarithmic plot of the zero-shear viscosity η_0 as a function of molecular weight for dendritic polyethers (Figure 2.7.a) indicates that the viscosity is a non-linear function of molecular weight in the low molecular weight range (10^3-10^4 g/mol). The absence of a sharp increase in viscosity over a wide range of molecular weights, as observed for linear polymers, indicates that there is no entanglement formation for polyether dendrimers.

In the high molecular weight range (Figure 2.7.b), a straight line with a slope of 1.1 is obtained (the amount of data available to confirm this trend is limited, however). This shows that no intermolecular entanglements are formed for these dendritic macromolecules, as would be expected for a globular structure. A high surface congestion and a high degree of branching should prevent interpenetration and entanglement formation in large dendrimer molecules.

The rheological properties of polyamidoamine dendrimers were investigated by

Dvornic *et al.* (24). The measurements showed that dendrimers, because of their unentangled structure, are characterized by Newtonian behavior, that is a viscosity independent of shear rate. This contrasts with the behavior of linear polymers that display shear thinning at high shear rates.

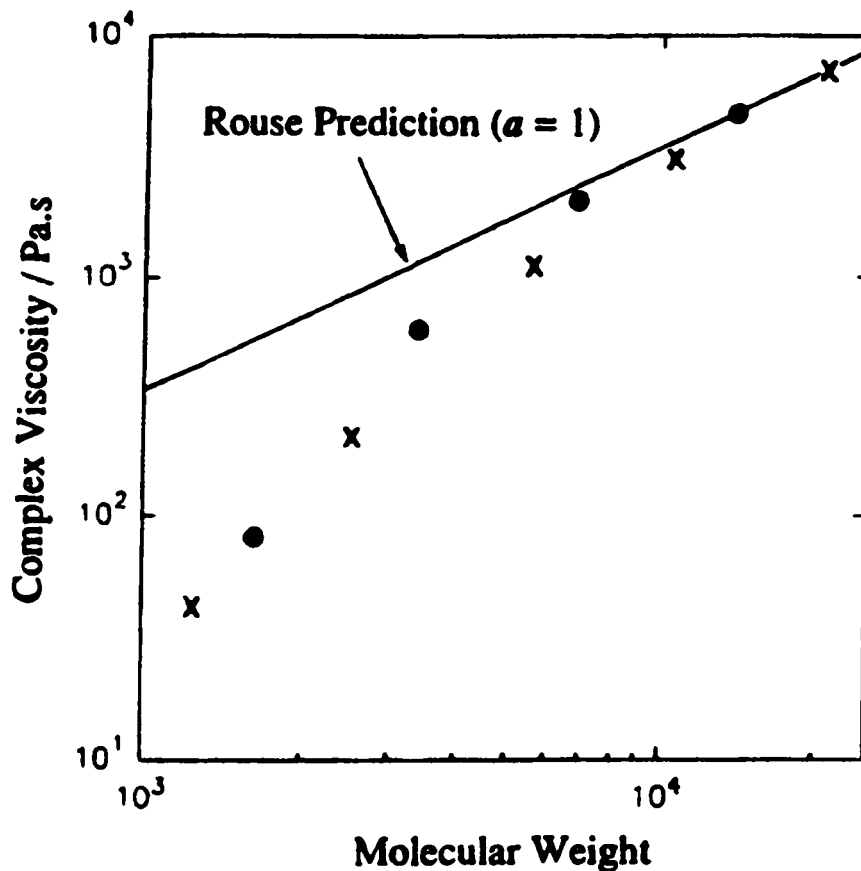


Figure 2.7.a. Viscosity of dendritic polyethers of successive generation for low molecular weight range (From reference 23)

2.1.3. Arborescent polymers

Arborescent polymers are highly branched polymers with a tree-like architecture first synthesized independently by Gauthier and Möller (25) and by Tomalia *et al.* (26). Their structure is well-defined in terms of branching functionality, branch length and

molecular weight distribution. The synthesis of these materials is based on a “graft-on-graft” strategy, consisting of successive grafting reactions of ‘living’ polymers.

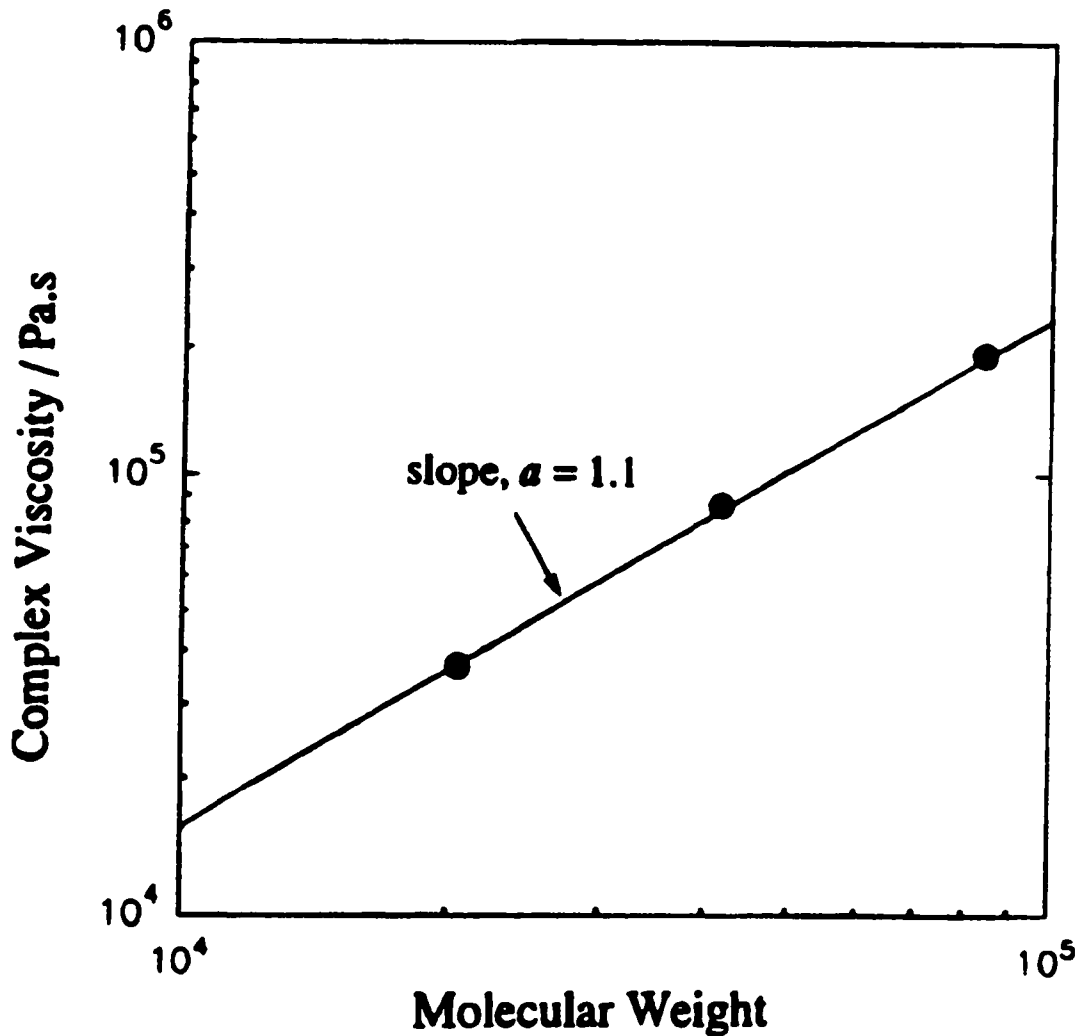


Figure 2.7.b. Viscosity of dendritic polyethers of successive generations in the high molecular weight range (From reference 23)

2.1.3.1. Synthesis

The synthetic scheme used for the preparation of arborescent polystyrenes is displayed in Figure 2.8 as an example. The random introduction of grafting sites along a

linear polystyrene with a narrow molecular weight distribution is accomplished through chloromethylation. The reaction of the partially chloromethylated backbone polymer with 'living' polystyrene anions leads to a polymer with a comb structure, identified as generation G0. Repetition of the chloromethylation and grafting reactions yields subsequent generations of arborescent polystyrenes G1, G2, and so on. The graft-on-graft procedure produces high molecular weight polymers in a few steps while maintaining good control over the structure and branching functionality of the molecules.

Graft copolymers incorporating an arborescent polystyrene core with end-linked poly(ethylene oxide) chains were prepared using a *grafting from* method (27), as shown in Figure 2.9. Linear polystyrene with a narrow molecular weight distribution was chloromethylated and grafted with polystyryllithium to generate a comb-branched structure.

A second grafting reaction was carried out in an analogous fashion but using a bifunctional initiator, 6-lithiohexyl acetaldehyde acetal (LHAA), for the preparation of polystyryllithium. Following hydrolysis and fractionation, a twice-grafted (G1) arborescent polystyrene bearing hydroxyl functionalities at the chain ends was obtained. The ethylene oxide copolymer was obtained by titrating the hydroxyl-terminated polymer with a potassium naphthalide solution and adding ethylene oxide.

Typical characterization results for arborescent polystyrenes are provided in Table 2.1. It can be seen that the weight-average molecular weight (M_w) and the branching functionality (f_w) of arborescent polymers increase rapidly for successive generations, while a low polydispersity is maintained for the graft polymers.

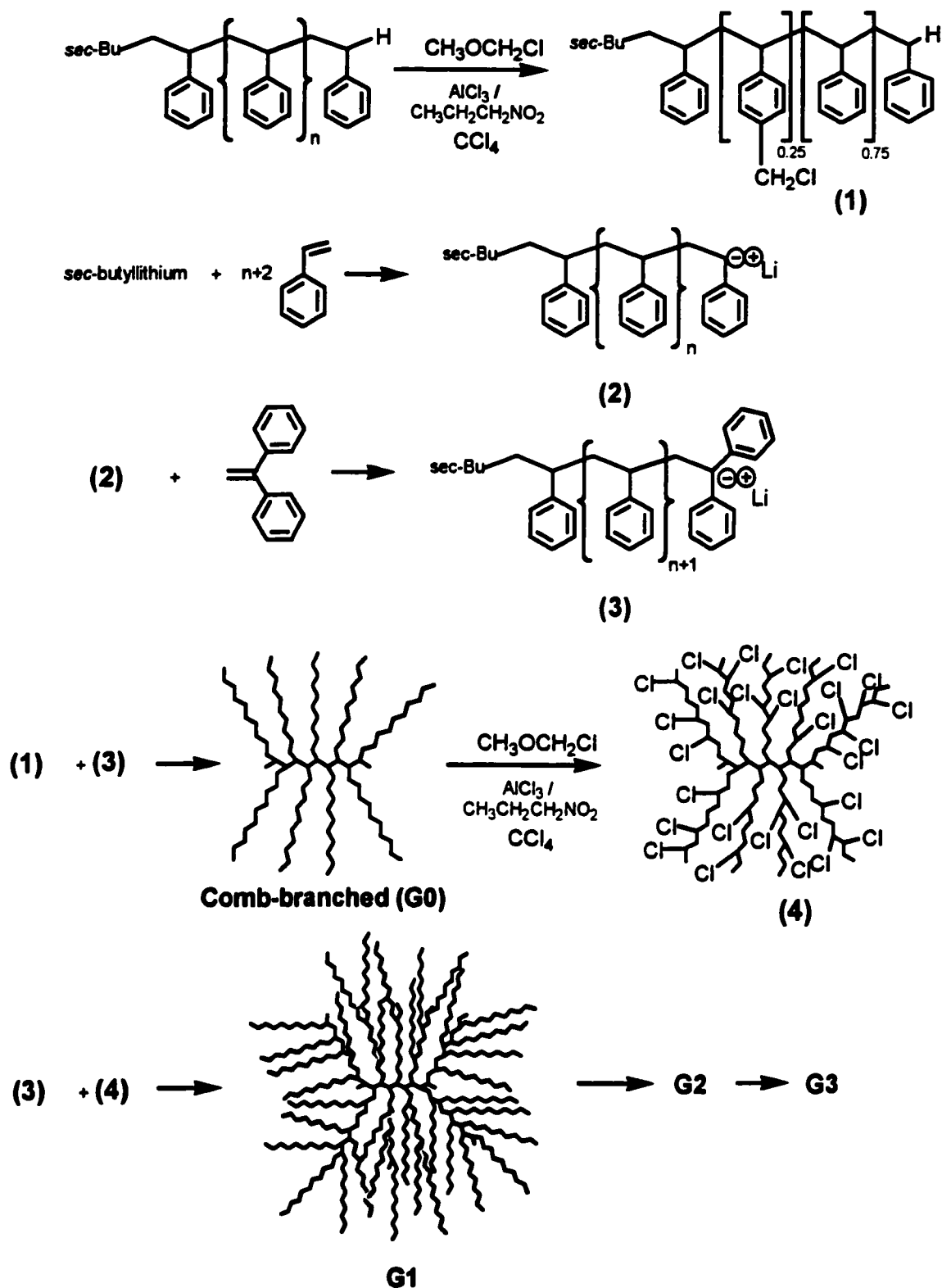


Figure 2.8. Synthetic scheme for the preparation of arborescent polystyrenes

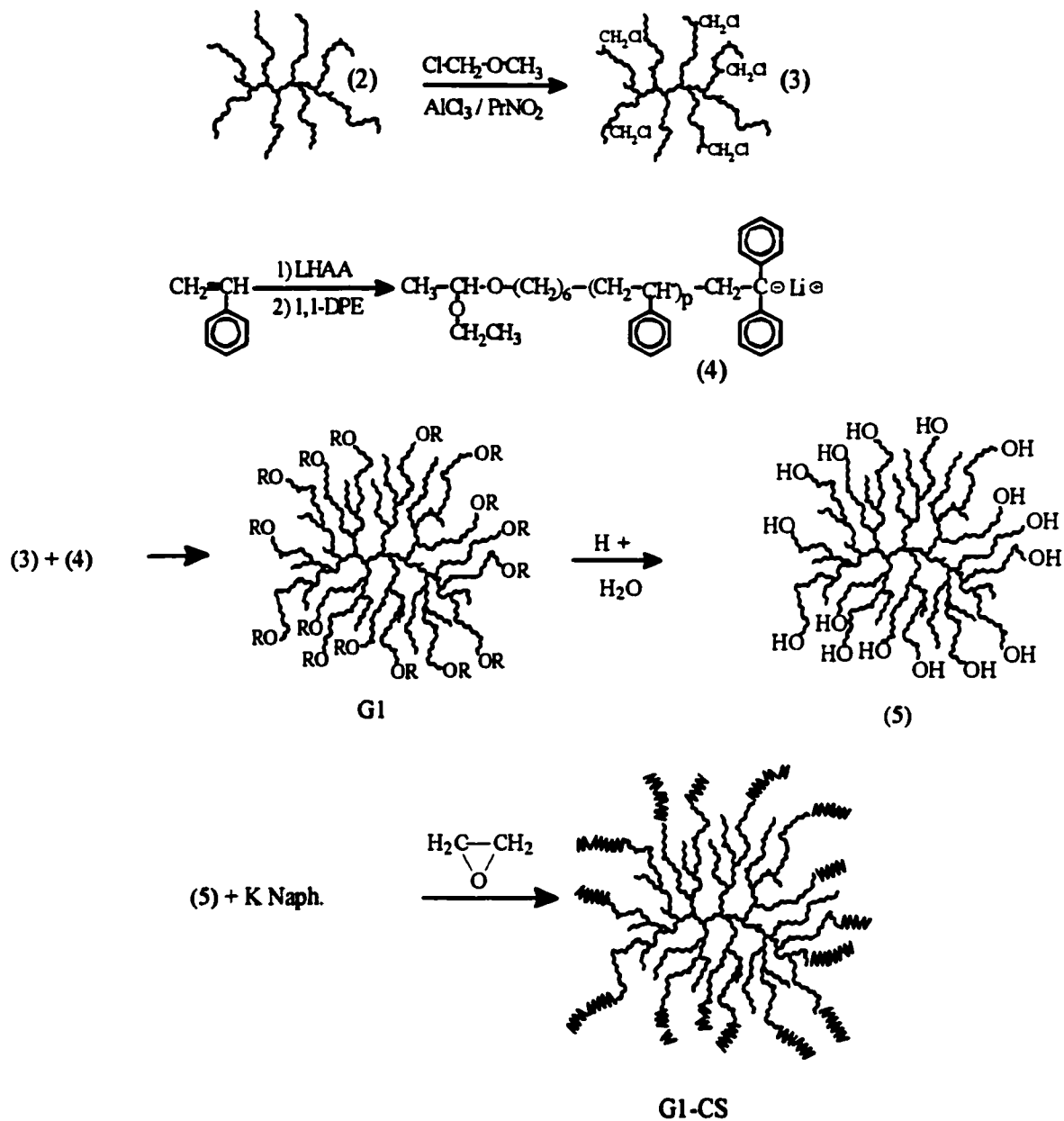


Figure 2.9. Arborescent poly(ethylene oxide) copolymer synthesis

Table 2.1. Characteristics of arborescent polystyrenes with 5 000 g×mol⁻¹ branches

Generation	M _w (g×mol ⁻¹)	M _w /M _n	f _w (total)
0	6.7×10 ⁴	1.07	16
1	8.7×10 ⁵	1.07	180
2	1.3×10 ⁷	1.20	2 800
3	8.8×10 ⁷	1.15	18 000

2.1.3.2. Physical Properties

The physical properties of arborescent polystyrenes in solution were investigated in relation to their structure (28). The variation in the intrinsic viscosity $[\eta]$ of these polymers with molecular weight is displayed in Figure 2.10. The measurements were carried out on two series of arborescent polymers having either 5 000 g/mol (S05-series) or 30 000 g/mol (S30-series) side chains, using either toluene or cyclohexane as a solvent. Compared to linear polymers, arborescent polymers have much lower intrinsic viscosities. The evolution of intrinsic viscosity with molecular weight displays a maximum, in analogy to star-branched and dendritic polymers. Furthermore, the intrinsic viscosity of higher generation polymers is comparable to that of the linear core polymers, even though the molecular weight of the arborescent polymers is up to 40 000 times larger than for the linear cores.

The film formation behavior of arborescent polystyrenes was investigated by atomic force microscopy (29). The photomicrographs presented in Figure 2.11 show that lower generation arborescent polymers have an open structure, allowing them to interpenetrate easily. The higher generation molecules, in contrast, have a compact globular structure with a low interpenetrability.

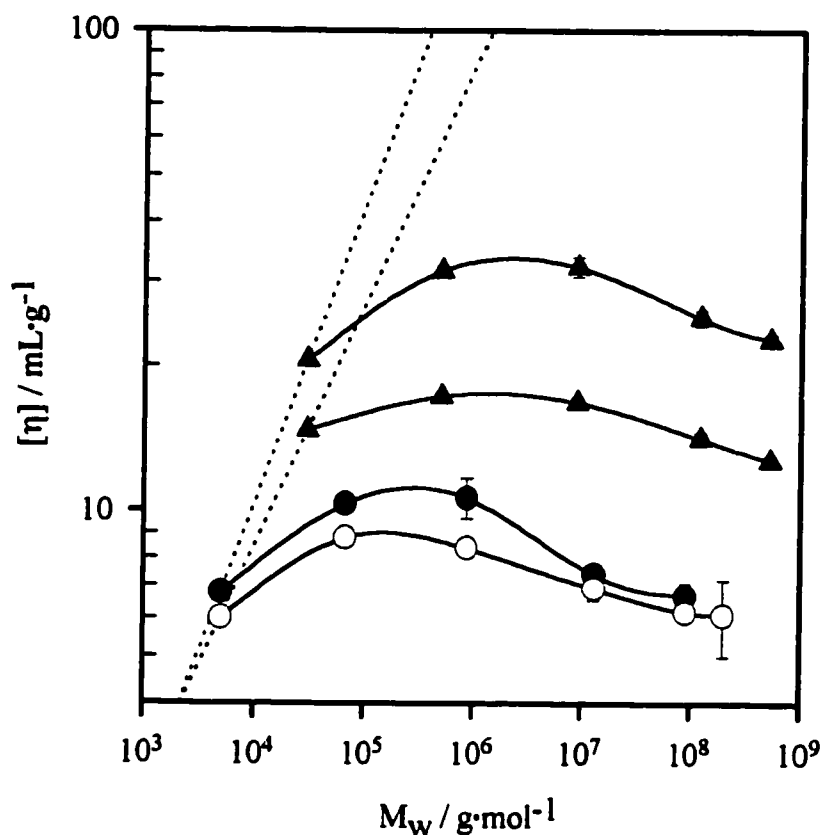


Figure 2.10. Intrinsic viscosity of arborescent polystyrenes of successive generations.

The curves, from top to bottom, are for S30-series polymers in toluene and in cyclohexane, and for S05-series polymers in toluene and in cyclohexane.

The dotted lines represent linear polystyrene in toluene and cyclohexane

(From reference 27)

The melt rheology of arborescent polystyrenes was investigated as a function of branch length and generation number (30). All arborescent polystyrenes displayed a zero shear viscosity η_0 lower than linear polymers of the same molecular weight. Furthermore, the difference in η_0 is more important for higher molecular weight samples, as shown in

Figure 2.12. For linear polymers with a molecular weight below the critical molecular weight for entanglement formation (M_c), the zero-shear viscosity varies linearly with the weight-average molecular weight ($\eta_o \propto M_w$). Above M_c , an exponential increase in η_o is observed ($\eta_o \propto M_w^{3.4}$). For arborescent polystyrenes of generations G0 (Sx-0) and G1 (Sx-1), the relation $\eta_o \propto M_w^{1.1}$ is obtained, corresponding to an essentially non-entangled structure. For the G2 polymers (Sx-2), in contrast, η_o decreases with M_w (Figure 2.12). This implies that second-generation polymers with short side chains (5 000 g/mol) are more strongly entangled than polymers with long side chains (20 000 g/mol). The unusual behavior of the G2 polymers can be rationalized in terms of a chain entrapment effect. The polymers with the short side chains are characterized by a denser, more brush-like structure than the polymers with the long side chains. When these molecules are forced to interpenetrate each other they are more likely to become immobilized by physical entrapment of the chains, leading to a higher melt viscosity.

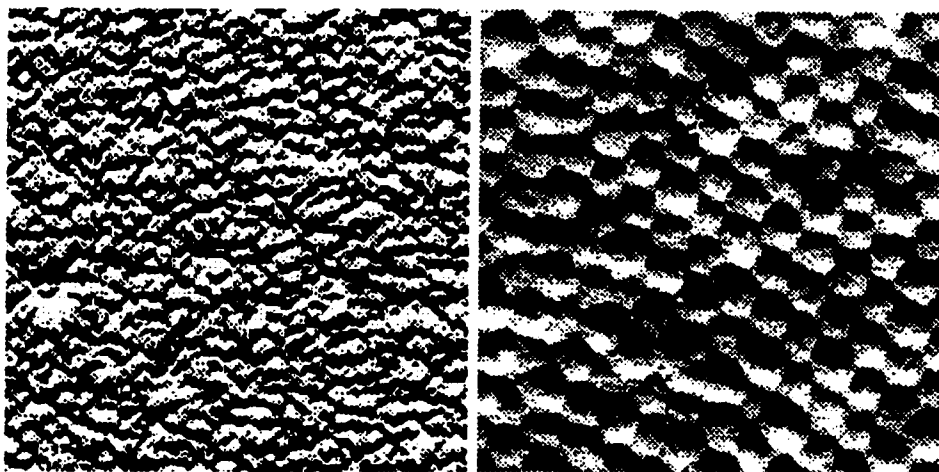


Figure 2.11. Atomic force microscopy pictures of monomolecular films of generation G1 (left) and G3 (right) arborescent polystyrenes. The width of each picture is 500 nm (From reference 29)

The unusual physical properties discussed demonstrate that arborescent polymers are interesting materials. Furthermore, mixtures of arborescent polymers with linear polymers should be interesting in terms of performance modification.

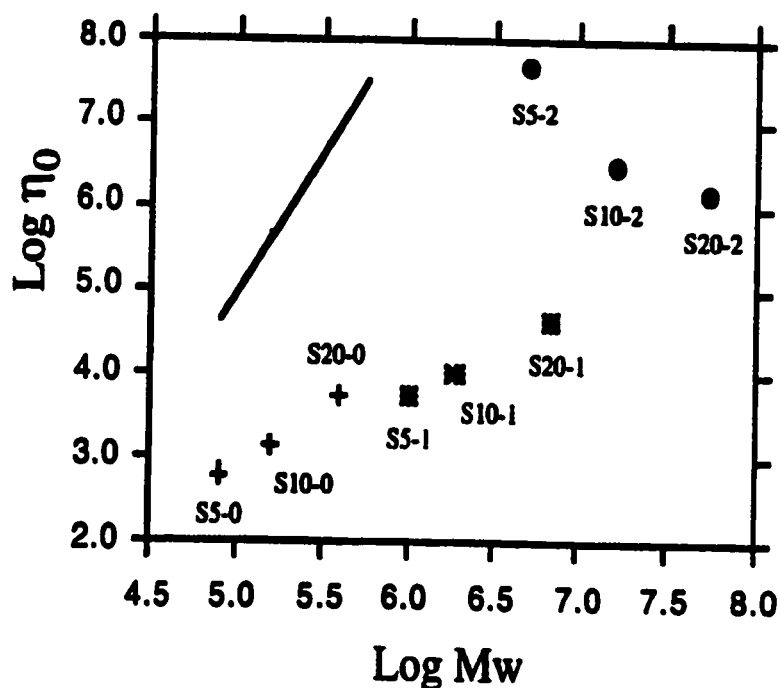


Figure 2.12. Zero-shear melt viscosity (η_0) of arborescent polystyrenes at 170°C. The labels (Sx-y) specify the side chain molecular weight (x) and generation number (y) (From reference 30)

2.2. Polymer Blends

Polymer blends are mixtures of two or more homopolymers or copolymers. Polymer blending should ideally be a method to obtain new materials with a combination of properties characteristic of those of the pure polymers. Blending is widely practiced industrially as an effective way to modify the properties of polymers. Consequently,

polymer blending is a very active area of polymer research (31-33). The composition of polymer blends can be tailored to control the physical properties of the final product. For example, blending can enhance mechanical properties such as the modulus, the impact resistance and the thermal stability. Blending can also serve to reduce the cost of an expensive polymer through 'dilution' with a less expensive material.

Blending offers many advantages over synthetic methods for the modification of physical properties. It requires a lower investment and also provides more flexibility, by variation of the proportions of each component. Furthermore, the synthesis of new copolymers requires more time compared to mixing pre-existing polymers.

A miscible polymer blend is defined as a system that is homogeneous at the molecular level. This blend consists of one single phase. It is characterized by one single glass transition temperature and thermodynamically by a negative free energy of mixing, as discussed in the next section.

There are numerous examples of commercially important polymer blends. Blending has been practiced in the rubber industry (34) where different polymers such as styrene-butadiene rubber (SBR) and ethylene-propylene-diene (EPDM) terpolymers are mixed with polybutadiene or natural rubber to improve the properties of the product. For instance, the addition of EPDM to polybutadiene or natural rubber enhances cracking resistance, while the addition of SBR to polybutadiene with a high *cis*-1,4 content improves processability.

A mixture of poly(2,6-dimethyl-1,4-phenylene oxide) (PPO) and polystyrene (PS) is another interesting example of a miscible system (35). Good mechanical properties and a high heat distortion temperature (HDT) are characteristic of PPO, which is however

very difficult to process (high melt viscosity) and expensive. Blending PS and PPO leads to enhanced mechanical and thermal properties since the incorporation of PS lowers the processing temperature. The blend is easier to process and more economical than pure PPO. In 1984, blends based on PPO and PS constituted 63% of the market share of all engineering resin blends, followed by nylon/elastomer blends representing a 17% market share (36).

The good heat resistance of poly(methyl methacrylate) (PMMA) and the flame resistance of poly(vinyl chloride) PVC led to the development of PMMA/PVC polymer blends used for injection molding and extrusion applications (36). Polymer blends based on PVC and acrylonitrile-butadiene-styrene (ABS) copolymers are also commercially important: The PVC imparts flame resistance, and ABS improves the toughness and processability of the blend.

2.2.1. Thermodynamics of Polymer Blending

Although a number of polymer blends are miscible, most combinations of two or more polymers are either immiscible or only partially miscible (37,38). This arises from unfavorable thermodynamics associated with mixing large molecules. The entropy of mixing for polymer blends tends towards zero with increasing molecular weight. The enthalpy of mixing is often positive, except in the presence of specific interactions between the polymeric components. Hence the overall free energy change for mixing is generally positive, which prohibits formation of a thermodynamically stable blend.

A polymer blend is miscible when the two components form a homogeneous and completely soluble system at the molecular level. From a thermodynamic standpoint, a

miscible polymer blend is associated with a negative free energy of mixing. The properties of the blend are generally intermediate between those associated with the constituent polymers. A single glass transition temperature (T_g) characterizes a miscible blend.

A polymer blend is immiscible when its components do not mix and form two or more phases. An immiscible blend is characterized by a positive free energy of mixing. The presence of two phases does not necessarily lead to an unfavorable behavior, and desirable physical properties may still be obtained. The utility of heterogeneous polymer blends lies in that desirable properties characteristic of each blend component can often be preserved, in particular when parameters such as the morphology, the interfacial adhesion, and the degree of dispersion of the phases can be controlled.

The characteristics of the interface between the two phases of an immiscible polymer blend strongly influence the final properties of the product (39). For this reason, block or graft copolymers are sometimes added to an immiscible blend to serve as interfacial agents or compatibilizers. Generally the chemical structure of the segments composing the copolymers is selected to be analogous to that of the blend components. The compatibilizers preferentially migrate to the interface between the two components, promoting good adhesion by reducing the difference in interfacial energy between the two phases of the blend (40).

Block and graft copolymer compatibilizers are typically used at low concentrations (less than 5 wt%). For example, high impact polystyrene (HIPS) is obtained by polymerizing styrene in the presence of polybutadiene. The polystyrene phase imparts hardness and good thermal properties to HIPS, while the rubbery phase improves impact resistance.

The free energy of mixing (ΔG_{mix}) for two polymers is a linear function of the enthalpy of mixing (ΔH_{mix}) and the entropy of mixing (ΔS_{mix}) (31)

$$\Delta G_{mix} = \Delta H_{mix} - T\Delta S_{mix} \quad (2.17)$$

where T is the temperature. The enthalpy of mixing is related to intermolecular interactions according to the equation

$$\Delta H_{mix} = RT\chi\phi_1\phi_2 \quad (2.18)$$

where χ is the interaction parameter, and ϕ_i represent the volume fractions of each component.

The entropy term describes the effect of molecular rearrangements. This term is inversely proportional to the molecular weight M_1 and M_2 of the polymeric components

$$\Delta S_{mix} = -R \left(\frac{w_1}{M_1} \ln \phi_1 + \frac{w_2}{M_2} \ln \phi_2 \right) \quad (2.19)$$

where w_1 and w_2 represent the weight fraction of each component.

Since the entropy of mixing for high polymers (M_1 and M_2 large) is usually very small, it is mainly the enthalpy of mixing that dictates whether a particular polymer blend is homogeneous or phase-separated. The expressions for the enthalpy and entropy of mixing can be combined to give the Flory-Huggins equation:

$$\Delta G_{mix} = RT \left(\frac{w_1}{M_1} \ln \phi_1 + \frac{w_2}{M_2} \ln \phi_2 + \chi\phi_1\phi_2 \right) \quad (2.20)$$

If the free energy of mixing ΔG_{mix} is positive at a given temperature, the polymer blend will phase separate. A polymer blend is completely miscible if the two following conditions are fulfilled (41):

- The Gibbs free energy of the mixture is negative.

- The second derivative of the Gibbs free energy with respect to the volume fraction of each component is positive (condition for stability):

$$\frac{\partial^2 \Delta G_{mix}}{\partial \phi_i^2} > 0 \quad (2.21)$$

In general the enthalpy (ΔH_{mix}) and entropy ($T\Delta S_{mix}$) terms are both positive for blends of non-polar polymers. The Gibbs free energy of mixing is negative if the enthalpy term is smaller than the entropy term. A polymer blend is usually miscible when the enthalpy of mixing is very small or negative.

If the two components of the blend contain polar groups, intermolecular interactions can favor miscibility. For example hydrogen bonding, acid-base or dipole-dipole interactions lead to a negative enthalpy of mixing. As a result, the Gibbs free energy is negative and the polymer blend is miscible. For instance, the miscibility of poly(acrylic acid) and poly(ethylene oxide) is attributed to hydrogen bonding (42).

The miscibility of poly(vinyl chloride) (PVC) and poly(caprolactone) has been attributed to hydrogen bonding between the α -hydrogens of PVC and the carbonyl groups of poly(caprolactone) (43). It has been shown that blends consisting of PVC and other polyesters are miscible if the ratio of CH_2 groups to carbonyl bonds in the polyester is between 4 and 10 for the same reason (44).

Polymer blends may display different phase separation behaviors. Many blends phase separate while the temperature is decreased. This behavior is due the existence of an upper critical solution temperature (UCST). One example of a blend that displays UCST behavior is the polystyrene/polyisoprene system. Polymer blends may exhibit a lower

critical solution temperature (LSCT) when phase separation is observed within the mixture with increasing temperature. Examples of blends which display a LCST include PS/poly(vinyl methyl ether), and PMMA/poly(styrene-*co*-acrylonitrile) (45).

2.2.2. Blending Methods

A wide range of methods may be used to blend polymers, depending on the amount and the nature of the components (32). Large amounts of polymer can be mixed together at a high shear rate using mechanical mixing. Consequently, this technique is widely used in the industry. The components of the blend can be mixed together at high temperature in the molten state using an extruder, although roll mills are sometimes employed.

Polymer blends can also be prepared *in situ* using reactive blending. Blending is accomplished by polymerizing a monomer in the presence of another pre-formed polymer. Often the polymerization is carried out within an extruder. The term reactive extrusion is accordingly used to describe this process.

When small quantities are required, blending can be conveniently performed in solution. The components are first dissolved in a common solvent, which is then removed by precipitation, evaporation, or by the freeze drying technique. These methods are highly suited to laboratory studies.

2.2.3. Linear and Branched Polymer Blends

A significant number of publications examining the experimental and theoretical aspects of polymer blends consisting of linear polymers have been reviewed (41).

However, due to the complex physical behavior associated with branched polymers, less attention has been given to blends consisting of linear and branched polymers.

The miscibility of linear and branched polymer blends based on chlorinated polyethylene was investigated (46). Chlorinated polyethylene with short branches exhibited relatively good miscibility with linear chlorinated polyethylene over a wide composition (chlorination) range. However, the composition range over which chlorinated polyethylene with long chain branching displayed miscibility with either linear or short chain-branched polymers was decreased. The effect was justified by a strong influence of branching points and chain ends on the interaction parameter χ dominating the miscibility of the blends.

The effect of chain structure on the phase separation kinetics of linear and star polymer blends was investigated (47). The blends examined were either based on linear poly(vinyl methyl ether) (PVME) and linear polystyrene (PS), or on linear PVME with four-arm star PS. A significant decrease in the phase separation kinetics of the four-arm star PS/linear PVME blends relative to the linear PS/linear PVME was observed for star polymers with a large arm molecular weight.

Phase separation in polyethylene blends with different architectures was recently investigated (48). The polymers used in the study were high density polyethylene (HDPE), linear low density polyethylene (LLDPE), and low density polyethylene (LDPE). For polymers with a low branching density, the blends were homogeneous in the melt. However, phase separation was observed in the melt for blends containing a component with a relatively high branching density. It was observed that for HDPE and LLDPE blends, phase separation occurs when the branching level is over eight branches per one

hundred carbon atoms.

In addition to mixing thermodynamics, the migration of branched polymer components to the surface of linear/branched polymer blends has also attracted considerable attention. This phenomenon is important since applications such as adhesion, lubrication and polymer processing are dominated by surface properties. The composition at the surface can have an important impact on the observable properties of a polymer blend. The segregation of a component to the surface of a blend is dictated by the surface energy of each component, and by the statistical segment length (stiffness) of the polymer chains (49).

A difference in surface energy between the blend components favors migration of the lower surface energy component to the surface. This is because the creation of a surface requires energy, to overcome intermolecular interactions and bring molecules from the bulk to the surface of the sample. The component with the lower surface energy requires less energy to break up intermolecular interactions than the higher surface energy component. Its migration to the surface is thus favored.

Increased structural stiffness (resulting from chain branching, for example) can also favor migration of a polymer to the surface of a sample, even when the chemical composition of the blend components is very similar. This is because entropy is lost when molecules are brought to the surface, since the chains at the interface have fewer accessible conformations. The number of accessible conformations for a branched polymer molecule is lower than for a linear polymer chain. The entropy penalty (loss) incurred by the branched molecule when it is brought to the surface is therefore lower than for a linear molecule, and its migration to the surface is energetically favored.

The surface characteristics of model branched diblock copolymers (prepared by hydrogenation of diene copolymers), containing linear polyethylene (PE), poly(ethylene-*alt*-propylene) and poly(1-butene) segments, were investigated (50,51). It was observed that the more highly branched components tend to migrate to the surface. This behavior was ascribed to differences in the structure, whereby the polymer with a shorter statistical segment length (a more compact structure) migrates preferentially to the surface.

One study of particular relevance to this work is the report by Kim and Webster (15) on the melt viscosity of linear polystyrene and polyphenylene hyperbranched polymer blends. While the morphology of the blends was not investigated, a 50% reduction in melt viscosity was observed at 180°C for a 5% concentration of the hyperbranched material. The melt viscosity decrease was further enhanced at higher temperatures and shear rates.

In light of the above investigations of linear and branched polymer blends, the following conclusions can be drawn. Depending on the branch length and branching functionality, different miscibility behaviors can be observed. When phase separation occurs between the two polymers, the branched component is expected to migrate preferentially to the surface of the blend.

2.2.4. Polymeric Processing Additives

Polymeric additives are often added to polymers such as polyolefins to facilitate their processing in extrusion and film blowing applications. The main advantage of these additives is that they decrease the formation of irregularities on film surfaces, known as sharkskin defects, in particular when processing polymers at high shear rates. Another benefit is that these substances facilitate the flow of the polymers on the surface of the

processing equipment, leading to 'apparent' decreases in melt viscosity of the matrix polymer. This allows the use of lower temperatures and/or higher throughputs in the processing operations. Two different mechanisms, namely slippage promotion and surface lubrication, have been suggested to explain the effects of two different types of polymeric additives on shark skin formation and on melt viscosity.

High molecular weight fluoroelastomers are often used as processing additives, primarily to reduce shark skin formation by promoting slippage of the polymer at the die/polymer interface. For example, the addition of 0.05% by weight of a vinylidene fluoride/hexafluoropropylene copolymer to linear low density polyethylene was shown to yield smooth extrudates and films at high shear rates (52). This behavior is ascribed to the formation of a uniform fluoroelastomer film on the metal of the barrel and die surfaces. The low surface energy of the film provides a sharp interface between the two polymers and facilitates slippage of the polyolefin extrudate. Optimum processing conditions are observed in these systems when the melt viscosity of the fluoroelastomer and the polyolefin are matched.

The incorporation of low viscosity polytetrafluoroethylene (PTFE) during the extrusion of poly(ether ether ketone) (PEEK) has been reported to lead to decreases in melt viscosity (53). The viscosity 'reduction' is enhanced as either the amount of PTFE or the rate of processing is increased. The decrease in melt viscosity in these systems is attributed to a surface lubrication effect arising from the migration of the low viscosity fluoropolymer to the surface. It is argued that the much lower surface tension of PTFE (19.1 mJ/m^2) relative to PEEK (36 mJ/m^2) favors migration of the PTFE component to the surface.

2.3. Synthesis and Properties of Polysiloxanes

Polysiloxanes, often identified by the generic name 'silicones', are polymers in which the backbone is composed entirely of silicon-oxygen bonds. The unique properties of polysiloxanes stem from the nature of the silicon-oxygen bond. Polysiloxanes are transparent, chemically inert, hydrophobic, thermally stable, highly permeable to gases, and are excellent thermal and electrical insulators. Polysiloxanes also have the lowest melting and glass transition temperatures observed of all polymers (54-58). One interesting feature of polysiloxanes is that their synthesis can be carried out using both step-growth and ionic ring opening polymerization techniques. This feature and the outstanding physical characteristics of these materials have been major driving factors for the commercial use of polysiloxanes. The synthesis and properties of polysiloxanes will be discussed in the following sections.

2.3.1. General Features of Siloxane Polymerization

Polysiloxanes can be prepared using both step-growth and ionic ring-opening polymerization methods. Step-growth polymerization is generally employed for the preparation of low molecular weight polysiloxanes when a narrow molecular weight distribution is unnecessary. The synthesis is simply carried out by hydrolysis of chlorosilane compounds. When precise control over the molecular weight distribution is required, or to synthesize block copolymers incorporating well-defined polysiloxane segments, ionic ring-opening polymerization is the only suitable route.

Ionic ring-opening polymerization can proceed by either anionic or cationic routes, depending on whether a base or an acid is used to catalyze the reaction of cyclic siloxane oligomers. Both reactions proceed by a living mechanism, and therefore sequential polymerization reactions leading to block copolymers are possible. Moreover, linear polysiloxanes with a well-defined molecular weight and a narrow molecular weight distribution are routinely prepared by these techniques (59).

Linear polysiloxanes are generally prepared by ring opening of the cyclic trimer (1) or tetramer (2) (Figure 2.13), where R and R' are either alkyl, substituted alkyl, or phenyl groups. A widely accepted shorthand notation used to describe the structure of methyl-substituted siloxane compounds is shown in Figure 2.14. The n -meric disubstituted siloxane cyclic oligomers are denoted D_n . For example, the tetramer (2) is referred to as D_4 . The notation MD_nM is used to denote linear oligomers and polymers capped with trimethylsilyl groups where there are $n+2$ silicon atoms present.

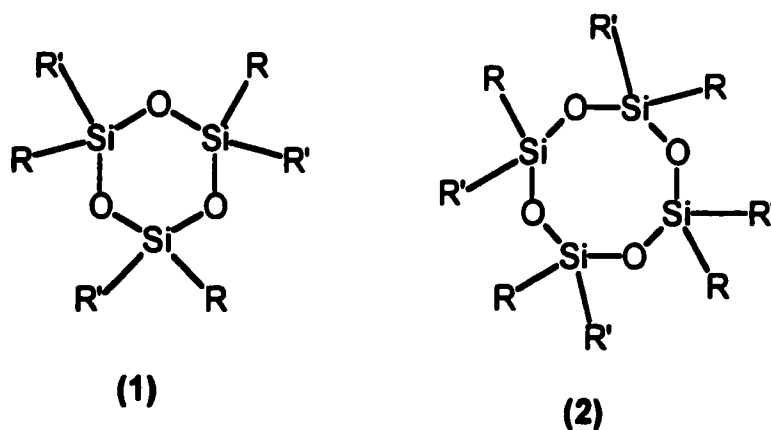


Figure 2.13. Cyclic siloxane monomers

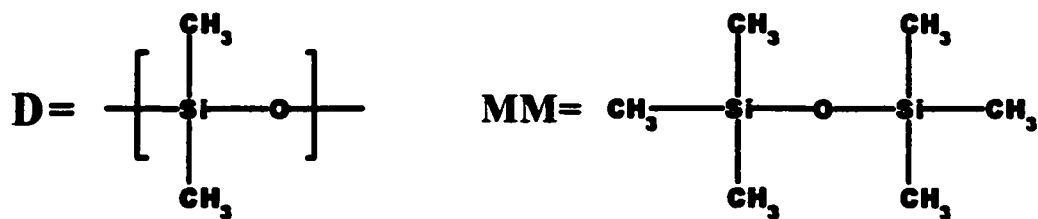


Figure 2.14. Nomenclature for methyl-substituted siloxane compounds

Cyclic siloxane oligomers (D_n , where $n \geq 3$) can be polymerized by anionic or cationic routes to yield high molecular weight polymers. With the exception of D_3 , the enthalpy change (ΔH) for the ring opening reaction to yield linear polymer is approximately zero. This arises because there is no net change in the number of siloxane bonds and there is essentially no ring strain in cyclic siloxanes with four or more siloxane units. For these compounds, the polymerization reaction is driven by a slight entropy gain associated with an open chain structure over the cyclic structure and proceeds under equilibrium conditions. However, in the case of D_3 , the alleviation of ring strain contributes about -15 kJ/mol to the ΔH of polymerization. Consequently D_3 is much more reactive, and the polymerization proceeds under kinetic control.

It was mentioned that three techniques can be used for the synthesis of polysiloxanes, namely the hydrolysis of chlorosilane compounds, and the cationic or anionic ring-opening reactions of the cyclic siloxanes. Each of these reactions will be discussed in more detail in the following sections.

2.3.1.1. Synthesis from Chlorosilane Compounds

Linear polysiloxanes can be prepared *via* hydrolysis of organosilicon dihalides,

according to the reactions given in Figure 2.15 (60,61). In addition to linear PDMS, the hydrolysis of dichlorodimethylsilanes produces cyclic siloxanes that can be recovered by fractionation and subsequently used in ring opening polymerization reactions.

The relative amounts of cyclic and linear products obtained can be controlled by varying the reaction conditions and the solvent used (62). For example, the formation of cyclic oligomers is favored when the hydrolysis proceeds at low temperatures, when ethers are used as solvent, or in the presence of amines or ammonium salts. In general this process leads to low molecular weight polysiloxanes.

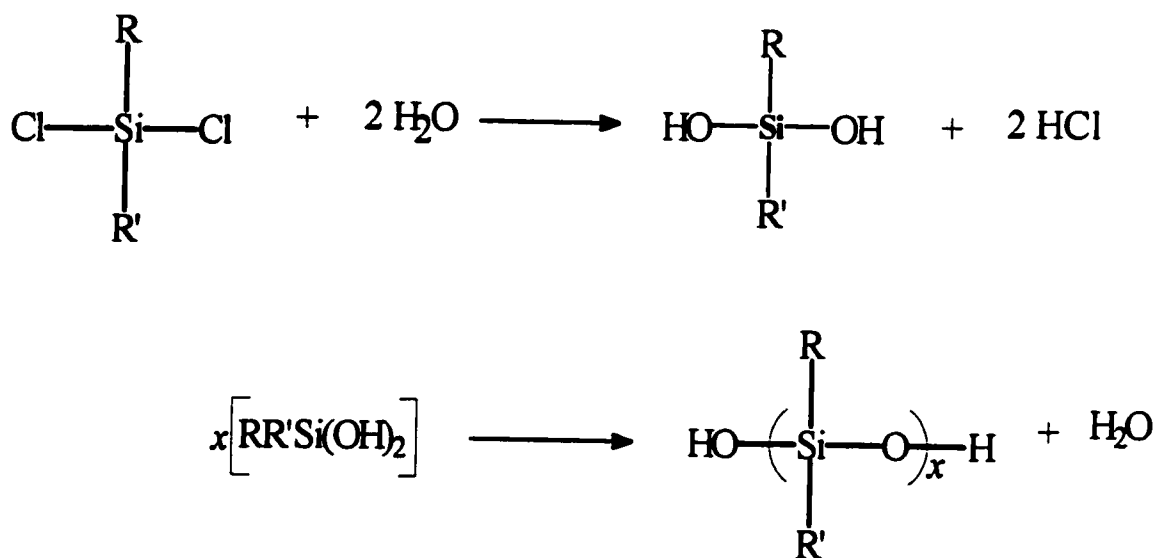
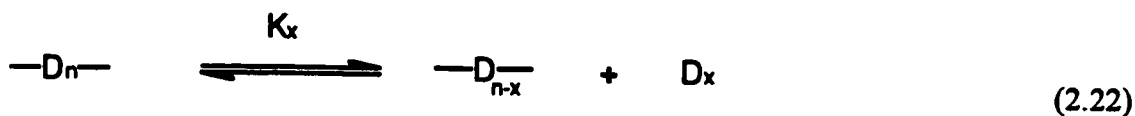


Figure 2.15. Hydrolysis of a dichlorosilane

2.3.1.2. Ionic Ring-Opening Polymerization Under Equilibrium Conditions

The equilibrium polymerization of D_4 is the most widely studied example of the thermodynamically controlled polymerization of siloxanes. The equilibrium state consists of cyclic siloxane rings, D_x where $x \geq 4$, and of linear polymeric chains, $-D_n-$. The polymerization equilibrium can be represented by the equation



The polymer yield, its molecular weight and polydispersity are thermodynamically controlled in the above equilibrium.

The position of the equilibrium between linear polymer chains and cyclic species determines the overall yield of polymer. The total concentration of cyclic species is independent of the initial monomer concentration (54,59). Diluting the system during polymerization will result in a decrease in overall yield of polymer, such that the concentration of cyclic species again reaches the equilibrium concentration. Consequently, equilibrium polymerization reactions of cyclic siloxanes are often performed in the bulk.

The equilibrium determines the average molecular weight of the polymer obtained. The number-average molecular weight (M_n) is related to the number of end groups by the equation

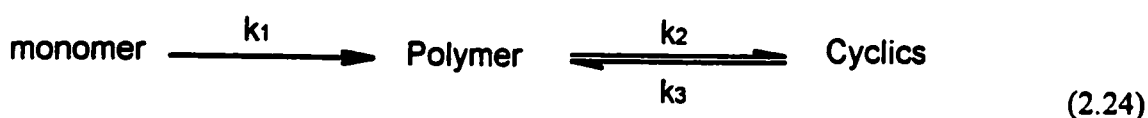
$$M_n = \frac{2[-Si(RR')O-]_{eq} M_o}{[end\ groups]} \quad (2.23)$$

where M_o is the molecular weight of the siloxane structural unit and $[-Si(RR')O-]_{eq}$ is the concentration of siloxane units incorporated in linear chains. The equilibrium involving redistribution amongst linear polymer chains is a result of random siloxane bond cleavage and formation. Thus the polymer formed under equilibrium conditions should have a molecular weight distribution characterized by a polydispersity index, M_w/M_n , that tends towards 2. This feature limits the utility of equilibrium polymerization when well-defined polymers are required. The number-average molecular weight can be controlled under these conditions by the addition of an appropriate amount of an “end-blocking” agent,

MM.

2.3.1.3. Ionic Ring-Opening Polymerization Under Kinetic Control

Kinetic control is possible because of the increased reactivity of some cyclic siloxanes due to ring strain, as it is the case for D_3 . Both anionic and cationic polymerization reactions can be carried out under kinetic control. The overall reaction can be represented by the equation



In general, $k_1 > k_2$ and a linear high molecular weight polymer is obtained. Depolymerization and redistribution reactions can be minimized or avoided with careful selection of the reaction conditions. Complete conversion is usually not possible, since at higher conversion depolymerization reactions become favored. Kinetic control over the polymerization reaction makes it possible to prepare polymers with a narrow molecular weight distribution ($M_w/M_n < 1.1$) and a predictable molecular weight ($M_n \propto [M]_0 / [I]$). Polymerization under kinetic control is also useful for the preparation of block copolymers, graft polymers and star polymers from cyclic trisiloxanes.

2.3.1.4. Cationic Ring-Opening Polymerization

Cationic ring-opening polymerization can be used for the preparation of linear homopolymers and block copolymers of siloxanes. Sulfuric acid, trifluoromethanesulfonic acid and some metallic cations can be used to initiate the cationic polymerization of cyclic siloxanes. The mechanisms for the initiation and the chain growth reactions are not well

understood (63). For both D_4 and D_5 the polymerization proceeds under thermodynamic control and redistribution reactions are pronounced, leading to low molecular weight products. For D_3 , however, the reaction may proceed under kinetic control and equilibrium conditions are only reached at long reaction times. The presence of water as a co-catalyst increases the polymerization rate but also leads to side reactions. Cationic polymerization tends to yield polymers with a relatively broad molecular weight distribution ($M_w/M_n = 1.3-1.4$).

2.3.1.5. Anionic Ring-Opening Polymerization Techniques

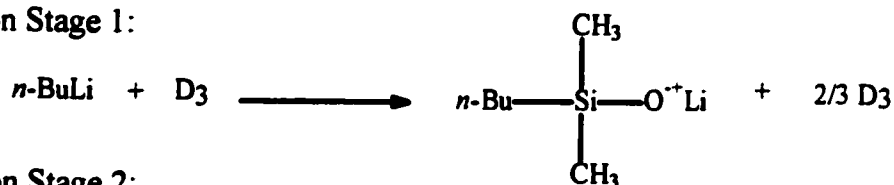
The anionic ring-opening polymerization of cyclic siloxanes can be carried out at room temperature in a variety of suitably purified solvents such as toluene, hexane, THF and benzene. The polymerization proceeds slowly unless a promoter cosolvent is added. Typical promoters include hexamethylphosphorous triamide (HMPT), N,N-dimethylformamide (DMF) and dimethylsulfoxide (DMSO) (64-66). Tetrahydrofuran (THF) has also been reported to be an effective promoter (67,68). The main role of the promoter is to increase the concentration of the more reactive solvent-separated ion pairs by solvating the counterion. This leads to an increased rate of polymerization.

Well-defined linear polydimethylsiloxane can be prepared by a two-step anionic polymerization reaction of the cyclic trimer (D_3) at room temperature (67). The first step consists of a seeding reaction where the initiator and a fraction of the monomer are left to react for at least 12 hours in toluene. The remaining monomer and THF are then added. The mechanism suggested for the two-step polymerization of D_3 initiated by *sec*-butyllithium is outlined in Figure 2.16. The termination reaction, also shown in Figure 2.16, will be discussed

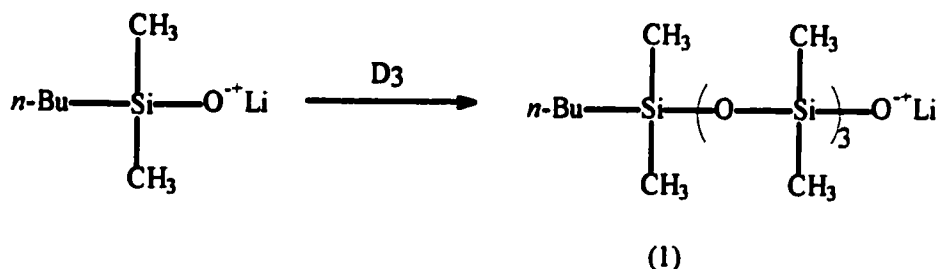
in more detail subsequently.

The nature of the metallic counterion affects the reactivity of the silanolate living ends, which in turn affects the polymerization rate. Reactivity decreases for smaller counterions, so that cesium silanolates are more reactive than potassium silanolates, which are in turn more reactive than sodium and lithium silanolates. However, even lithium silanolates can become very reactive when used in the presence of a promoter (59).

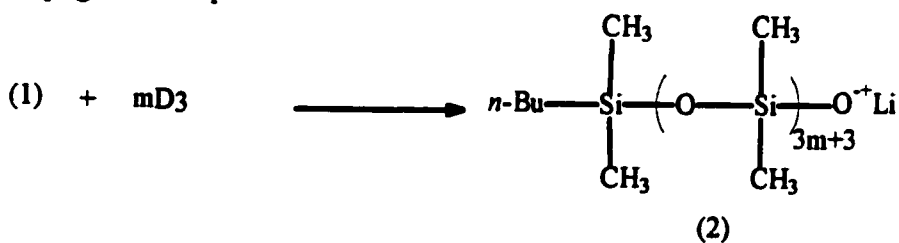
Initiation Stage 1:



Initiation Stage 2:



Propagation Step:



Termination Step:

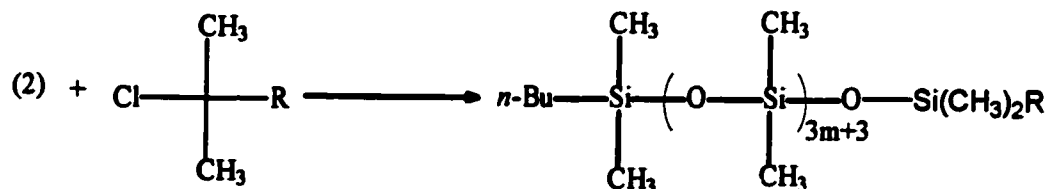


Figure 2.16. Preparation of linear PDMS by a two-step anionic polymerization reaction

2.3.1.5.1. Cryptands in Ring-Opening Polymerization

Evidence demonstrating the formation of polymeric silanolate aggregates during the ring-opening polymerization of cyclic siloxanes has been reported (69). It was shown that the rate of polymerization displayed a fractional order with respect to the concentration of silanolate species in kinetic investigations. In order to suppress aggregation, the use of macrobicyclic ligands and other cryptands has been investigated (70). It was observed that the polymerization rate becomes first-order with respect to the concentration of active centers in the presence of cryptands. Viscosity measurements for solutions of 'living' and deactivated PDMS also yielded identical molecular weights, providing further evidence for the suppression of silanolate anion aggregation in the presence of cryptands.

Polymerization of D_3 at room temperature initiated with an alkali metal hydroxide (KOH) in the presence of a macrobicyclic cryptand such as Kryptofix 2.2.2 (4,7,13,16,21,24-hexaoxa-1,10-diazabicyclo[8.8.8]hexacosane), shown in Figure 2.17, led to linear PDMS with a high molecular weight at 60% conversion within five minutes (71). The usefulness of cryptands has also been demonstrated in the anionic polymerization of a wide range of other monomers such as methyl methacrylate, ethylene oxide, propylene sulfide, styrene, and isoprene (72).

2.3.1.6. Termination of the Polymerization

Termination of the polymerization reaction is crucial, since the living polysiloxane chains carrying silanolate groups can undergo redistribution and depropagation reactions. The most commonly used end-capping reagent is chlorotrimethylsilane, since it leads to a

stable polymer preventing depropagation and redistribution reactions. The silanolate living ends can displace the chloride anion to yield a trimethylsilyl-terminated chain, as shown in Figure 2.16.

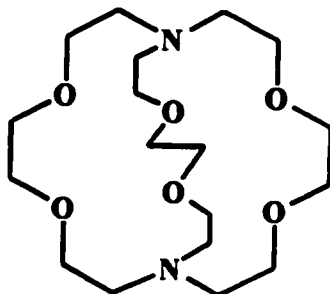


Figure 2.17. Structure of Kryptofix 2.2.2, a cryptand

Reactive chain ends can also be introduced in the living polymer through termination reactions. For instance the addition of water yields silanol end groups. Termination with chlorodimethylvinylsilane yields a vinyl-terminated polysiloxane (73). Other terminating agents have been used to introduce various other functional groups including *p*-vinylphenyl, propyl methacrylate, and pentyl methacrylate functionalities (73-76).

2.3.2. Branched Polymers with Well-Defined Architectures Based on Polysiloxanes

The synthesis of branched siloxane polymers and copolymers with graft, star and dendritic architectures has been reported. These polymers are of considerable interest since they are tailor-designed materials with unique properties. Star-branched and dendritic polysiloxanes display unusual physical properties because of their compact

structure. These polysiloxanes are also suitable for the formation of networks.

2.3.2.1. Graft Copolymers

Different methods can be employed to prepare polysiloxane graft copolymers. For example vinyl-terminated polysiloxanes can be used as macromers, and copolymerized with a suitable vinyl monomer to yield a graft copolymer. Alternatively, pre-existing polysiloxane side chains may be coupled with a polymer backbone bearing suitable functional groups, or a suitably functionalized backbone polymer can be used to initiate the polymerization of cyclic siloxanes.

2.3.2.1.1. Copolymerization of Macromers

Many studies have reported the use of macromers in the synthesis of copolymers based on siloxanes, since this approach allows control over the molecular weight and the average number of branches in the molecule. Examples of this approach include the copolymerization of vinyl-terminated polydimethylsiloxane macromers with vinyl monomers such as styrene, methyl methacrylate or vinyl acetate (73,75,77,78). Macromers are obtained with a narrow molecular weight distribution by anionic ring-opening polymerization of D_3 , and termination with a substituted dimethylsilylchloride compound bearing a vinyl group. Free-radical copolymerization of the vinyl-terminated PDMS with a second monomer yields the graft copolymer. The synthesis of a comb-branched graft copolymer based on the copolymerization of a methacrylate-terminated PDMS macromer with methyl methacrylate (79) is shown in Figure 2.18.

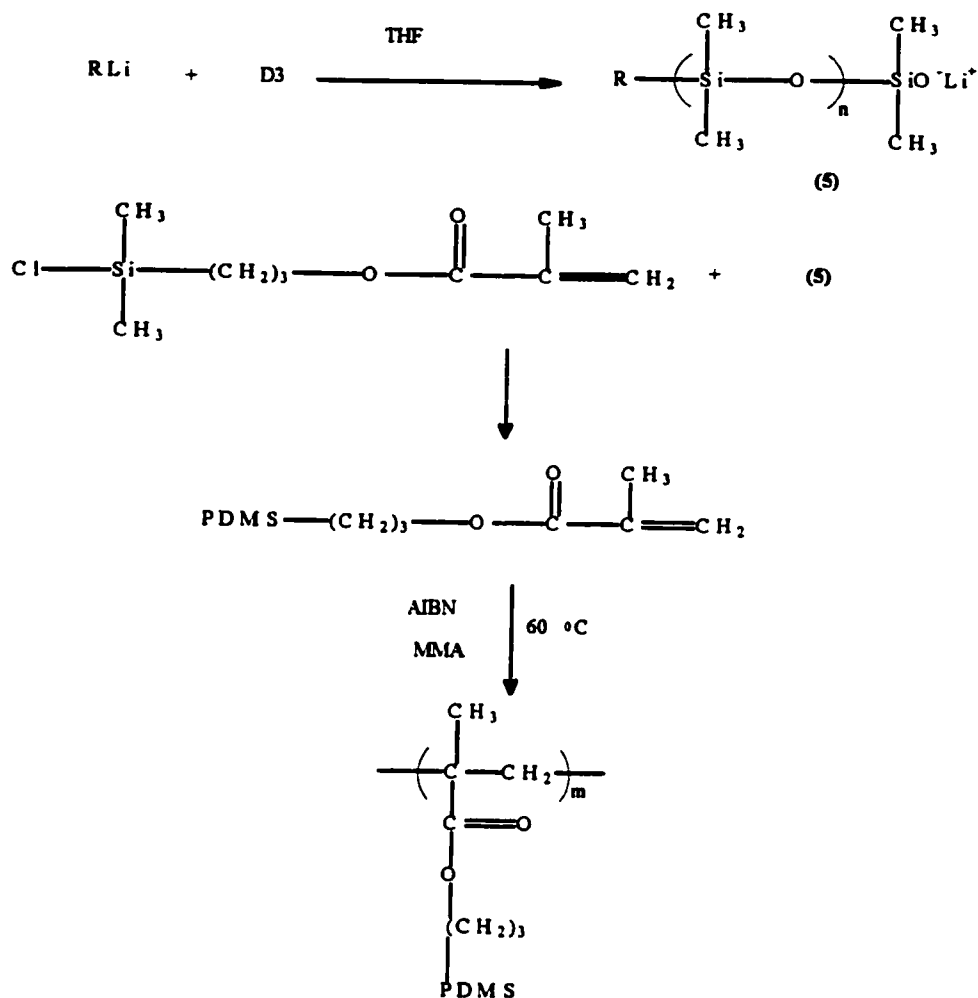


Figure 2.18. Preparation of poly(methyl methacrylate)-g-polydimethylsiloxane

2.3.2.1.2. Grafting Reactions

The preparation of graft copolymers consisting of a linear polymer bearing PDMS side chains has been achieved using both *grafting onto* and *grafting from* schemes. For example, hydrosilyl-terminated PDMS is suitable for grafting PDMS *onto* a linear backbone polymer through the hydrosilylation of pendent double bonds. An alternative method for preparing graft copolymers uses a *grafting from* technique, whereby reactive sites capable of initiating the anionic polymerization of D_3 are created along a polymer

backbone. One example of a *grafting onto* scheme yielding a comb-branched graft copolymer is the reaction of vinyltrimethylsilylated polysulfone with hydrosilyl-terminated PDMS depicted in Figure 2.19 (80). The metalation of polysulfone with *n*-butyllithium in THF, followed by reaction with vinyltrimethylchlorosilane, yields vinyltrimethylsilylated polysulfone. In the presence of a platinum catalyst, the hydrosilyl-terminated PDMS can be coupled with the linear backbone.

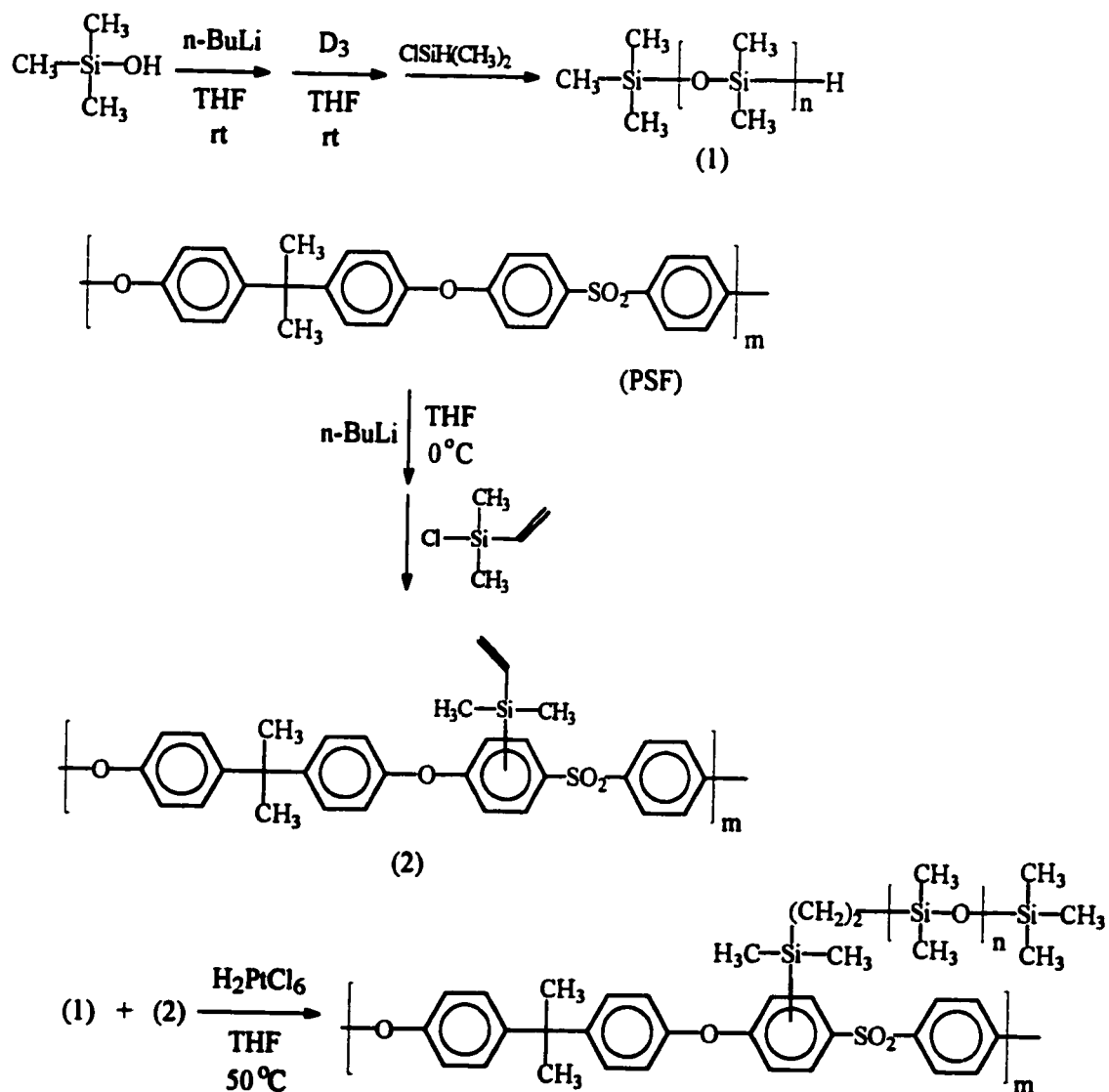


Figure 2.19. Preparation of polysulfone-g-polydimethylsiloxane

A graft copolymer consisting of a poly(1-phenyl-1-propyne) (PPP) backbone with PDMS branches was prepared using a *grafting from* scheme. In this case, metalation of PPP in cyclohexane with *n*-butyllithium yielded a polyfunctional initiator from which PDMS branches were grown by polymerization of D_3 according to the scheme of Figure 2.20 (81).

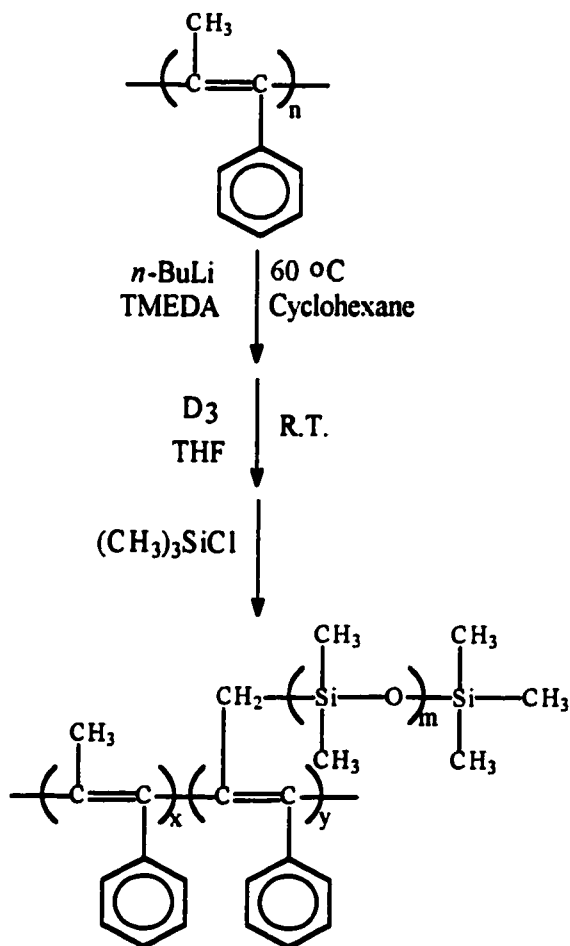


Figure 2.20. Preparation of poly(1-phenyl-1-propyne)-*g*-polydimethylsiloxane

2.3.2.2. Star-Branched Telechelic Polymers

Telechelic polymers consist of chains terminated with functional groups at one or more chain ends, including star-branched topologies (82,83). For example, an amino-

terminated three-arm star-branched PDMS was obtained according to the scheme shown in Figure 2.21. The anionic ring-opening polymerization of D_3 was initiated with p -(N,N -bis(trimethylsilyl)amino) styryllithium, a protected form of p -amino-functionalized initiator. The living polymer chains were then deactivated with trichloromethylsilane or tetrachlorosilane, to yield three- or four-arm star-branched polymers, respectively. The bis (trimethylsilyl) amino groups were subsequently deprotected using mild acid-catalyzed hydrolysis.

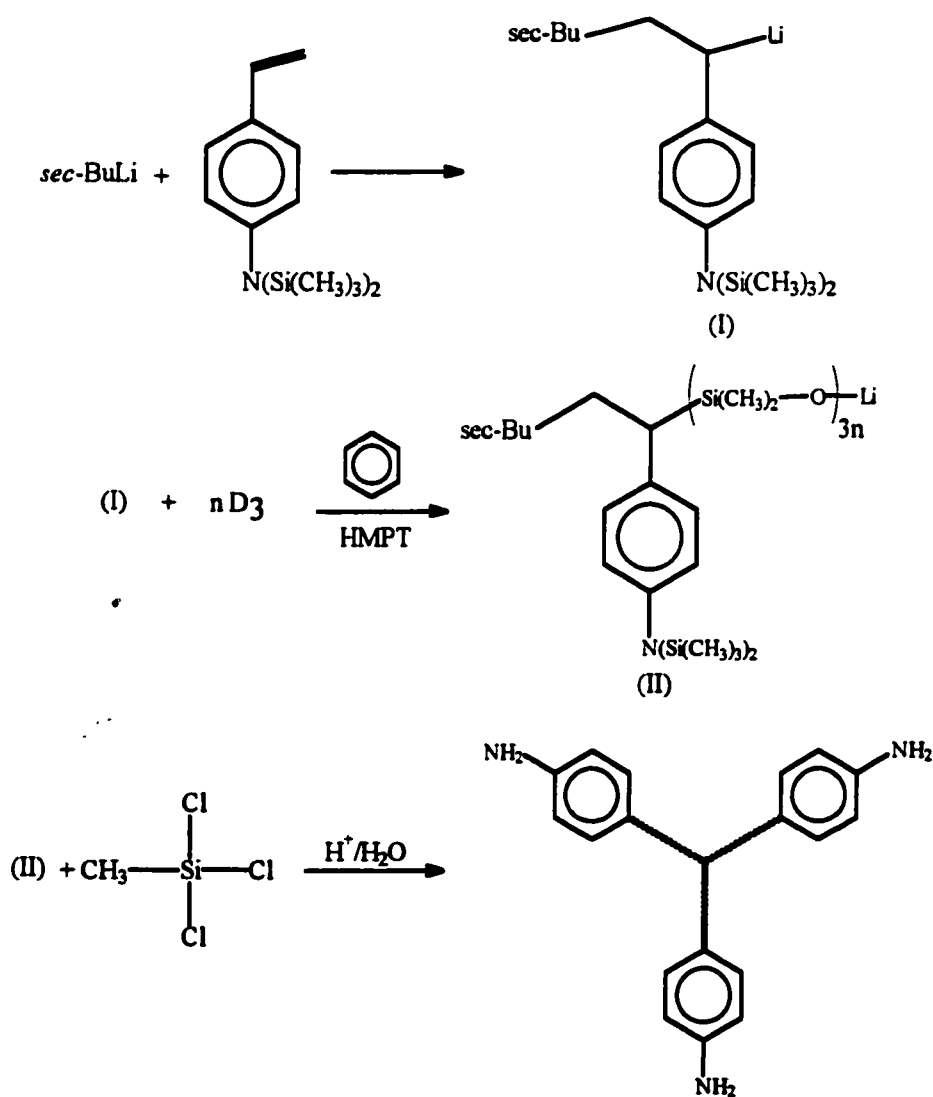


Figure 2.21. Preparation of amino-terminated three-arm star-branched PDMS

2.3.2.3. Networks Based on PDMS Segments

Model PDMS networks with precisely controlled molecular structures in terms of average molecular weight between crosslinks, M_c , and the functionality of the junction points have been reported (84-88). The PDMS segments were prepared by anionic ring-opening polymerization to ensure a narrow molecular weight distribution, and were end-functionalized with vinyl groups. The vinyl-terminated PDMS segments were then reacted with tetrakis(dimethylsiloxy)silane by hydrosilylation in the presence of a platinum catalyst, to yield a network with a structure shown in Figure 2.22. The elastomeric networks were used as model systems to study the relationship between network structure and performance, and as high impact materials (89). Polysiloxane networks were also obtained by the reaction of hydroxyl-terminated PDMS chains with a cross-linking agent bearing four functional sites (such as tetraethyl orthosilicate) in the presence of a catalyst (85).

2.3.2.4. Dendritic Polysiloxanes

A few methods for the preparation of dendritic macromolecules based on polysiloxanes have been reported (90-92). In one case, the synthesis was based on repetitive reactions between electrophilic silicon species and a nucleophilic silanol, as shown in Figure 2.23 (91). Methyltrichlorosilane was used as a starting material for the preparation of tris(phenyldimethylsiloxy)methylsilane (**13**), serving as a core. Successive reactions of the core with bromine and diethylamine yielded the corresponding N,N-diethylaminosilane derivative [G0-DEA: (**14**)]. The additional reaction step with

diethylamine resulted in higher yield (85%) compared to the direct reaction of the bromosilane with the sodium siloxide (30-50% yield). Addition of a new building block, phenyldimethylsilanol, to G0-DEA led to the following generation (G1-Ph) dendritic polysiloxanes. The synthesis of higher generations was carried out following the same sequence of bromination, amination and addition of the building blocks.

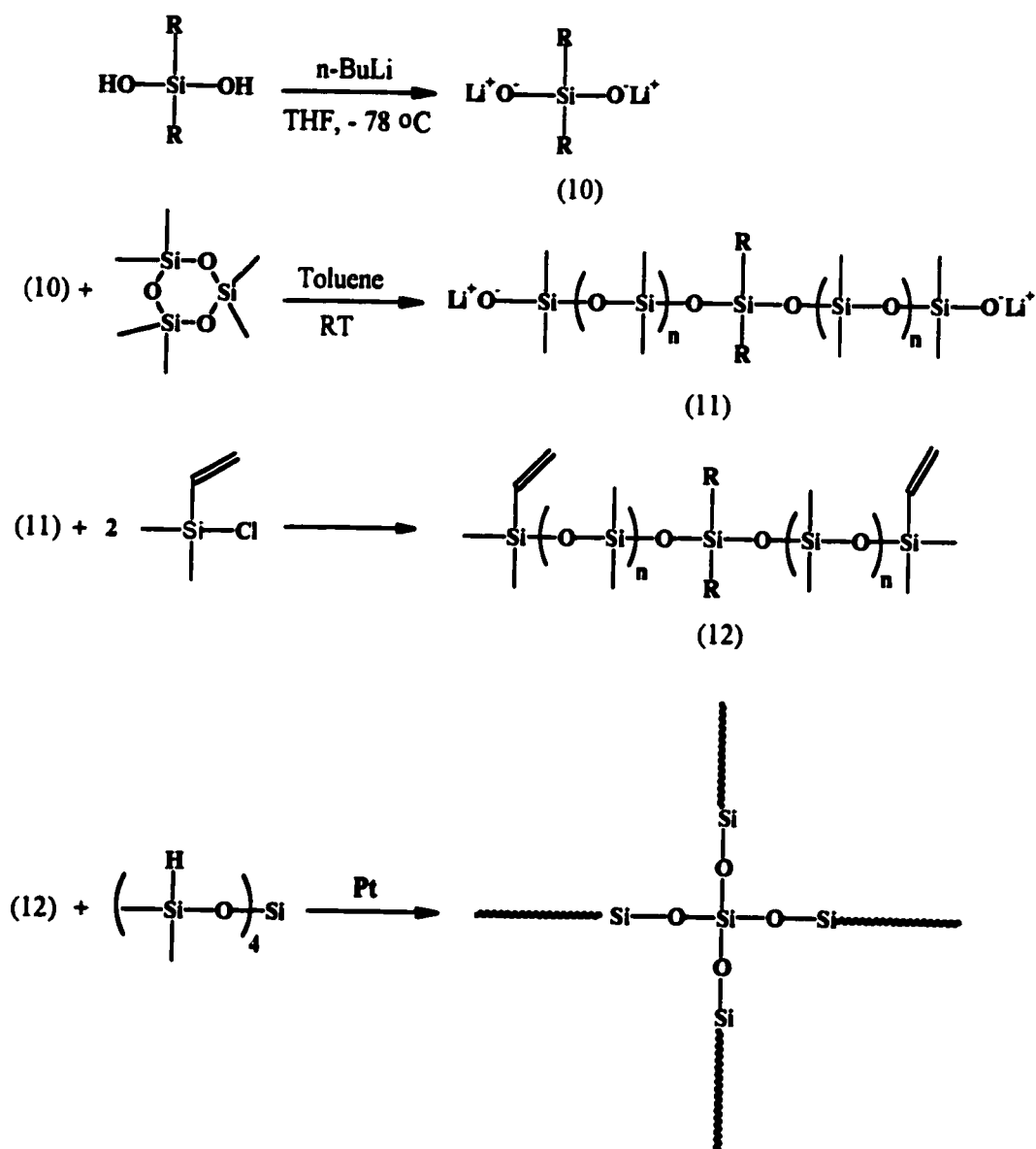


Figure 2.22. Preparation of networks based on PDMS segments

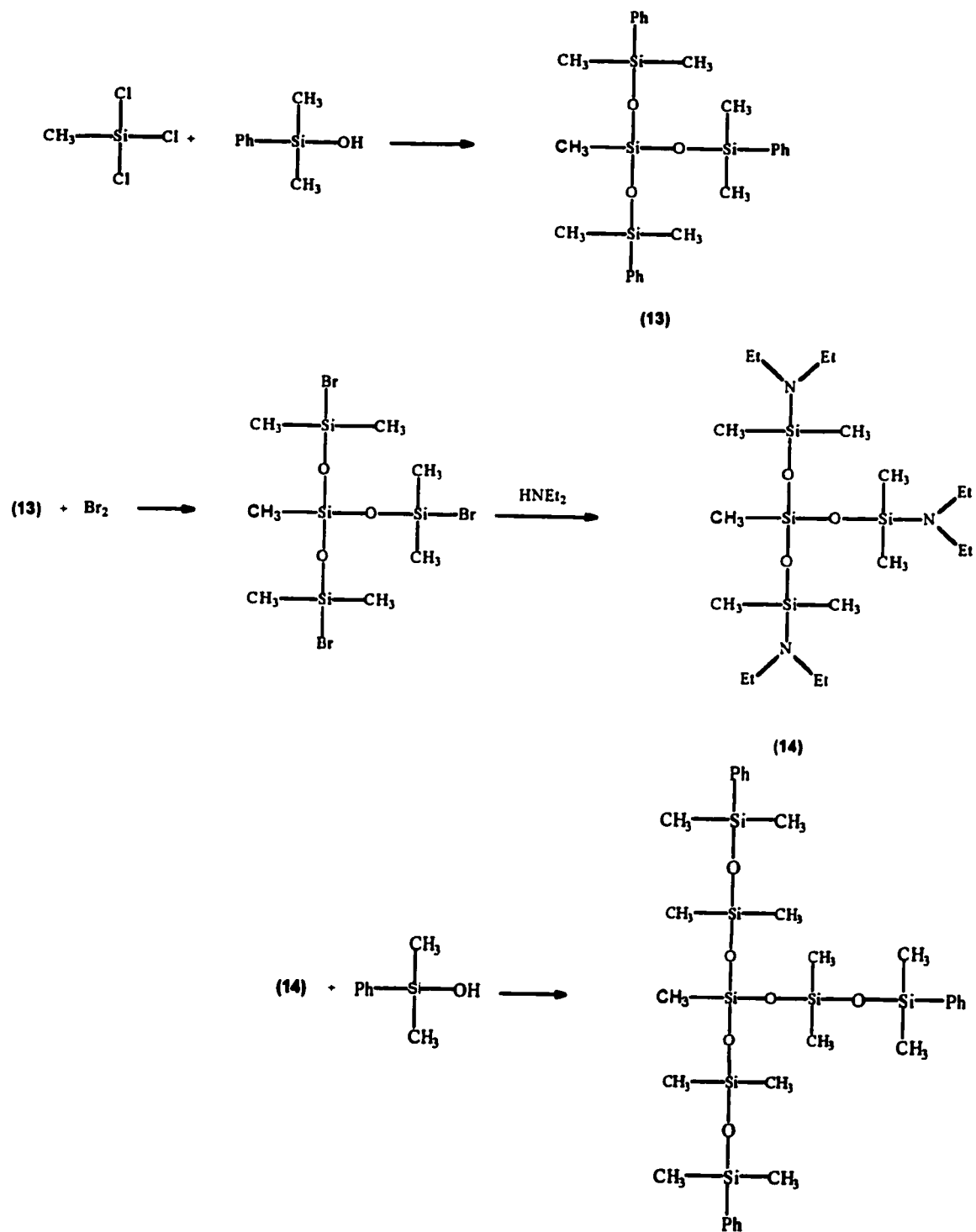


Figure 2.23. Preparation of a dendritic polysiloxane

2.4. Physical Characteristics of Polysiloxanes

The average *Si-O* bond length in polysiloxanes is longer than for typical *C-C* bonds, 1.64 Å compared to 1.53 Å, respectively (54). The *Si-O-Si* bond angle of 143° is also much larger than typical *C-C-C* bond angles (109°). Furthermore, the oxygen atoms within the polysiloxane backbone do not bear substituents. All these factors lead to very low rotational energy barriers for the *Si-O-Si* bond, which translates into a high extensibility, in addition to low glass transition (T_g) and melting (T_m) temperatures. Polysiloxanes exhibit some of the lowest glass transition temperatures known among polymers. For example, the T_g of polydimethylsiloxane (PDMS) and polymethylhydrosiloxane are -123 °C and -137 °C, respectively, resulting in exceptional elastomeric behavior even at low temperatures.

Polysiloxanes also exhibit high thermal stability, good resistance to oxidation and to UV radiation. The bond dissociation energy for the *Si-O* bond is high (460 kJ/mol) compared to typical *C-C* bonds (348 kJ/mol), making polysiloxanes suitable for high temperature applications where other polymers fail. For example, polydimethylsiloxane depolymerizes significantly after 20 hours at 200°C (93) to yield mainly hexamethylcyclotrisiloxane. The type of termination agent used in the polymerization plays a major role in the thermal stability of polysiloxanes. Polymers with trimethylsilyl end groups are more stable than the ones carrying silanol groups.

The polarization and the free rotation of the *Si-O* bond endow polysiloxanes with unique adhesive properties. Polar substrates such as water-based adhesives and glasses are attracted to the oxygen atoms within the polymer backbone. The organic substituents (for example the -CH₃ substituent in PDMS) are repelled by the substrate, and create a hydrophobic

barrier at the surface.

2.4.1. Surface Properties

With the exception of fluorinated polymers, polysiloxanes have the lowest surface energy of all polymers. This is due to the low intermolecular forces between the organic substituents, and to the flexibility of the silicone–oxygen bond that allows the backbone to rearrange easily. Consequently, polysiloxanes are highly suited for surface modification, pressure-sensitive adhesives and as water repellents.

2.5. Synthesis and Properties of Poly(ϵ -caprolactone)

Poly(ϵ -caprolactone) is of considerable interest since it is a biocompatible, biodegradable semicrystalline polymer. It is characterized by a low glass transition temperature and a high permeability, making it well-suited for use in biodegradable drug delivery systems. Another important advantage of poly(ϵ -caprolactone) is its compatibility with a variety of polymers, useful in the preparation of polymer blends.

2.5.1. Synthesis of Linear Poly(ϵ -caprolactone)

The anionic ring-opening polymerization of ϵ -caprolactone can be initiated by a wide range of nucleophiles (94). The lithium *tert*-butoxide-initiated anionic polymerization of ϵ -caprolactone at room temperature in THF was also reported (95). This study is particularly relevant to the present work, because it can serve as a model reaction for the initiation method used in this study. The anionic polymerization with a lithium counterion

is characterized by fast propagation, and full conversion is reached within a few minutes. The molecular weight distribution of poly(ϵ -caprolactone) prepared under these conditions is broad, however, due to the occurrence of intermolecular and intramolecular transesterification reactions (96). These side reactions are described in Figure 2.24. The intermolecular transesterification reaction leads to chain scission and transfer of the propagating center to the cleaved chain. The intramolecular transesterification reaction results in depolymerization and the formation of cyclic oligomeric products through a backbiting mechanism.

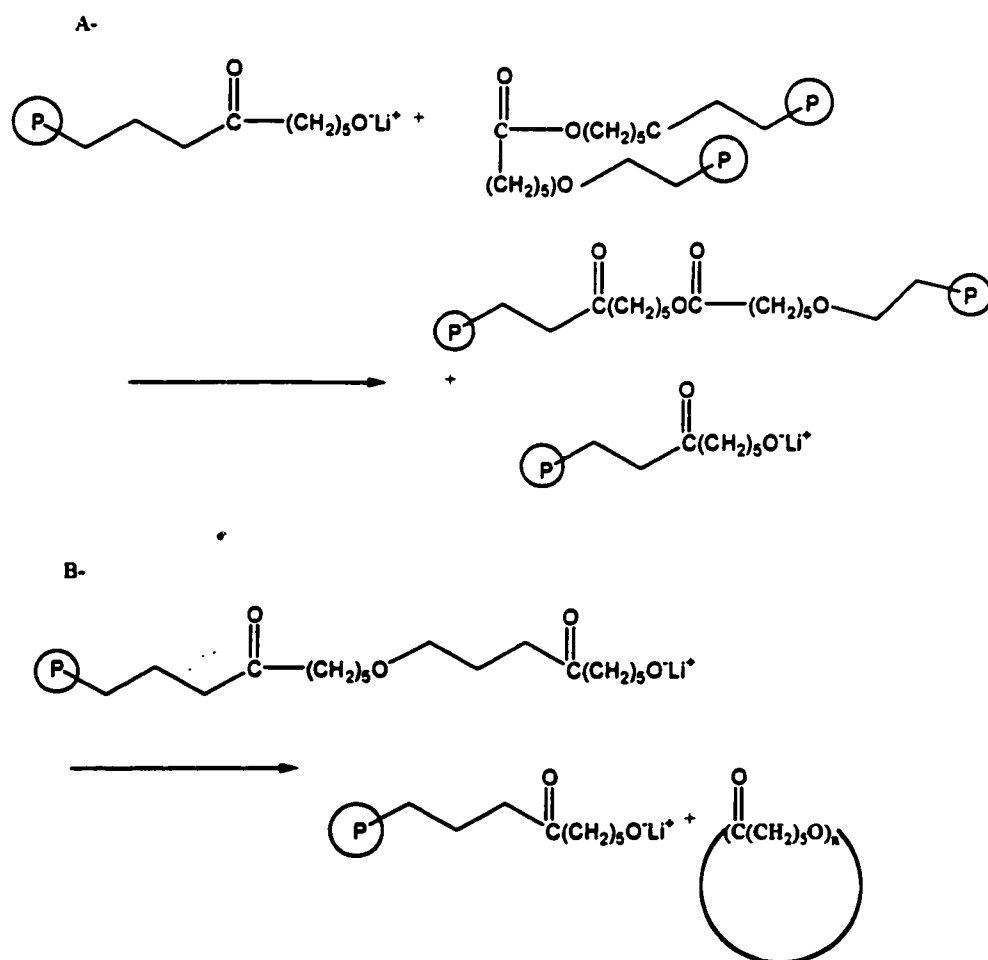


Figure 2.24. Intermolecular (A) and intramolecular (B) transesterification in ϵ -caprolactone polymerization. (P) represents the polymer chains

The side reactions described can be avoided, and a narrow molecular weight distribution obtained if the ring-opening polymerization of ϵ -caprolactone is carried out using coordination catalysts such as alkylaluminum compounds. For example, $(\text{CH}_3\text{CH}_2)_2\text{AlOCH}_3$ in THF at room temperature yields living polymers with a narrow molecular weight distribution ($M_w/M_n=1.03-1.13$) without cyclic oligomer formation (96).

2.5.2. Branched Poly(ϵ -caprolactone)s

Star-branched poly(ϵ -caprolactone)s were synthesized using polyol molecules such as erythritol, xylitol, and sorbitol as polyfunctional initiators for the ring-opening polymerization of ϵ -caprolactone. These alcohols bear 4, 5 and 6 reactive hydroxyl groups, respectively. The polymerizations were carried out in the bulk at 140°C in the presence of stannous octoate (97). The molecular weight distribution of the polymers was narrow initially, but M_w/M_n increased to 1.8-1.9 at higher conversions.

The synthesis of well-defined hyperbranched aliphatic polyesters based on ϵ -caprolactone was also reported (98). Ring opening polymerization was first initiated with benzyl alcohol in combination with aluminum isopropoxide or stannous octoate, to give hydroxyl-terminated polycaprolactone chains (Figure 2.25). After coupling of the hydroxyl end group with a dibenzylidene ketal unit, catalytic hydrogenation was used to cleave the benzyl ether and ketal functionalities and obtain an AB_2 macromer. The hyperbranched polyester was prepared by the self-condensation of the macromer.

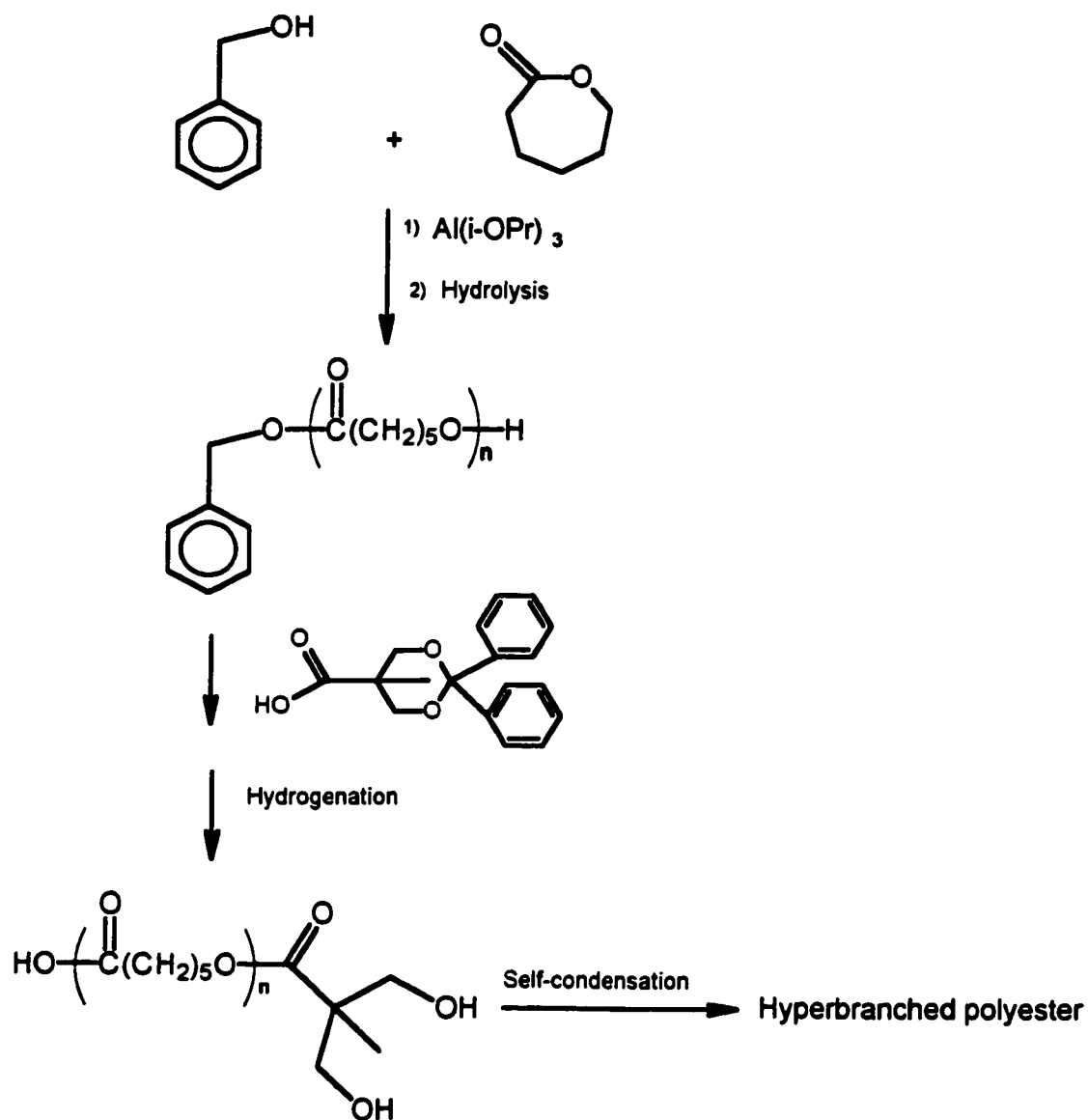


Figure 2.25. Synthesis of hyperbranched polyesters

2.6. References

1. Rempp, P. F., Lutz, P. J. In *Comprehensive Polymer Science*; Bevington, J. C., Ed.; Wiley: New York, 1989; Vol. 4, Chapter 12.
2. Roovers, J. E. L.; Bywater, S. *Macromolecules* **1974**, *7*, 443.
3. Hadjichristidis, N.; Roovers, J. E. L. *J. Polym. Sci.* **1974**, *12*, 2521.

4. Hadjichristidis, N.; Guyot, A.; Fetters, L. J. *Macromolecules* **1978**, *11*, 668.
5. Grest, G. S.; Fetters, L. J.; Huang, J. S. *Adv. Chem. Phys.* **1996**, *94*, 67.
6. Klein, J.; Fletcher, D. *Nature* **1983**, *304*, 526.
7. Doi, M.; Edwards, S. F. *The Theory of Polymer Dynamics*; Clarendon : Oxford, 1986.
8. Klein, J.; Fletcher, D.; Fetters, L. J. *J. Chem. Soc. Faraday Symp.* **1983**, *18*, 159.
9. Graessley, W. W. *Acc. Chem. Res.* **1977**, *19*, 332.
10. Graessley, W. W.; Massuda, T.; Roovers, J. E. L.; Hadjichristidis, N. *Macromolecules* **1976**, *9*, 127.
11. Roovers, J.; Graessley, W. W. *Macromolecules* **1981**, *14*, 766.
12. Masuda, T.; Ohta, Y.; Onogi, S. *Macromolecules* **1971**, *4*, 763.
13. Hawker, C.; Fréchet, J. M. J. *J. Chem. Soc., Perkin Trans.* **1992**, *1*, 2459.
14. Hawker, C.; Fréchet, J. M. J. *J. Am. Chem. Soc.* **1991**, *113*, 4583.
15. Kim, Y. H.; Webster, O. W. *Macromolecules* **1992**, *25*, 5561.
16. Tomalia, D. A.; Naylor, A. M.; Goddard, W. A. III *Angew. Chem. Int. Ed. Engl.* **1990**, *29*, 138.
17. Sahota, H. S.; Llyold, P. M.; Yeates, S. G.; Derrick, P. J.; Taylor, P. C.; Haddleton, D. M. *J. Chem. Soc., Chem. Commun.* **1994**, 2445.
18. Mourey, T. H.; Turner, S. R.; Rubinstein, M.; Fréchet, J. M. J.; Wooley, K. L. *Macromolecules* **1992**, *25*, 2401.
19. Hester, R. D.; Mitchell, P. H. *J. Polym. Sci., Polym. Chem. Ed.* **1980**, *18*, 1729.
20. Tomalia, D. A.; Baker, H.; Dewald, J.; Hall, M.; Kallos, G.; Martin, S.; Rock, J.; Ryder, J.; Smith, P. *Polym. J.* **1985**, *17*, 117.

21. Wooley, K. L.; Hawker, C. J.; Pochan, J. M.; Fréchet, J. M. J. *Macromolecules* **1993**, *26*, 1514.
22. Kim, Y. H.; Beckerbauer, R. *Macromolecules* **1994**, *27*, 1968.
23. Hawker, C. J.; Farrington, P. J.; Mackay, M. E.; Wooley, K. L.; Fréchet, J. M. J. *J. Am. Chem. Soc.* **1995**, *117*, 4409.
24. Dvornic, P. R.; Uppuluri, S.; Tomalia, D. A. *Polym. Mater. Sci. Eng.* **1995**, *73*, 131.
25. Gauthier, M.; Möller, M. *Macromolecules* **1991**, *24*, 4548.
26. Tomalia, D. A.; Hedstrand, D. M.; Ferritto, M. S. *Macromolecules* **1991**, *24*, 1435.
27. Gauthier, M.; Tichagwa, L.; Downey, J. S.; Gao, S. *Macromolecules* **1996**, *29*, 519.
28. Gauthier, M.; Li, W.; Tichagwa, L. *Polymer* **1997**, *38*, 6363.
29. Sheiko, S. S.; Gauthier, M.; Möller, M. *Macromolecules* **1997**, *30*, 2343.
30. Hempenius, M. A.; Zoetelief, W. F.; Gauthier, M.; Möller, M. *Macromolecules* **1998**, *31*, 2299.
31. Datta, S., Lohse, D. J. *Polymeric Compatibilizers Uses and Benefits in Polymer Blends*; Hanser: New York, 1996.
32. Utracki, L. A. *Polymer Alloys and Blends Thermodynamics and Rheology*; Hanser: New York, 1990.
33. Folkes, M. J.; Hope, P. S. *Polymer Blends and Alloys*; Chapman & Hall: New York, 1993.
34. Manson, J. A.; Sperling, L. H. *Polymer Blends and Composites*; Plenum: New York, 1976, Chapter 9.
35. Robeson, L. M. *Polym. Eng. Sci.* **1984**, *24*, 587.
36. Rappaport, M.; Kline, C. F. *Plast. Eng.* **1985**, *85*, 33.

37. Paul, D. R.; Barlow, J. W. In *Polymer Compatibility and Incompatibility*; Solc, K., Ed., MMI Press Symposium Series; Harwood: New York, 1980; Vol. 2, Chapter 1.
38. Sperling, L. S. *Polymer Multicomponent Materials: An Introduction*; Wiley: New York, 1997.
39. Fayt, R.; Jérôme, R.; Teyssié, P. In *Multiphase Polymers: Blends and Ionomers*; Utracki, L. A. and Weiss, R. A., Eds.; ACS Symposium Series 395; American Chemical Society: Washington, 1989; Chapter 2.
40. Paul, D. R. R. In *Polymer Blends*; Paul, D.; Newman, S., Eds.; Academic: New York, 1978; Vol. 2, Chapter 12.
41. Kammer, H. W.; Kressler, J. K.; Kummerloewe, C. *Adv. Polym. Sci.* **1993**, *106*, 31.
42. Smith, K. L.; Winslow, A. E.; Peterson, D. E. *Ind. Eng. Chem.* **1959**, *51*, 1361.
43. Olabishi, O. *Macromolecules* **1975**, *8*, 316.
44. Prud'homme, R. E. *Polym. Eng. Sci.* **1982**, *22*, 90.
45. Cowie, J. M. G. In *Encyclopedia of Polymer Science and Engineering*, 2nd Ed.; Wiley: New York, 1985; Supplement Volume, page 455.
46. Chai, Z.; Sun, R.; Li, S.; Karasz, F. E. *Macromolecules* **1995**, *28*, 1126.
47. Factor, B. J.; Russell, T. P.; Smith, B. A.; Fetters, L. J.; Bauer, B. J.; Han, C. C. *Macromolecules* **1990**, *23*, 4452.
48. Mandelkern, L.; Alamo, R. G.; Wignall, G. D.; Stehling, F. C. *Trends Polym. Sci.* **1996**, *4*, 377.
49. Yethiraj, A. Kumar, S.; Hariharan, A.; Schweizer, K. S. *J. Chem. Phys.* **1994**, *100*, 4691.
50. Sikka, M.; Singh, N.; Karim, A.; Bates, F. S.; Satija, S. K.; Majkrzak, C. F. *Phys. Rev.*

- Lett.* **1993**, *70*, 307.
51. Bates, F. S.; Rosedale, J. H.; Bair, H. E.; Russell, T. P. *Macromolecules* **1989**, *22*, 2557.
52. Stewart, C. W. *J. Rheol.* **1993**, *37*, 499.
53. Chan, C; Nixon, A. Venkatraman, S. *J. Rheol.* **1992**, *36*, 807.
54. Clarson, S.J.; Semlyen, J. A. *Siloxane Polymers*; Prentice Hall: Englewood Cliffs, 1993.
55. Jones, R. G.; *Silicon-Containing Polymers*; The Royal Society of Chemistry: Cambridge, 1995.
56. Sheats, J. Jr.; Carraher, C. E.; Zeldin, M.; Currell, B.; Pittman, Jr. *Inorganic and Metal Containing Polymeric Materials*; Plenum: New York, 1991.
57. Allock, H.; Lampe, F.W. In *Contemporary Polymer Chemistry*; 2nd Ed.; Prentice Hall: Englewood Cliffs, 1990, Chapter 24.
58. Mark, J. E.; Allcock, H. R.; West R. *Inorganic Polymers*; Prentice Hall: Englewood Cliffs, 1992.
59. Kendrick, T. C.; Parbhoo, B. M.; White, J. W. In *Comprehensive Polymer Science*; Bevington, J. C., Ed.; Wiley: New York, 1989; Vol. 4, Chapter 25.
60. Godovsky, Y. K.; Papkov, V.S. *Makromol. Chem., Macromol Symp.* **1986**, *4*, 71.
61. Arkles, B.; Crosby, J. In *Silicon-Based Polymer Science: A comprehensive Resource*; Zeigler, J. M. and Gordon, F. W., Eds.; Advances in Chemistry Series 224; American Chemical Society: Washington, 1990; pp 181-198.
62. Burger, C.; Kreuzer, F. H. In *Silicon in Polymer Synthesis*; Kricheldorf, H. R., Ed.; Springer: Berlin, 1996.

63. Sigwalt, P.; Stannet, V. *Makromol. Chem., Macromol. Symp.* **1990**, *32*, 217.
64. Wright, P. V. In *Ring Opening Polymerization*; Ivin, K.J. and Saegusa, T., Eds.; Elsevier: London, 1984; Vol. 2, Chapter 14.
65. Lee, C. L.; Johannson, O.K. *J. Polym. Sci., Polym. Chem. Ed.* **1976**, *14*, 729.
66. Lee, C. L.; Johannson, O.K. *J. Polym. Sci., Polym. Chem. Ed.* **1976**, *14*, 743.
67. Maschke, U.; Wagner, T. *Makromol. Chem.* **1992**, *193*, 2453.
68. Morton, M.; Bostick, E. E. *J. Polym. Sci., Polym. Chem. Ed.* **1964**, *2*, 523.
69. Lestel, L.; Boileau, S. *Makromol. Chem., Macromol. Symp.* **1991**, *47*, 293.
70. Boileau, S. In *Ring Opening Polymerization: Kinetics Mechanism and Synthesis*; McGrath, J. E., Ed.; ACS Symposium series 286; American Chemical Society: Washington, 1985; pp 23-35.
71. Boileau, S.; Hemy, P.; Kaempf, B.; Schué, F.; Viguier, M. *J. Polym. Sci.* **1974**, *12*, 217.
72. Boileau, S.; Hemy, P.; Kaempf, B.; Schué, F.; Lehn, J. M. *J. Polym. Sci.* **1974**, *12*, 203.
73. Kawakami, Y. *Progr. Polym. Sci.* **1994**, *19*, 203.
74. Kawakami, Y.; Murthy, R. A. N.; Yamashita Y. *Makromol. Chem.* **1984**, *185*, 9.
75. Kawakami, Y.; Miki, Y.; Tsuda, T.; Murthy, R. A. N.; Yamashita, Y. *Polym. J.* **1982**, *14*, 913.
76. Owen, M. J.; Thompson, J. *Br. Polym. J.* **1972**, *4*, 297.
77. Kawakami, Y.; Yamashita Y. In *Ring Opening Polymerization: Kinetics Mechanism and Synthesis*; McGrath, J. E., Ed.; ACS Symposium series 286; American Chemical Society: Washington, 1985; pp 245-261.
78. Cameron, G. G.; Chisholm, M. S. *Polymer* **1985**, *26*, 137.

79. Smith, S. D.; York, G.; Dwight, D.W. McGrath, J. E. In *Chemical Reactions on Polymers*; Benham, J. L.; Kinstle, J. F., Eds.; ACS Symposium series 364; American Chemical Society: , Washington, 1988; pp 85-96.
80. Nagase, Y.; Naruse, A. Matsui, K. *Polymer* **1989**, *60*, 1931.
81. Nagase, Y.; Mori, S.; Matsui, K.; Uchikuda, M. *J. Polym. Sci., Polym. Chem. Ed.* **1988**, *26*, 3131.
82. Lefebvre, P. M.; Jérôme, R.; Teyssié, P. *Macromolecules* **1977**, *10*, 871.
83. Dickstein, W. H.; Lillya, C. P. *Macromolecules* **1989**, *22*, 3886.
84. Bontems, S. L.; Stein, J.; Zumburum, M. A. *J. Polym. Sci., Part A* **1993**, *31*, 2697.
85. Mark, J. E.; Sullivan, J. L. *J. Chem. Phys.* **1977**, *66*, 1006.
86. Mark, J. E. *Makromol. Chem. Suppl.* **1979**, *2*, 87.
87. Mark, J. E.; Rahalkar, R. R.; Sullivan, J. L. *J. Chem. Phys.* **1979**, *70*, 1794.
88. Gottlieb, M.; Makosko, C.W.; Benjamin, G.S.; Meyers, K.O.; Merrill, E.W. *Macromolecules* **1981**, *14*, 1039.
89. Gnanou, Y. and Rempp, P. *Makromol. Chem.* **1988**, *189*,1997.
90. Dvornic, P. R.; De Leuze-Jallouli, A. M.; Owens, M. J.; Perz, S. V. *Polym. Prepr.* **1998**, *39(1)*, 473.
91. Morikawa, A.; Kakimoto, M.; Imai, Y. *Macromolecules* **1991**, *24*, 3469.
92. Morikawa, A.; Kakimoto, M.; Imai, Y. *Macromolecules* **1992**, *25*, 3247.
93. Grassi, N.; MacFarlane, I.G. *Eur. Polym. J.* **1978**, *14*, 875.
94. Löfgren, A.; Albertsson, A.; Dubois, P.; Jérôme, R. *J. Macromol. Sci.-Rev. Macromol. Chem. Phys.* **1995**, *C35*, 379.
95. Morton, M.; Wu, M. In *Ring Opening Polymerization: Kinetics Mechanism and*

- Synthesis*; McGrath, J. E., Ed.; ACS Symposium Series 286; American Chemical Society: Washington, 1985; pp. 175-182.
96. Duda, A.; Florjanczyk, Z.; Hofman, A.; Słomkowski, S.; Penczek, S. *Macromolecules* **1990**, *23*, 1640.
97. Schindler, A.; Hibionada, Y. M.; Pitt, C. G. *J. Polym. Sci., Polym. Chem. Ed.* **1982**, *20*, 319.
98. Trollsas, M.; Hedrick, J. L.; Mecerreyes, D.; Dubois, Ph.; Jérôme, R. *Polym. Mater. Sec. Eng.* **1997**, *77*, 208.

Chapter 3: Arborescent Polystyrenes as Melt Viscosity Modifiers for Linear Polymers

3.1. Introduction

Polymer blending is a very active field of polymer science. It is often possible to tailor the composition of polymer mixtures in such a way as to control the properties of the final product. However, most of the studies in this area have focused on blends of linear polymers of different chemical compositions (1-4). Few investigations have been dedicated to blends of linear and branched polymers. In order to systematically assess the effect of branching on the physical properties of polymers blends, materials are necessary where the degree of branching and branch molecular weight are well-defined.

The compact structure of branched polymers leads to properties in solution and in the molten state that are very different from linear polymers (5-12). For example, the intrinsic viscosity of arborescent polystyrenes is much lower than for linear polymers of comparable molecular weight, due to their smaller hydrodynamic volume (7). In the molten state, arborescent polystyrenes have viscosities up to 10^4 times lower than linear polymers of comparable molecular weight (12).

The influence of chain architecture on the properties of blends incorporating branched and linear polymers has been the object of very few investigations. Segregation of the branched component to the surface of the blend is predicted in theoretical studies (13,14). Phase separation is also expected to be enhanced at higher branching densities and higher concentrations of the branched component.

In a study more directly relevant to this work, the addition of highly branched polyphenylene dendrimers to a polystyrene matrix led to significant decreases in melt viscosity (15). For example, a 50% reduction in melt viscosity is reported at 180°C for a blend of polystyrene containing 5% w/w of the hyperbranched material. The decrease becomes more significant at higher temperatures and higher shear rates.

Arborescent polymers are highly branched dendritic macromolecules prepared by sequences of functionalization and anionic grafting reactions (16-18). The synthetic procedure used leads to a geometric increase in molecular weight and branching functionality for each reaction cycle (generation), while precise control over the branching density and side chain molecular weight is maintained. It is thus possible to prepare highly branched polymers with a very high molecular weight in a few synthetic steps. The preparation of arborescent polystyrenes involves the chloromethylation of linear polystyrene and coupling with living polystyryl anions to yield a comb-branched polystyrene, designated as generation G0. Repetition of the chloromethylation and grafting reactions with the comb polymer yields subsequent generations of arborescent polystyrenes (G1, G2, etc.). These materials should be useful to assess the effects of branching in blends with linear polymers.

The results of an investigation of the effect of arborescent polystyrenes on the melt viscosity of blends with linear polymers are presented in this Chapter. The influence of branch length, branching functionality, and the concentration of arborescent polystyrene are investigated. To examine the role of the polymer matrix composition, blends based on commercial linear polystyrene (PS) and poly(methyl methacrylate) (PMMA) samples are compared. While miscibility is not necessarily expected for blends

of linear and arborescent polystyrene, the polymers should at least display some degree of compatibility, because of their identical chemical composition. The blends of PMMA and arborescent polystyrene are intrinsically immiscible and should exhibit phase separation.

3.2. Experimental Procedures

3.2.1. Preparation of Blends

Blends of the linear polymers and arborescent polystyrenes with different side chain molecular weights and branching functionalities were investigated. The commercial polystyrene sample used has a number-average molecular weight $M_n = 1.55 \times 10^5$ g/mol and a weight-average molecular weight $M_w = 3.55 \times 10^5$ g/mol, and the poly(methyl methacrylate) sample has $M_n = 1.96 \times 10^5$ g/mol and $M_w = 2.90 \times 10^5$ g/mol. The M_w and the branching functionality (f_w) of the arborescent polystyrenes used in the study are listed in Table 3.1. These materials were prepared and characterized as previously described (16).

The two components were dissolved in benzene (100 mL, BDH) at a concentration of 5% (w/v) and stirred for 24 hours. The solvent was then removed by freeze-drying under vacuum. The polymer blends were dried further in a vacuum oven for 48 hours at room temperature, at 80°C for three days, and pressed at 180°C into discs (ca. 25 mm × 2.3 mm) with a hydraulic press.

3.2.2. Characterization

The viscoelastic properties of the pure linear polymers and of the blends were

measured on a Rheometrics RMS 605 Mechanical Spectrometer. A parallel plate geometry with a diameter of 25 mm and a gap range of 1.8-2.0 mm was used for the measurements. All tests were performed under nitrogen atmosphere to prevent sample degradation. The samples were first equilibrated at the high temperature limit (250°C in most cases) for twenty minutes. The measurements were initiated while ramping the temperature downward at a rate of 1°C per minute. Temperature sweep (time cure sweep) measurements were carried out at a frequency of 1 Hz and 10% strain.

Table 3.1. Characteristics of the arborescent polystyrenes used

Arborescent Polymer	Branch Molecular Weight, M_w^{br} /g \times mol $^{-1}$	Total Molecular Weight, M_w /g \times mol $^{-1}$	Branching Functionality f_w
G1(5K)	4.6×10^3	8.7×10^5	180
G2(5K)	4.2×10^3	1.3×10^7	2 800
G3(5K)	4.4×10^3	9.0×10^7	18 000
G1(30K)	2.7×10^4	9.0×10^6	310
G2(30K)	2.7×10^4	1.0×10^8	4 200
G3(30K)	2.7×10^4	5.0×10^8	17 000

3.3. Results and Discussion

The arborescent polymers used in this study have a structure comparable to star-branched molecules, except for their much higher branching functionality ranging from 180 to 18 000. The length of the side chains of the arborescent polymers is clearly below (5 000 g/mol) or comparable (30 000 g/mol) to the critical molecular weight for entanglement formation (M_c) of polystyrene. Therefore, the ability of arborescent polystyrene molecules to entangle with each other is expected to be quite limited.

A recent investigation (19) demonstrated major differences in the film formation

behavior of first-generation (G1) and third-generation (G3) arborescent polystyrenes. Thin films of the third-generation polymers, when characterized by atomic force microscopy (AFM), exhibited long range lattice-like ordering, in analogy to hard latex particles of very uniform size. In contrast, films of the first generation polymer only displayed a grainy, irregular structure, showing that lower generation arborescent polymers are easily interpenetrable. This seems reasonable, considering the roughly 100-fold difference in branching functionality between the G1 and G3 polymers.

3.3.1. Polystyrene Matrix

Blends of arborescent and linear polystyrene are expected to be at least compatible, if not miscible, because of their identical chemical composition. Two distinct mechanisms, namely chain entanglement and chain entrapment effects, can be identified as potentially affecting the viscosity of these blends. Entanglement formation with the linear polymer chains should be a function of the structure of the arborescent molecules. The G1 polymers, because of their high interpenetrability (or open structure), are expected to entangle with the linear polystyrene matrix efficiently, thus hindering the flow of the individual molecules. For blends incorporating the higher generation polymers (G2 and above), it is the physical chain entrapment mechanism discussed in Section 2.1.3.2 that is expected to have the most influence on melt viscosity.

Rheological measurements are generally considered to be reproducible to within ± 5 -10%. For comparison purposes, error bars corresponding to a 10% uncertainty have been included for the curve corresponding to the pure linear polymer (forming the matrix in the blends) on all viscosity-temperature plots.

3.3.1.1. Effect of Branched Polymer Content

The temperature dependence of the complex dynamic melt viscosity (η^*) for blends of linear polystyrene and either 5% or 10% w/w G1 arborescent polystyrene with a side chain $M_w \approx 5\,000$ g/mol is compared with that of pure polystyrene in Figure 3.1. Significant differences in melt viscosity are only observed in the high-temperature range, i.e., the flow region. The addition of arborescent polystyrene to linear polystyrene leads to melt strengthening at high temperature, and the increase in η^* is more pronounced at higher branched polymer contents in the blend.

The fact that the melt viscosity only increases noticeably in the high temperature region can be rationalized as follows. The G1(5K) arborescent polystyrene molecules are characterized by a high interpenetrability (19) and a highly branched structure. When these molecules are dispersed in the linear polystyrene matrix, they should efficiently entangle with the matrix and cause a slight increase in the average entanglement level of the chains. These additional entanglements may not be sufficient to increase the viscosity at lower temperatures, however, because the high viscosity of the matrix polymer dominates in that temperature range. As the temperature increases and the viscosity of the matrix polymer decreases, the additional contribution to η^* from arborescent-linear polymer entanglements becomes more significant and flow is hindered. A higher concentration of branched polymer in the blend should lead to the formation of more entanglements, and thus a higher viscosity in the flow region, as experimentally observed.

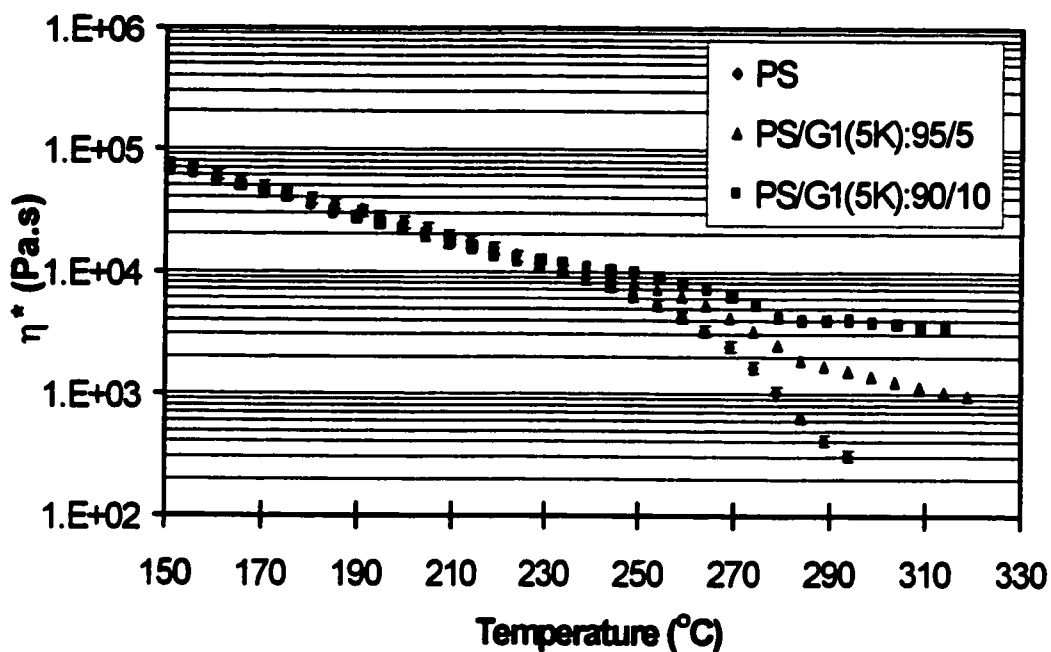


Figure 3.1. Effect of concentration of arborescent polystyrenes on the melt viscosity of linear polystyrene

3.3.1.2. Effect of Branch Length

The complex melt viscosity-temperature curves for polystyrene containing 5% w/w G3 polymers with either short ($M_w \approx 5\,000$ g/mol, 5K) or long ($M_w \approx 30\,000$ g/mol, 30K) branches are compared with the curve obtained for linear polystyrene in Figure 3.2. The G3(30K) arborescent polymer has no influence on the melt viscosity of the polystyrene matrix, whereas the PS/G3(5K) blend displays melt strengthening in the high-temperature range. It was mentioned in Section 2.1.3.2 that G2 arborescent polymers are characterized by enhanced zero-shear viscosity relative to lower generation polymers (12). The viscosity enhancement, most pronounced for polymers with short side chains (higher branching densities), was explained in terms of physical chain entrapment

occurring when the molecules are forced to interpenetrate. Likewise in the present case, the ability of the G3(5K) polymer to physically entrap linear polymer chains in its structure should be more pronounced than for the G3(30K) polymer. If both arborescent polymer samples are blended at the same concentration with linear polystyrene, sample G3(5K) is therefore expected to affect η^* most noticeably.

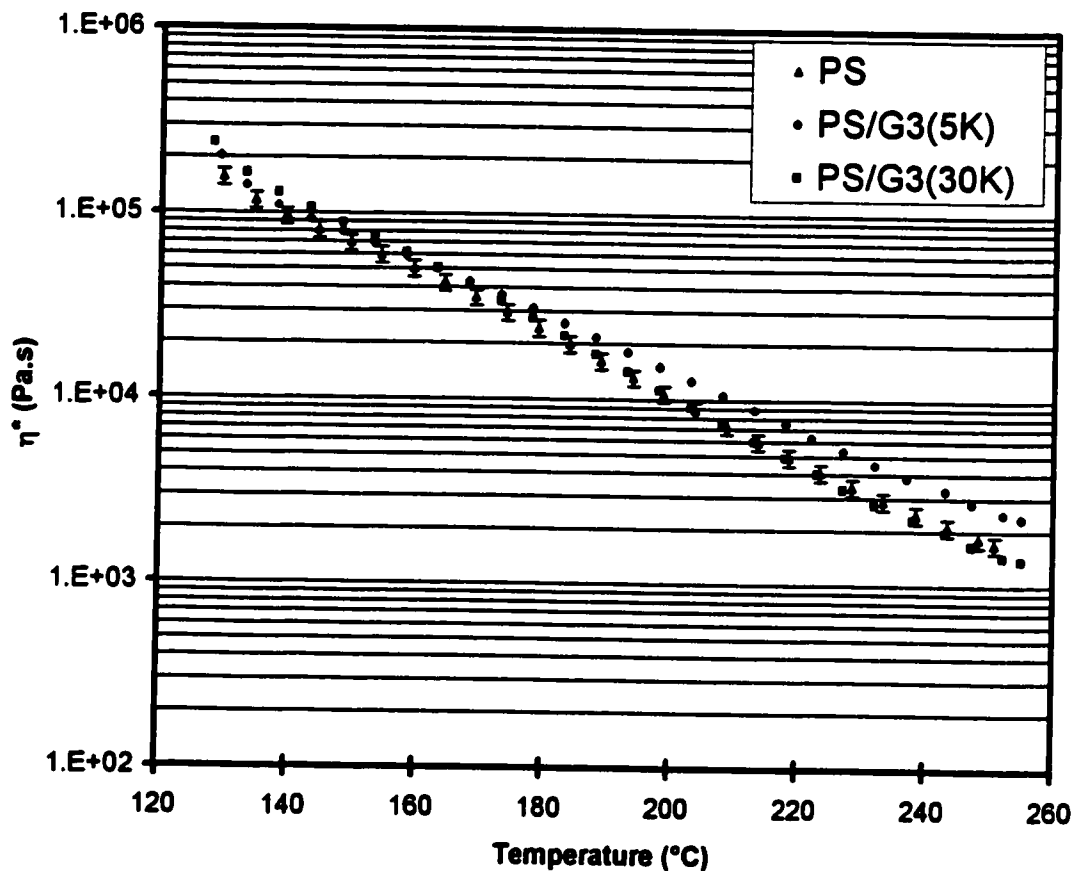


Figure 3.2. Effect of branch length of arborescent polystyrenes on the melt viscosity of polystyrene

3.3.1.3. Effect of Branching Functionality

The temperature dependence of the complex melt viscosity for linear polystyrene and for its blends with 5% w/w G1, G2, and G3 arborescent polystyrenes with

$M_w \approx 30\,000$ g/mol side chains are compared in Figure 3.3. Slight melt strengthening is observed for the G1 and G2 arborescent polystyrenes, but no significant effect is seen for the G3 additive. The behavior of the G3(30K) sample was explained in Section 3.3.1.2 in terms of reduced chain entrapment effects, due to its lower branching density. The G1(30K) and G2(30K) samples have a lower branching functionality than G3(30K) (Table 3.1). The AFM investigation of arborescent polymer film formation (19) discussed earlier showed that lower generation molecules are characterized by a greater interpenetrability. This should favor entanglement formation with the linear polymer matrix for the G1 and G2 polymers, to give the small increases in η^* observed.

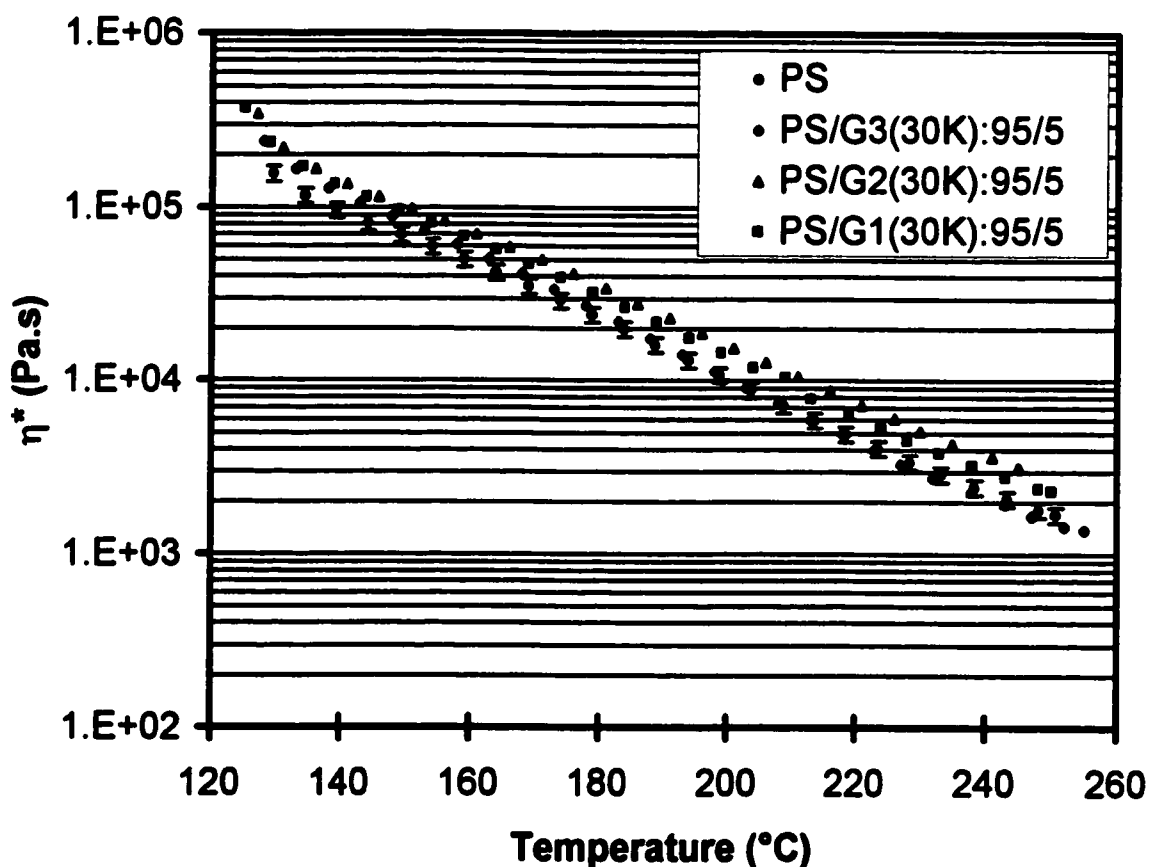


Figure 3.3. Effect of branching functionality of arborescent polystyrenes with long branches on the melt viscosity of polystyrene

For arborescent polymers with short branches ($M_w \approx 5\,000$ g/mol, Figure 3.4), melt strengthening is also observed. Considering the dense branched structure of these polymers (corresponding to about 10 side chains per backbone chain, or one branching point for every five repeat units), it seems that chain entrapment effects should have a dominant role in increasing the viscosity of the blends.

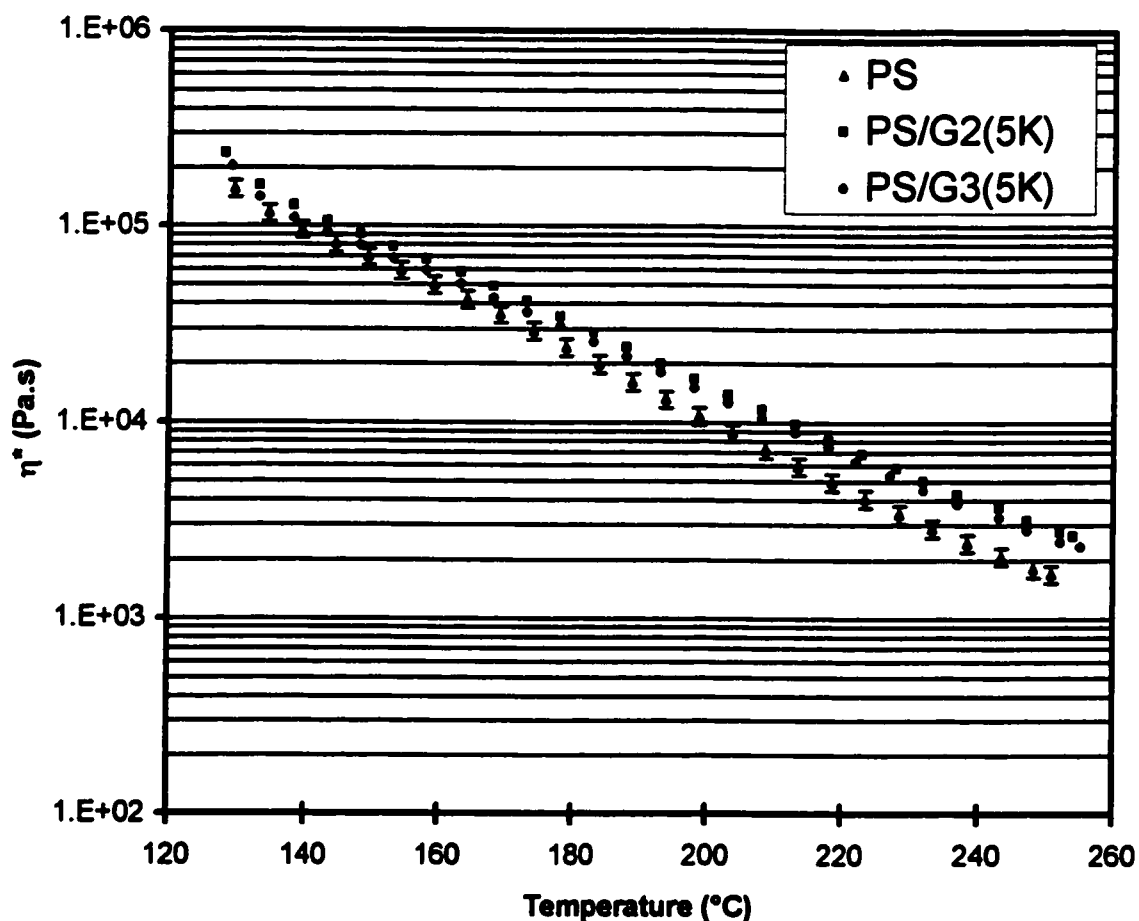


Figure 3.4. Effect of branching functionality of arborescent polystyrenes with short branches on the melt viscosity of polystyrene

3.3.2. Poly(methyl methacrylate) Matrix

Polystyrene and poly(methyl methacrylate) are intrinsically immiscible polymers, and phase separation is expected to occur. This is confirmed by the opaque appearance of the blend samples prepared. According to the Flory-Huggins theory, the free energy of mixing for a blend is given by the equation

$$\Delta G_{mix} = \Delta H_{mix} - T\Delta S_{mix} \quad (3.1)$$

The more positive the Gibbs free energy of mixing becomes, the more phase separation is favored. The free energy of mixing can be also expressed as a function of the interaction parameter χ , the volume fraction ϕ_i and the volume per molecule V_i of each component, the monomer segment volume V_r and the total sample volume V :

$$\frac{\Delta G_{mix}}{kTV} = \chi \frac{\phi_1\phi_2}{V_r} + \left(\frac{\phi_1}{V_1} \ln \phi_1 + \frac{\phi_2}{V_2} \ln \phi_2 \right) \quad (3.2)$$

The interaction parameter for linear PS and linear PMMA was reported to be 0.041 at 25°C, decreasing only slightly to 0.035 at 250°C (20). This leads to a significant positive contribution to ΔG_{mix} over the whole temperature range investigated.

The very high molecular weight (large molecular volume V_i) and branched structure of arborescent polymers are obvious factors contributing to phase separation in the PMMA/arborescent polystyrene blends. Linear polymers with a high molecular weight are invariably less miscible than those with a lower molecular weight, because their entropy contribution (term between brackets in Equation 3.2) to ΔG_{mix} is smaller. Arborescent polymers also have a lower entropy of mixing than linear polymers, because branching decreases the number of conformations accessible to the polymer chains. Phase separation is therefore expected to be most favored for the third-generation arborescent polymers, since they combine a very high branching functionality with an extremely high

molecular weight.

In a theoretical study on polymer blends (14) with one component stiffer than the other, it was shown that the stiffer component migrates preferentially to the surface. While the simulations used in the study were limited to chains with a degree of polymerization $N=10-100$, it was also pointed out that as the molecular weight increases, the segregation of the stiffer component is expected to become more pronounced. A stiffer structure results in weaker intermolecular interactions. The creation of a surface requires moving molecules from the bulk of the blend to the interface, and hence requires breaking intermolecular interactions. Since the arborescent polystyrene molecules are stiffer and more weakly interacting, they can move to the surface of the PMMA/arborescent polystyrene blends most easily. The investigation of Hempenius *et al.* (12) demonstrated that arborescent polystyrenes have a very low melt viscosity. The compact structure and low viscosity of arborescent polymers are expected to facilitate their migration (diffusion) to the surface of the blend. The viscosity measured in a rheometer under these conditions does not represent the bulk properties of the sample. It is rather an apparent viscosity due primarily to surface lubrication of the sample by the arborescent component.

Phase separation and migration can potentially occur at different steps of sample preparation and handling. Drying of the freeze-dried samples at 80°C should have no significant influence on the properties of the blends. This is because the polystyrene matrix ($T_g \approx 100^{\circ}\text{C}$) remains glassy at that temperature, effectively preventing demixing of the blend and the migration of the branched component. Sample molding (180°C), equilibration at 250°C and the measurements are all carried out well above the matrix T_g ,

and phase separation/migration may occur at each step. Considering that the melt viscosity of polymers decreases exponentially with temperature, it seems that sample molding should have the least influence on the observed properties. Phase separation and migration presumably occurred predominantly at higher temperatures (during sample equilibration and the measurements), when the viscosity was much lower.

3.3.2.1. Effect of Branched Polymer Content

The effect of varying the arborescent polymer concentration between 2.5 and 10% w/w on the melt viscosity of a blend of PMMA with an arborescent polystyrene containing side chains with $M_w \approx 30\,000$ g/mol [G3(30K)] is illustrated in Figure 3.5. The branched polymer concentration has little or no influence on the complex melt viscosity, and a 2- to 2.5-fold decrease in η^* is observed in all cases. The concentration independence of the decrease is consistent with a surface modification mechanism. This is because, depending on the thickness of the interface, very small amounts of arborescent polymer may suffice to coat the surface of the blend and lead to the surface lubrication effect observed. The concentration-independent decrease in η^* observed is very encouraging, since it suggests that a small amount of branched polymer may be sufficient to achieve a significant reduction in the melt viscosity of PMMA. Moreover, from a practical point of view, this implies not only lower costs for the branched polymer, but also that any potential deleterious effects of the additive on the mechanical properties of the polymer matrix due to phase separation should be less significant.

3.3.2.2. Effect of Branching Functionality

Two series of arborescent polystyrenes of generations G1-G3 and either 5 000 g/mol or 30 000 g/mol side chains were blended (5% w/w) with linear PMMA. The variation in the complex dynamic melt viscosity of PMMA blends containing arborescent polystyrene ($M_w \approx 30\ 000$ g/mol side chains) with temperature is illustrated in Figure 3.6. A decrease of up to 3-fold in η^* is observed over the temperature range investigated.

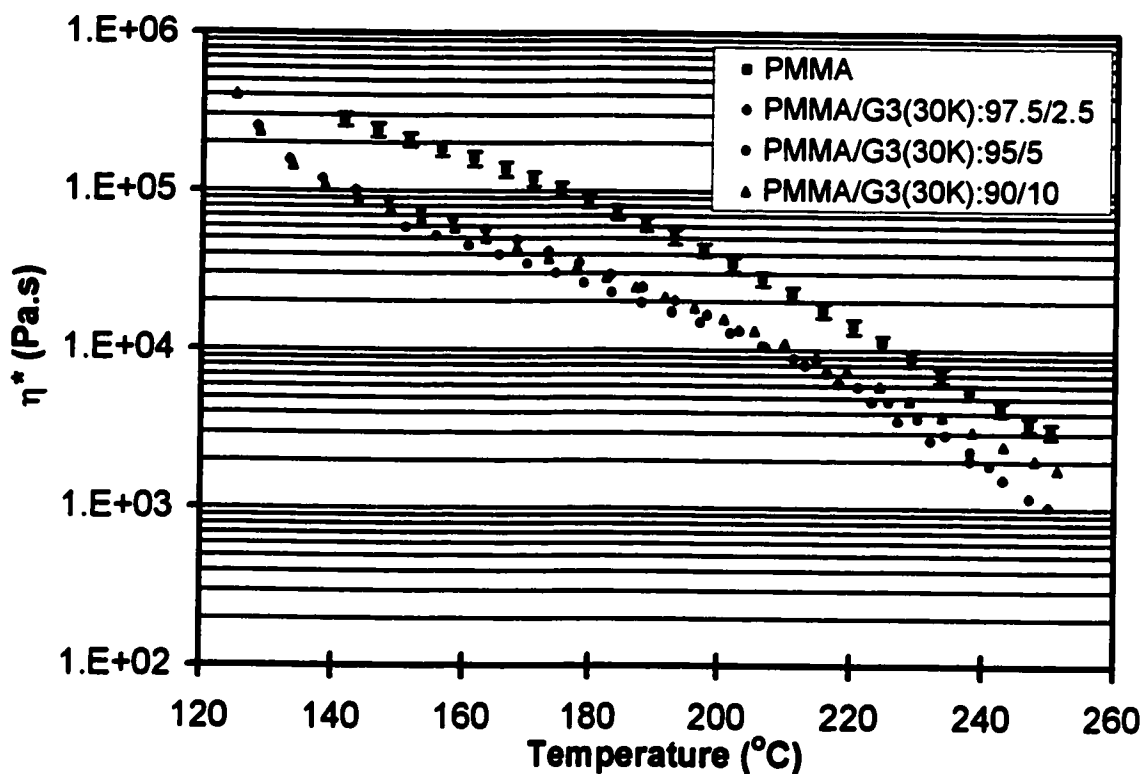


Figure 3.5. Effect of concentration of arborescent polystyrenes on the melt viscosity of PMMA

A decrease in melt viscosity is also observed for blends incorporating polymers with short branches ($M_w \approx 5\ 000$ g/mol, Figure 3.7), although the effect is not as pronounced as for samples with long branches. The large decreases observed for the polymers with 30 000 g/mol side chains can be explained at least in part by their much

higher molecular weight than the polymers with 5 000 g/mol side chains (Table 3.1). The molecular weight also increases with the generation number within a series, so a decrease is likewise expected. The blends based on G3 polymers in both series display the largest viscosity drop on Figures 3.6 and 3.7 as expected, although the differences observed among the different generation polymers remain small.

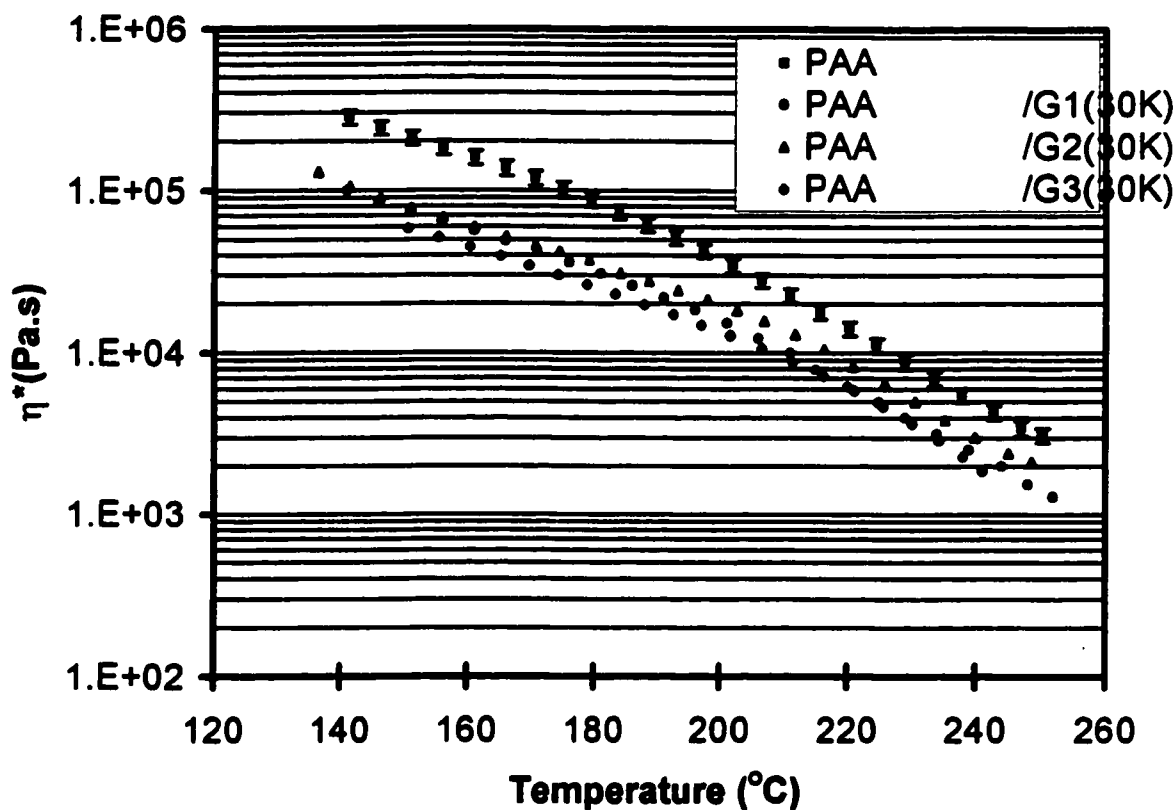


Figure 3.6. Effect of branching functionality of arborescent polystyrenes with long branches on the melt viscosity of PMMA

3.4. Conclusions

This study demonstrates that arborescent polystyrenes, when blended in small amounts with linear polystyrene and poly(methyl methacrylate), can have a significant

influence on melt viscosity. Arborescent polymers with a low branching functionality produce melt strengthening effects in a polystyrene matrix at high temperatures. The increase in melt viscosity is proportional to the amount of arborescent polymer added. For a PMMA matrix, all blends display a decrease in melt viscosity over the whole temperature range studied. The magnitude of the decrease seems to be essentially independent of the branched polymer concentration, so that small amounts of additives maybe sufficient to bring about a significant decrease in melt viscosity. The decrease is more pronounced for higher generation arborescent polystyrenes.

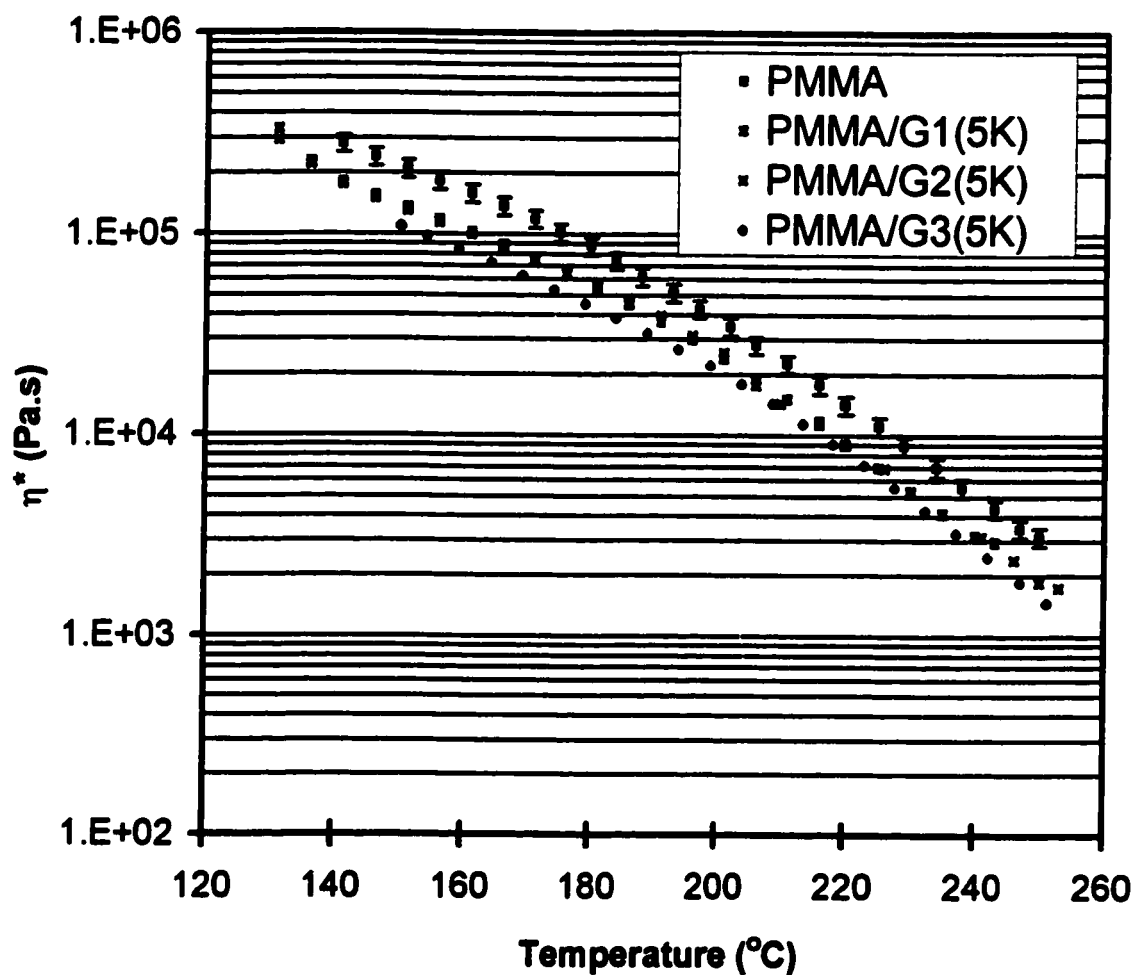


Figure 3.7. Effect of branching functionality of arborescent polystyrenes with short branches on the melt viscosity of PMMA

These results show that depending on the nature of the matrix, arborescent polymers can influence the melt viscosity of linear polymers in various ways. The enhancement of melt viscosity is of industrial importance in operations such as blow molding. Blending with PMMA to decrease the melt viscosity can be useful for other processes such as injection molding or extrusion, to increase processing throughput and minimize shark skin formation.

3.5. References

1. Utracki, L.A. *Polymer Alloys and Blends, Thermodynamics and Rheology*; Hanser: New York, 1990.
2. Datta, S., Lohse, D. J. *Polymeric Compatibilizers Uses and Benefits in Polymer Blends*; Hanser: New York, 1996.
3. Folkes, M. J.; Hope, P. S. *Polymer Blends and Alloys*; Chapman & Hall: New York, 1993.
4. Olabishi, O.; Robeson L.M.; Shaw, M.T. *Polymer-Polymer Miscibility*; Academic: New York, 1979.
5. Mourey, T. H.; Turner, S. R.; Rubinstein, M.; Fréchet, J. M. J.; Hawker, C. J.; Wooley, K. L. *Macromolecules* **1992**, *25*, 2401.
6. Klein, J.; Fletcher, D.; Fetters, L. J. *Nature* **1983**, *304*, 526.
7. Gauthier, M.; Li, W.; Tichagwa, L. *Polymer* **1997**, *38*, 6363.
8. Grest, G.S.; Fetters, L.J.; Huang, J.S. In *Advances in Chemical Physics*; Progogine, I. and Rice, S. A., Eds.; Wiley: New York, 1996; Vol. 94, p.67.

9. Graessley, W.W.; Masuda, T.; Roovers, J.E.L.; Hadjichristidis, N. *Macromolecules* **1976**, *9*, 127.
10. Graessley, W.W.; Roovers, J. *Macromolecules* **1979**, *12*, 959.
11. Hawker, C.J.; Farrington, P.J.; Mackay, M.E.; Wooley, K.L.; Fréchet, J.M.J. *J. Am. Chem. Soc.* **1995**, *117*, 4409.
12. Hempenius, M.A.; Zoetelief, W.F.; Gauthier, M.; Möller, M. *Macromolecules* **1998**, *31*, 2299.
13. Yethiraj, A. *Phys. Rev. Lett.* **1995**, *74*, 2018.
14. Yethiraj, A.; Kumar, S.; Hariharan, A.; Schweiser, K.S. *J. Chem. Phys.* **1994**, *100*, 4691.
15. Kim, Y. H.; Webster, O.W. *Macromolecules* **1992**, *25*, 5561.
16. Gauthier, M.; Möller, M. *Macromolecules* **1991**, *24*, 4548.
17. Gauthier, M., Tichagwa, L.; Downey, J.S.; Gao, S. *Macromolecules* **1996**, *29*, 519.
18. Kee, R. A.; Gauthier, M. *Polym. Mater. Sci. Eng.* **1997**, *77*, 177.
19. Sheiko, S. S.; Gauthier, M.; Möller, M. *Macromolecules* **1997**, *30*, 2343.
20. Russell, T. P.; Hjelm, R. P.; Seeger, P. A. *Macromolecules* **1990**, *23*, 890.

Chapter 4: Polyisoprene Arborescent Copolymers as Melt Viscosity Modifiers for Linear Polymers

4.1. Introduction

The compact structure of branched polymers leads to properties in the molten state and in solution very different from linear polymers (1-6). For example, the viscosity of star-branched polystyrenes with side chains below the entanglement molecular weight is lower than for linear polymers of comparable molecular weight (4). For polyether dendrimers, the zero-shear viscosity η_0 increases linearly with molecular weight, a behavior consistent with an unentangled structure (7). The rheological properties of arborescent polystyrenes in the molten state were investigated by Hempenius *et al.* (8). The zero-shear viscosity of arborescent polystyrenes with short side chains is up to 10^4 times lower than for linear polymers of comparable molecular weight.

Miscibility is an important factor influencing the viscosity of blends of linear and branched polymers. Miscibility is usually disfavored at higher branching levels and at higher concentrations of the branched component (9,10). A few investigations of the effect of chain architecture on polymer segregation in blends incorporating branched and linear polymers are available in the literature (9-14). The migration of branched polymer components to the surface of linear/branched polymer blends has attracted considerable interest. The extent of migration of the branched polymer to the surface is dependent on intermolecular interactions between the blend components, and also on interactions with the surface itself (11). The composition of a blend at the surface can have an important

influence on the observable properties of the sample. Theoretical studies of linear and branched polymers have predicted that small differences in structure can induce phase separation, and that the branched polymer preferentially migrates to the surface (12).

A systematic examination of the effect of branching on blend properties should ideally rely on branched polymers with a well-defined structure in terms of branch length and degree of branching. Arborescent polymers, prepared by anionic polymerization techniques, fulfill these requirements (15-17). The synthesis of arborescent polymers is based on successive functionalization and anionic grafting reactions. The procedure for the preparation of arborescent copolymers incorporating polyisoprene (PIP) segments of the type used in this study is described in Figure 4.1. Control over the chemical composition such as achieved in arborescent copolymers may be advantageous from various perspectives. It provides control over the interactions between the two components of the blend, and hence the extent and the kinetics of phase separation. Furthermore, other physical properties such as the glass transition temperature and the viscosity of the additive can be controlled.

In order to explore the usefulness of these materials as processing additives, copolymers based on a comb polystyrene substrate grafted with polyisoprene side chains were blended with linear polystyrene and linear poly(methyl methacrylate) (PMMA). The copolymers used in the investigation contain polyisoprene as a major component (over 80% w/w), and polyisoprene side chains with a molecular weight of either 3 600, 5 500 or 30 000 g/mol. The effect of the arborescent copolymer content on the melt viscosity of commercial PMMA and polystyrene samples is investigated in the 1-10% w/w range.

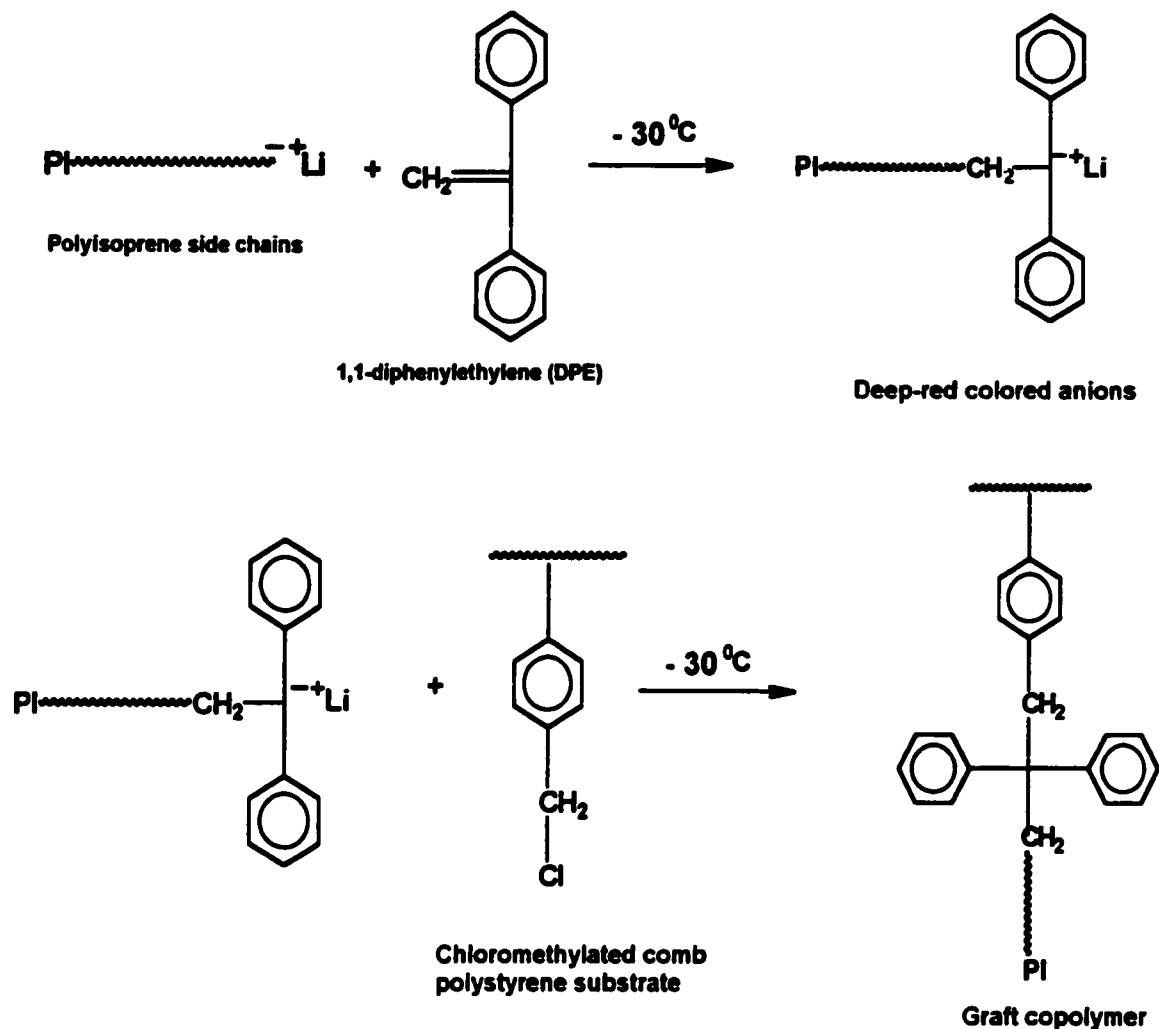


Figure 4.1. Synthetic scheme for the preparation of arborescent polyisoprene copolymers

4.2. Experimental Procedures

4.2.1. Preparation of Blends

Blends of linear homopolymers and arborescent copolymers with different branch lengths were investigated. The linear polystyrene sample used has a number-average molecular weight $M_n = 1.55 \times 10^5$ g/mol and a weight-average molecular weight $M_w = 3.55 \times 10^5$ g/mol, and the poly(methyl methacrylate) sample has a

$M_n = 1.96 \times 10^5$ g/mol and $M_w = 2.90 \times 10^5$ g/mol. The M_w and branching functionality (f_w) of the arborescent polyisoprene copolymers used for the study are listed in Table 4.1. The samples were prepared and characterized as previously described, by grafting a chloromethylated comb-branched polystyrene with polyisoprene side chains (17). Sample PIP3.6K, prepared by anionic polymerization of isoprene in tetrahydrofuran, contains side chains with a 1:1:1 ratio of 1,2-, 3,4- and 1,4-microstructures. The other copolymers, synthesized in cyclohexane, have polyisoprene side chains with a 1,4- to 3,4-microstructure ratio of about 19:1.

The two components of the blends were first dissolved in benzene (100 mL, BDH) at a concentration of 5% (w/v) by stirring for 24 hours. The solvent was then removed by freeze-drying under vacuum for 24 hours. The polymer blends were dried further in a vacuum oven for 48 hours at room temperature, at 80°C for three days, and pressed at 180°C into discs (ca. 25 mm × 2.3 mm) with a hydraulic press.

Table 4.1. Characteristics of the arborescent polyisoprene copolymers used

Arborescent Copolymers	M_w^{br} ($g \times mol^{-1}$) ^a	M_w/M_n ^a	Total M_w ^b ($g \times mol^{-1}$)	Branching Functionality f_w
PIP3.6K	3 600	1.09	6.2×10^5	180
PIP5.5K	5 500	1.06	8.7×10^5	149
PIP30K	30 000	1.06	3.8×10^6	125

^a PIP side chains, apparent values from SEC analysis

^b Absolute M_w of copolymer from light scattering

4.2.2. Characterization

The viscoelastic properties of the pure linear polymers and of the blends were determined on a Rheometrics RMS 605 Mechanical Spectrometer. A parallel plate geometry with a diameter of 25 mm and a gap range of 1.8-2.0 mm was used. All tests were performed under nitrogen atmosphere to prevent sample degradation. The samples were first equilibrated at the high temperature limit (250°C) for twenty minutes. The measurements were initiated while ramping the temperature downward at 1°C per minute. Temperature sweep (time cure sweep) measurements were carried out at 1 Hz and 10% strain.

Size exclusion chromatography (SEC) served to characterize the linear polystyrene and poly(methyl methacrylate) samples, and some of the polymer blends after the rheological measurements. The instrument used consisted of a Waters 510 HPLC pump, a Jordi DVB 500 mm linear mixed bed column and a Waters 410 differential refractometer detector. Tetrahydrofuran served as the eluent, at a flow rate of 1 mL/min. Molecular weights were determined using a linear polystyrene standards calibration curve.

The glass transition temperature of some blends was determined with a Perkin-Elmer Differential Scanning Calorimeter (DSC, model DSC-2C). Samples (10 mg) were sealed in aluminium pans, annealed at 160°C for 5 minutes, quenched to -60°C and scanned to 160°C at a rate of 20°C/minute.

Tensile measurements were performed on an Instron machine. The polymer samples were pressed into dog bone-shaped specimens on a hydraulic press (3.2 mm width × 1.6 mm thickness). The tensile force was recorded as a function of elongation, at a constant deformation rate of 0.02 inch/minute. The results were averaged for

measurements on three samples for pure PMMA and for a PMMA/PIP3.6K blend (1% w/w).

4.3. Results and Discussion

The free energy of mixing in a blend is a function of the interaction parameter χ , the volume fraction ϕ_i and the volume per molecule V_i of each component, and the total sample volume V . According to the Flory-Hugging theory (18), the free energy of mixing is given by the equation

$$\frac{\Delta G_{mix}}{kTV} = \chi \frac{\phi_1 \phi_2}{V_r} + \left(\frac{\phi_1}{V_1} \ln \phi_1 + \frac{\phi_2}{V_2} \ln \phi_2 \right) \quad (4.1)$$

where V_r is the monomer segment volume and k is Boltzmann's constant. Interaction parameters for the PIP/PMMA, PIP/PS and PS/PMMA systems found in the literature are listed in Table 4.2 (19-21). The larger the interaction parameter for the two components in the blend, the more positive (less favorable) is the enthalpy contribution (leftmost term in Equation 4.1) to the Gibbs free energy of mixing, and phase separation is more strongly favored. Based on the data listed in Table 4.2, the free energy of mixing is expected to be more positive for PMMA/PIP blends than for PS/PIP blends.

Table 4.2. Interaction parameters for PMMA/PIP, PS/PIP and PMMA/PS

Polymer	Interaction Parameter χ	Temperature (°C)	Reference
PMMA/PIP	0.077	22	20
PS/PIP	0.038	45	21
PMMA/PS	0.041	25	19
PMMA/PS	0.029	70	20

Arborescent polymers are characterized by a high molecular weight and a highly branched structure, both leading to a more positive free energy of mixing and enhanced phase separation. A high molecular weight results in a small entropy contribution (term within brackets in Equation 4.1), because the molecular volume V_i is correspondingly large. Branching also reduces the number of conformations accessible to the arborescent polymers in the blends, further decreasing their contribution to the entropy of mixing.

It was pointed out in Section 2.2.3 that branching and a low surface energy both favor migration of a polymer to the surface of a blend. Surface energy data for linear polyisoprene, polystyrene and poly(methyl methacrylate) are compared in Table 4.3 (22). Polyisoprene has by far the lowest surface energy, and is therefore expected to migrate preferentially to the surface of polystyrene and poly(methyl methacrylate) blends. The tendency of arborescent isoprene copolymers to migrate to the surface of the blends should be further enhanced on the basis of their low viscosity, and under the influence of shearing during the rheological measurements.

Table 4.3. Surface energy of linear polymers

Polymer	Surface tension γ (mN/m)
Polyisoprene	32
Polystyrene	40.7
PMMA	41.1

4.3.1. Effect of Copolymer Branch Length

Complex dynamic melt viscosity (η^*)-temperature curves obtained at 1 Hz for

PMMA blends containing 5% w/w copolymers with polyisoprene side chains of either 3 600 g/mol (PIP3.6K), 5 500 g/mol (PIP5.5K) or 30 000 g/mol (PIP30K) and for pure PMMA are compared in Figure 4.2. Rheological measurements are generally considered to be reproducible to within ± 5 -10%. Error bars corresponding to a 10% uncertainty are included on all plots for the measurements done on the pure matrix polymer, for comparison purposes.

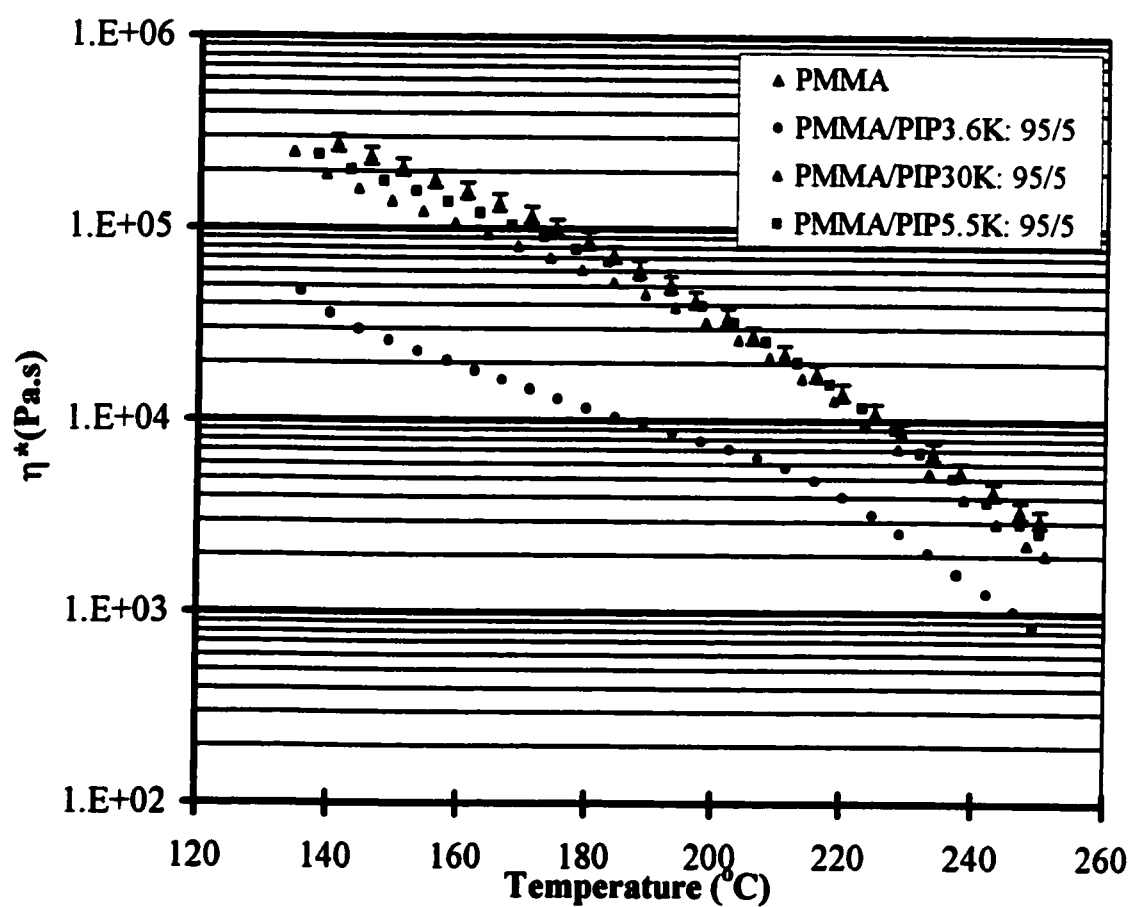


Figure 4.2. Effect of branch length of polyisoprene copolymers on the melt viscosity of PMMA

A dramatic decrease (4- to 10-fold) in melt viscosity is observed over the whole temperature range for the blend containing the short side chain copolymer (PIP3.6K). The decrease for the copolymer with 5 500 g/mol side chains is much less significant. The blend incorporating the PIP30K copolymer yielded results almost identical with pure PMMA.

The large decrease in melt viscosity observed for the copolymer with 3 600 g/mol chains relative to the copolymer with 5 500 g/mol side chains may seem unexpected, considering the relatively small difference in molecular weight of the side chains. The fact that the *microstructure* of the side chains in each copolymer is different should also be considered, however. The PIP5.5K sample contains polyisoprene side chains with a 1,4-microstructure. For a molecular weight of 5 500 g/mol, the degree of polymerization is 80, corresponding to 320 carbon-carbon bonds in the side chains. Sample PIP3.6K has side chains with a molecular weight of 3 600 g/mol and a mixed microstructure (an approximately 1:1:1 ratio of 1,2- 3,4- and 1,4-microstructures), corresponding to a degree of polymerization of 53. Since the 1,2- and 3,4-microstructures each contribute only two carbon-carbon bonds in the polyisoprene backbone, the side chains only contain 141 carbon-carbon bonds. This calculation shows that the polyisoprene side chains in PIP3.6K are 2.3 times shorter than the ones in PIP5.5K. An arborescent copolymer with shorter side chains should migrate more easily to the surface than the one with longer side chains, because of its smaller size. Since arborescent polymers have a much lower viscosity than linear polymers (8), migration of the copolymers to the surface should result in a surface lubrication effect and a very low apparent viscosity.

The variation in the complex dynamic melt viscosity as a function of temperature

at 1 Hz for blends of polystyrene containing 5% w/w copolymer with either 3 600 g/mol or 30 000 g/mol polyisoprene branches and for pure polystyrene are compared in Figure 4.3. The addition of the arborescent copolymer did not decrease the viscosity of the polystyrene matrix, but actually caused melt strengthening at high temperatures. It was suggested, based on the surface energy data provided in Table 4.3, that migration of polyisoprene to the surface of the sample should be equally favored in both polystyrene and poly(methyl methacrylate) blends. While this is true in blends of the homopolymers, one major distinction must be considered for the samples used in this study: The arborescent polymers are not isoprene homopolymers, but rather copolymers incorporating a polystyrene core and polyisoprene side chains. Because of the relatively low branching functionality ($f_w \leq 180$) of the copolymers used, it seems likely that the linear polystyrene matrix chains can penetrate inside (and possibly entangle with) the polystyrene core of the copolymer molecules. Favorable interactions between the polystyrene core and the polystyrene matrix should lead to a decreased tendency for the branched molecules to phase-separate and migrate to the surface. Additional entanglement formation between the linear polystyrene and the arborescent copolymer can also lead to the viscosity enhancement observed at high temperature, as discussed in Section 3.3.1.1.

4.3.2. Effect of Copolymer Concentration on the Melt Viscosity of PMMA

The temperature dependence of the complex dynamic melt viscosity at 1 Hz for blends of poly(methyl methacrylate) and the copolymer with 5 500 g/mol branches

(PIP5.5K) containing 1% to 10% w/w arborescent copolymer and for pure PMMA are compared in Figure 4.4. At lower arborescent copolymer concentrations (1 and 2.5% w/w), a significant decrease (up to 3-fold) in viscosity is observed over the whole temperature range. At higher concentrations (5% w/w and above), in contrast, melt strengthening is apparent.

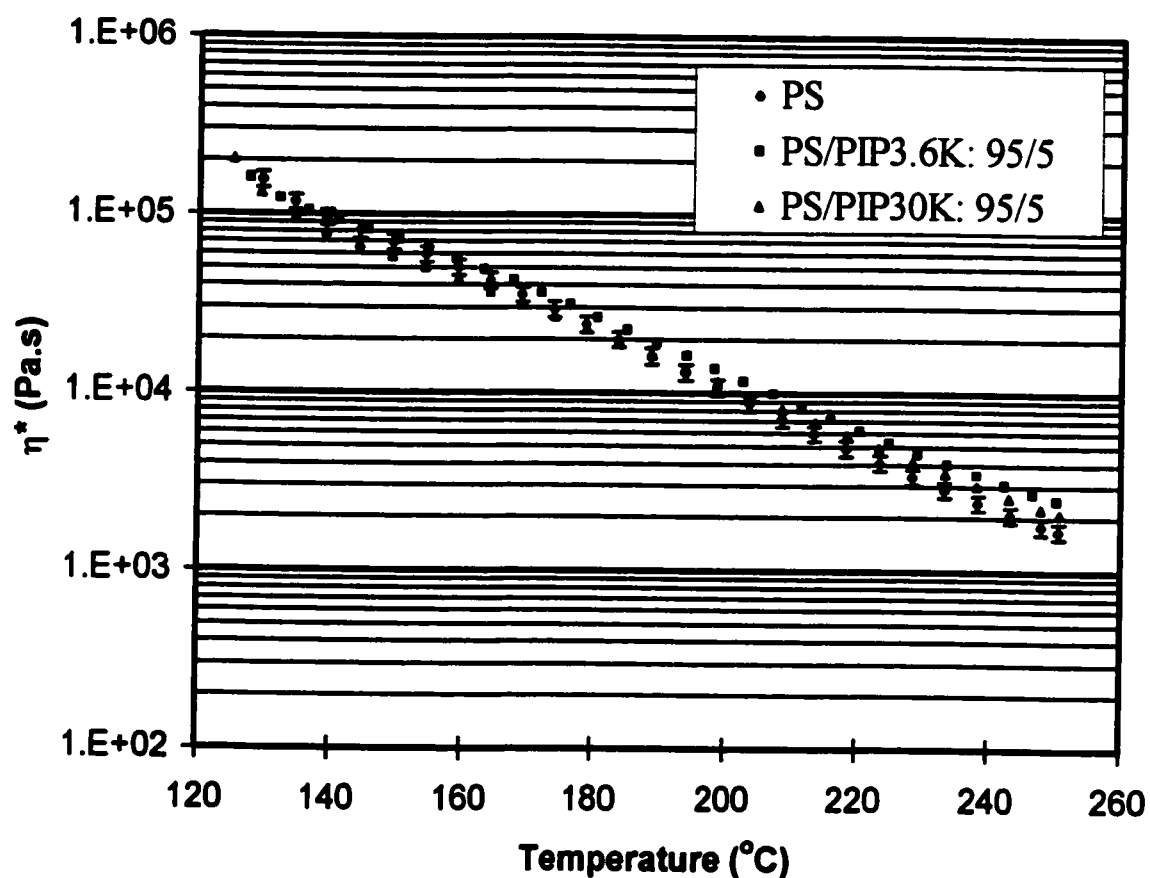


Figure 4.3. Effect of branch length of polyisoprene copolymers on the melt viscosity of polystyrene

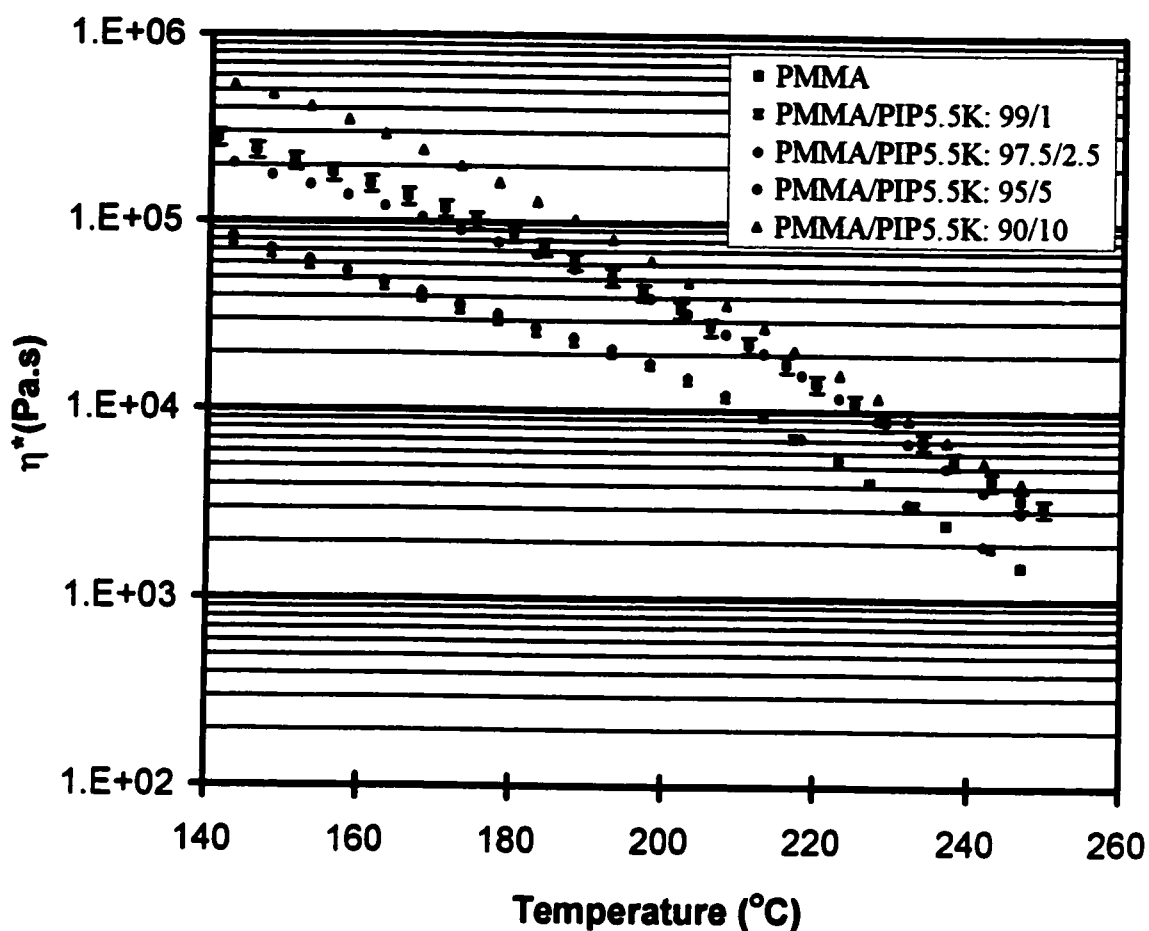


Figure 4.4. Effect of polysioprene copolymer concentration on the melt viscosity of PMMA

It was suspected that the increase in melt viscosity with copolymer concentration was due to cross-link formation between vinyl pendant groups of the polyisoprene side chains in the blends. To verify this hypothesis, dissolution of the blend containing 10% w/w copolymer was attempted in different solvents after the rheological measurements. Sample dissolution was incomplete, and gel particles were apparent even after stirring for a few days. This confirms that cross-link formation occurred during the measurements at high temperatures, leading to the observed increase in melt viscosity. The blends with lower arborescent copolymer concentrations, in contrast, dissolved completely in the

same solvents. The effect of arborescent polyisoprene copolymer concentration on the melt viscosity of PMMA can be easily rationalized. At low concentrations (1 and 2.5% by weight), the arborescent molecules or phase-separated domains dispersed in the polymer matrix form a diluted system, where the domains or molecules remain isolated from each other. Network formation inside the domains does not have much influence on the bulk viscosity of the sample, because there is no connectivity between the domains. At higher concentrations (5% and 10% by weight) overlapping of the domains becomes increasingly likely, leading to the formation of a three-dimensional network as a result of cross-linking. The formation a network (gel particles) should be favored at high arborescent polyisoprene copolymer contents, in particular for copolymers with longer branches, as the phase-separated domains and/or molecules start to overlap.

The fact that a significant (2- to 3-fold) decrease in melt viscosity was achieved at low polyisoprene copolymer concentrations is very interesting. A low branched polymer concentration is preferable for melt processing additives not only in terms of cost, but also because the mechanical properties of the matrix polymer should be less affected.

To confirm that the observed decreases in melt viscosity are related to the addition of the copolymers and not due to degradation of the PMMA matrix, size exclusion chromatography (SEC) measurements were performed on the blends before and after the rheological measurements. No detectable changes in the molecular weight distribution of PMMA could be observed in the blend containing 5% w/w PIP3.6K.

Entanglement and cross-link formation are unlikely to occur in blends of arborescent polyisoprene copolymers with short side chains. When these materials are blended with PMMA, phase separation and migration of the branched polymer to the

surface are expected (12). Because of their low viscosity, the copolymers act as lubricants on the sample surface, leading to the observed 'apparent' decreases in melt viscosity.

Further evidence in support of a surface lubrication mechanism to explain the 'decrease' in melt viscosity observed was found in dynamic scanning calorimetry (DSC) measurements. If the decrease is related to a bulk effect, the glass transition temperature (T_g) of the blend should also be lowered. This is the case, for example, when plasticizers are added to polymers. However, no change in T_g is expected if the decrease is only related to surface effects. A PMMA/PIP3.6K blend containing 5% w/w arborescent polyisoprene was investigated by DSC. No change in the glass transition temperature of the matrix could be detected.

4.3.4. Tensile Measurements

Tensile measurements were performed for pure PMMA samples and for blends of PMMA with 1% w/w arborescent polyisoprene with 5 500 g/mol side chains. The measurements were found to be reproducible to within 15%. The modulus was essentially unaffected by the addition of the branched polymer, increasing insignificantly from 2.2₀ to 2.2₆ GPa. The stress at break was significantly reduced from 87 to 64 MPa, and the elongation at break also decreased from 5 to 3% for the blend. These results confirm that the addition of graft copolymers should be limited to small amounts, and ideally to less than 1% w/w for optimal results.

4.4. Conclusions

The results presented show that blending of arborescent polyisoprene copolymers

with PMMA can lead to large decreases in melt viscosity (melt thinning). The magnitude of the decrease was most pronounced for copolymers with short polyisoprene side chains. In contrast, no effect was observed for blends based on polystyrene.

Arborescent copolymers with relatively long side chains led to a decrease in melt viscosity at low concentrations (1 and 2.5 % w/w) in the poly(methyl methacrylate) blends. At higher concentrations (up to 10% w/w) melt strengthening was observed, and related to cross-linking occurring in the sample.

Future work will concentrate on blends with concentrations of arborescent copolymers below 1% w/w, to minimize the impact of the additives on the mechanical properties of the matrix.

4.5. References

1. Mourey, T. H.; Turner, S. R.; Rubinstein, M.; Fréchet, J. M. J.; Hawker, C. J.; Wooley, K. L. *Macromolecules* **1992**, *25*, 2401.
2. Klein, J.; Fletcher, D.; Fetters, L. J. *Nature* **1983**, *304*, 526.
3. Gauthier, M.; Li, W.; Tichagwa, L. *Polymer* **1997**, *38*, 6363.
4. Grest, G.S.; Fetters, L.J.; Huang, J.S. In *Polymeric Systems*; Prigogine, I. And Stuart, A.R., Eds.; *Advances in Chemical Physics*: Wiley: New York, 1996; Vol. *XCIV*, page 67.
5. Graessley, W.W.; Masuda, T.; Roovers, J.E.L.; Hadjichristidis, N. *Macromolecules* **1976**, *9*, 127.
6. Graessley, W.W.; Roovers, J. *Macromolecules* **1979**, *12*, 959.

7. Hawker, C.J.; Farrington, P.J.; Mackay, M.E.; Wooley, K.L.; Fréchet, J.M.J. *J. Am. Chem. Soc.* **1995**, *117*, 4409.
8. Hempenius, M.A.; Zoetelief, W.F.; Gauthier, M.; Möller, M. *Macromolecules* **1998**, *31*, 2299.
9. Mandelkern, L.; Alamo, R. G.; Wignall, G. D.; Stehling, F. C. *Trends Polym. Sci.* **1996**, *4*, 377.
10. Chai, Z.; Sun, R.Li.; Karasz, F.E. *Macromolecules* **1995**, *28*, 2297.
11. Yethiraj, A. *Phys. Rev. Lett.* **1995**, *74*, 2018.
12. Yethiraj, A.; Kumar, S.; Hariharan, A.; Schweiser, K.S. *J. Chem. Phys.* **1994**, *100*, 4691.
13. Sikka, M.; Singh, N.; Karim, A.; bates, F.S.; Satija, S. K.; Majkarzak, C. F. *Phys. Rev. Lett.* **1993**, *70*, 307.
14. Wu, D.T.; Fredrickson, G.H. *Macromolecules* **1996**, *29*, 7918.
15. Gauthier, M.; Möller, M. *Macromolecules* **1991**, *24*, 4548.
16. Gauthier, M.; Tichagwa, L.; Downey, J.S.; Gao, S. *Macromolecules* **1996**, *29*, 519.
17. Kee, R.A.; Gauthier, M. *Polym. Mater. Sci. Eng.* **1995**, *73*, 335.
18. Sperling, L. S. *Polymer Multicomponent Materials: An Introduction*; Wiley: New York, 1997.
19. Russell, T. P.; Hjelm, R. P.; Seeger, P. A. *Macromolecules* **1990**, *23*, 890.
20. Tcherkasskaya, O.; Ni, S.; Winnik, M. A. *Macromolecules* **1996**, *29*, 610.
21. Tseng, H., Lloyd, D. R. *J. Polym. Sci., Polym. Sci. Phys. Ed.* **1987**, *25*, 325.
22. Wu, S. *Polymer Handbook*, 3rd Edition, J. Brandrup and E. H. Immergut, Page VI/411, 1989.

Chapter 5: Arborescent Polydimethylsiloxane Graft Copolymers

5.1. Introduction

Polysiloxanes are known for their exceptional properties that have made them popular for a wide range of industrial applications. A convenient way to combine the properties of polysiloxanes with those of other polymers is by the preparation of copolymers. Further control over the properties of these materials can be attained by varying the architecture of the chains, for example by the introduction of branching. Branched polymers with a dendritic structure, the arborescent polymers, can be prepared using anionic grafting techniques (1). Graft copolymers consisting of an arborescent polystyrene core and either polyisoprene or poly(ethylene oxide) side chains were also prepared. The synthesis of arborescent polyisoprene copolymers, shown in Figure 4.1, is based on a *grafting onto* scheme whereby polyisoprenyl anions are reacted with a chloromethylated branched polystyrene substrate (2).

Graft copolymers incorporating an arborescent polystyrene core with end-linked poly(ethylene oxide) chains were also prepared using a *grafting from* method (3), as shown in Figure 2.9. Linear polystyrene with a narrow molecular weight distribution was chloromethylated and grafted with polystyryllithium to generate a comb-branched structure. A second grafting reaction was carried out in an analogous fashion but using a bifunctional initiator, 6-lithiohexyl acetaldehyde acetal, for the preparation of polystyryllithium. Following hydrolysis and fractionation, a twice-grafted (G1)

arborescent polystyrene bearing hydroxyl functionalities at the chain ends was obtained. The ethylene oxide copolymer was obtained by titrating the hydroxyl-terminated polymer with a potassium naphthalide solution and adding ethylene oxide.

The goal of this research was to investigate the usefulness of the *grafting from* method for the synthesis of arborescent copolymers containing polydimethylsiloxane segments. The procedure was based on hydroxyl-functionalized polystyrene cores of different architectures acting as polyfunctional initiators for the polymerization of hexamethylcyclotrisiloxane (D_3).

5.2. Experimental Procedures

Anionic polymerization is very sensitive to protic impurities that can easily react with the living chain ends and cause premature termination of the polymerization. Stringent purification of all reagents, crucial to the success of the procedure, is typically achieved with high-vacuum purification techniques. The nitrogen gas used in the inert atmosphere procedures was also purified to remove trace amounts of water and oxygen. The purified reagents were contained within specially designed glass ampules sealed with Young polytetrafluoroethylene (PTFE) greaseless stopcocks.

5.2.1. Reagent and Solvent Purification Procedures

5.2.1.1. Reagents

sec-Butyllithium (Aldrich, 1.4 M in cyclohexane) and *n*-butyllithium (Aldrich, 2.5 M in hexanes) were used as received; the exact activity of the initiators was determined by the procedure of Lipton *et al.* (4). Chloromethyl methyl ether was

prepared according to a known procedure (5). All other reagents were used as obtained from the suppliers unless otherwise indicated.

A lithium naphthalide solution in tetrahydrofuran (THF) was prepared in a three-necked flask containing a glass-encased magnetic stirring bar. After the flask was evacuated, flamed and filled with nitrogen, dry THF (200 mL) was added followed by naphthalene (6.4 g, 50 mmol, Baker) and lithium metal (1.62 g, 42 mmol, Aldrich). After stirring overnight at room temperature, the dark green-colored solution was filtered using a Schlenk funnel and stored in a Schlenk flask at -20°C until needed. The concentration of the lithium naphthalide solution was determined by the titration of 2,6-di-*tert*-butyl-4-methylphenol (BHT) (300 mg) dissolved in dry THF (50 mL) in a nitrogen-filled flask fitted with a septum. The endpoint was indicated by the appearance of a persistent faint green color. The exact molar concentration of lithium naphthalide (0.95 M) was calculated from the average of three determinations.

5.2.1.2. Purification of Solvents

Tetrahydrofuran (Caledon, Reagent) was dried by refluxing with sodium-benzophenone ketyl under dry nitrogen for two hours and distilled immediately prior to use. Toluene (BDH, Omnisolv) was dried by refluxing with oligostyryllithium under dry nitrogen for three hours, and distilled immediately prior to use. Carbon tetrachloride (Caledon, Reagent) was dried by distillation from P_4O_{10} (BDH).

5.2.1.3. Monomer Purification

The cyclic dimethylsiloxane monomer, hexamethylcyclotrisiloxane (D_3 , Aldrich, 99%) was first dissolved in toluene at a concentration of 40% (w/w), and left to stir over calcium hydride for 24 hours. The solution was distilled at 116-117°C and collected in a flask maintained at -78°C. The monomer solution was stored at -5°C until needed.

The D_3 solution was further purified immediately prior to polymerization with a second distillation from CaH_2 under vacuum. The manifold assembly used for the purification is shown in Figure 5.1. The manifold was evacuated (10^{-4} mm Hg) and flamed to remove adsorbed water, then allowed to cool and filled with nitrogen. The required volume of monomer solution (15 mL, 4 g D_3 , 0.0179 mol) was added to flask A through the opening on the top with a syringe while maintaining a flow of nitrogen within the assembly. The drying agent (CaH_2 , 2 g) was added to the monomer solution using a funnel. The solution was stirred over CaH_2 for 30 minutes under nitrogen, then degassed with three freezing-pumping-thawing cycles under vacuum. The monomer solution was slowly recondensed to the ampule frozen in liquid nitrogen, and the ampule was then filled with a slight overpressure of purified nitrogen.

Styrene (Aldrich, 99%) was first purified by distillation from CaH_2 under reduced pressure and stored under nitrogen at -5°C until needed. The monomer was further purified prior to polymerization using the manifold shown in Figure 5.1. Phenylmagnesium chloride (Aldrich, 2.0 M solution in THF, 5 mL) was transferred to flask A through the opening on the top of the manifold using a syringe, and the THF was removed under vacuum. Styrene (33 mL, 30 g, 0.288 mol) was then added to flask A with a syringe, and degassed using three successive freezing-pumping-thawing cycles. The pure monomer

was slowly recondensed to an ampule with a PTFE stopcock that was finally filled with nitrogen and stored at $-5\text{ }^{\circ}\text{C}$ until needed.

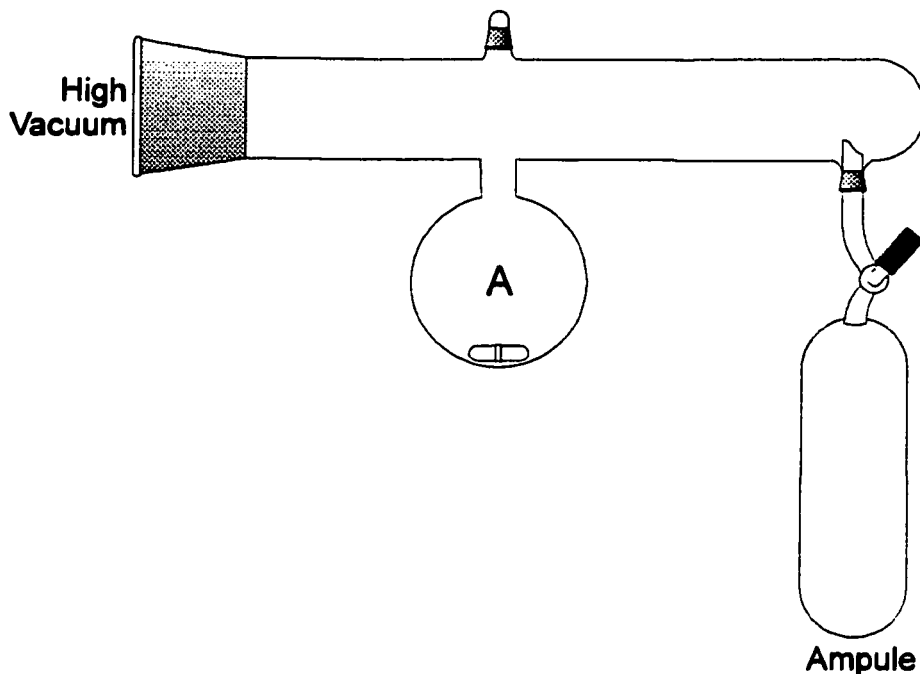


Figure 5.1. Apparatus for monomer purification

5.2.1.4. Azeotropic Purification of 1,1-Diphenylethylene and Core Polymers

1,1-Diphenylethylene (DPE; Aldrich, 97%) was distilled under reduced pressure after adding enough *n*-butyllithium solution (Aldrich, 2.5 M in hexanes) to obtain the deep red coloration of 1,1-diphenylhexyllithium. Further purification of DPE was carried out by azeotropic distillation employing the manifold shown in Figure 5.2. The side arm on flask B was coupled with the THF line from the still and the ampule containing DPE and a PTFE-coated magnetic stir bar was mounted on the manifold. The assembly was evacuated and flamed (except the DPE ampule). THF was added to flask B and recondensed to the ampule immersed in liquid nitrogen. The solution was thawed and stirred 20 minutes. Flask

C was then immersed in liquid nitrogen to recondense the THF from the ampule. Two additional azeotropic distillation cycles were performed to complete the removal of volatile protic impurities from DPE. Finally, a fresh portion of THF was recondensed to the ampule that was filled with a slight overpressure of nitrogen.

The azeotropic distillation procedure was also used to remove residual water from samples of chloromethylated polystyrene, hydroxyl-functionalized polystyrene and cryptand (whenever used) prior to the grafting reaction.

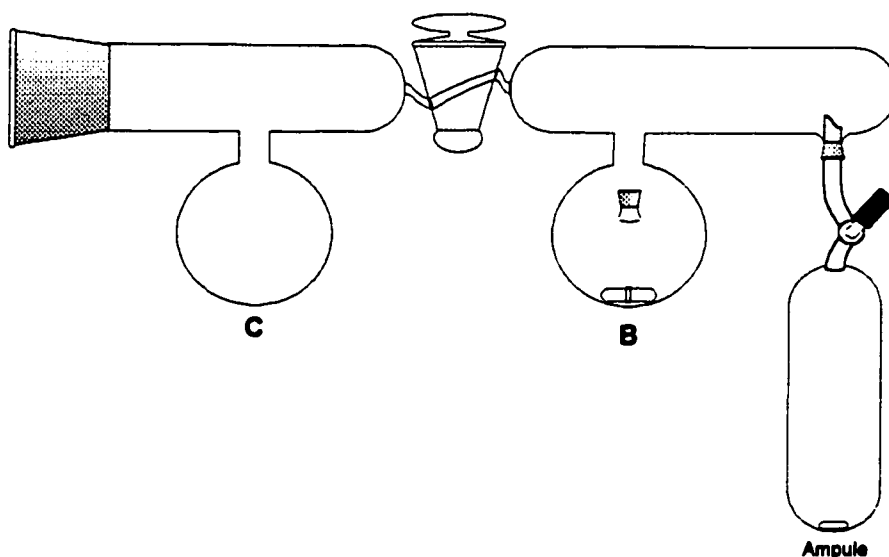


Figure 5.2. Apparatus for purification by azeotropic distillation

5.2.2. Synthesis of Linear Polydimethylsiloxane

5.2.2.1. Anionic Polymerization of D_3 Initiated with *n*-Butyllithium

Linear polydimethylsiloxane was synthesized using a modification of a procedure reported by Maschke and Wagner (6). The polymerization reaction was carried out in a three-necked flask mounted on the high-vacuum line. The purified D_3 monomer ampule

(15 mL solution, 4 g, 0.0179 mol), THF and toluene lines were mounted on the flask. The apparatus was evacuated, flamed and filled with nitrogen. Toluene (100 mL) was added, followed by the *n*-butyllithium solution (0.8 mL, 2 mmol, for a target $M_n = 5\,000$ g/mol) and the monomer solution. The seeding reaction was allowed to proceed for 12 hours at room temperature, and THF (100 mL) was added. The polymerization reaction was carried out for 48 hours at room temperature. The living polydimethylsiloxane chains were terminated by stirring with chlorotrimethylsilane (1 mL, 8 mmol) for 24 hours. The solvent was removed on a rotary evaporator, the polymer residue was dissolved in hexane and washed once with 25% (v/v) hydrochloric acid/water and once with distilled water. The solvent was again removed, and the polymer was dried overnight under high vacuum to remove residual monomer. The polymer was characterized by size exclusion chromatography (SEC).

5.2.2.2. Anionic Polymerization of D_3 Initiated by Lithium *n*-Butoxide

In order to establish satisfactory conditions for the preparation of PDMS using a lithium alcoholate initiator, a model polymerization reaction initiated by lithium *n*-butoxide was carried out. Two different conditions were considered for the reaction. In the first case the seeding step was done in toluene and in the second case, in THF. The reaction was carried out in a three-necked flask as outlined previously, using an ampule containing 4 g of D_3 dissolved in Toluene. THF (100 mL) and *n*-butanol (0.1 mL, 1.1 mmol) were added to the flask, and the solution was titrated with the lithium naphthalide solution until a persistent green color was obtained. The THF was then removed under vacuum, the flask was filled with nitrogen and toluene (100 mL) was

added. The monomer solution was transferred to the flask for the seeding reaction. After 16 hours, THF (100 mL) was added, and the reaction was left to proceed further for 48 hours at room temperature. The living polydimethylsiloxane chains were terminated by reaction with chlorotrimethylsilane (0.5 mL, 4 mmol) for 24 hours. For the reaction in THF, the polymerization was carried out directly in THF after titration of the core without replacement of the solvent with toluene as in the previous case. Isolation and characterization of the polymers were done as described previously.

5.2.3. Synthesis of Polystyrene Grafting Substrates

5.2.3.1. Linear Polystyrene

The polymerization of styrene was carried out in the reactor shown in Figure 5.3. The flask was fitted with a septum, inlets for the THF and toluene lines, and the ampule containing the purified styrene monomer (11 mL, 10 g, 0.096 mol). A vacuum-tight, magnetically coupled stirring shaft was placed on the flask. The reactor was evacuated, flamed and filled with dry nitrogen gas. Toluene (200 mL) was transferred to the reactor. Two drops of styrene monomer were added from the ampule, followed by *sec*-butyllithium, dropwise, until a stable pale orange color was observed. The required amount of *sec*-butyllithium (0.34 mL, 0.476 mmol, for a $M_n = 25\ 000$ g/mol) was added, followed by the contents of the monomer ampule. The reaction was stirred at room temperature for 15 minutes, and cooled to -78°C using a dry ice/2-propanol bath. THF (100 mL) was then added to the mixture, that was stirred further for 15 minutes at -78°C . The reaction was terminated with degassed methanol, and the polymer isolated by precipitation into methanol and characterized by SEC.

5.2.3.2 Chloromethylation of Linear Polystyrene

Partially chloromethylated polystyrene was prepared using a modification of a previously reported procedure, in a well-ventilated fumehood (1). A typical reaction consisted of dry polystyrene (5 g, 48 mmol styrene units) dissolved in dry carbon tetrachloride (500 mL), and chloromethyl methyl ether (50 mL). A catalyst solution of anhydrous aluminium chloride (3 g, 22.5 mmol) dissolved in 1-nitropropane (100 mL) and carbon tetrachloride (140 mL) was added, and the mixture was stirred at room temperature for 30 minutes. The reaction was quenched with glacial acetic acid (10 mL) and the solvent was removed under reduced pressure, using two traps to minimize the risk of exposure to carcinogenic chloromethyl methyl ether. The polymer residue was redissolved in chloroform, extracted with three portions of 50% (v/v) glacial acetic acid/water and precipitated into methanol. The polymer was redissolved in toluene and reprecipitated twice. The chloromethylated polymer was characterized by SEC and by $^1\text{H-NMR}$ spectroscopy.

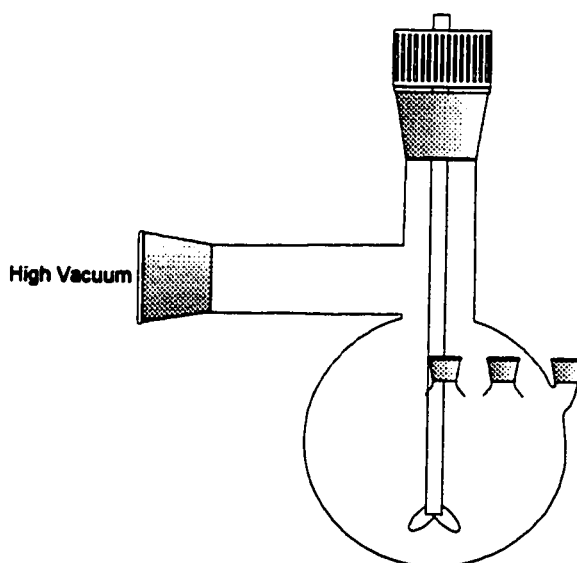


Figure 5.3. Polymerization reactor

5.2.3.3. Living Free Radical Copolymerization

An alternate route for the preparation of linear polystyrene grafting substrates was examined, based on a procedure for the living stable free radical copolymerization of styrene and *p*-chloromethylstyrene (7). The bulk copolymerization reaction was performed in a three-necked flask with a magnetic stirring bar and a reflux condenser. The flask was purged with nitrogen during the reaction. Styrene (85.9 g, 0.825 mol, Aldrich, 99%), 4-vinylbenzylchloride (14.1 g, 0.092 mol, Aldrich, 90%) and 2,2,6,6-tetramethyl-1-piperidinyloxy (TEMPO, 0.446 g, 3.7 mmol, Aldrich, 98%), were added to the flask. After heating to 138°C, benzoyl peroxide (0.692 g, 2.857 mmol, Aldrich, 97%) was added. The polymerization was carried out for 4 hours at 138°C with constant stirring. The flask was cooled to room temperature, the polymer solution diluted in toluene and precipitated into methanol. The polymer was further purified by two reprecipitations from toluene into methanol, and analyzed by SEC and by ¹H-NMR spectroscopy. An overall monomer conversion of 60% was obtained.

5.2.3.4. Preparation of 6-Lithiohexyl Acetaldehyde Acetal

The bifunctional initiator 6-lithiohexyl acetaldehyde acetal was prepared using a modification of a previously reported method (8). 6-Chloro-1-hexanol (Aldrich, 96%) was distilled over anhydrous sodium carbonate at reduced pressure prior to use. Ethyl vinyl ether (99 mL, 1.03 mol, Aldrich, 99%) and purified 6-chloro-1-hexanol (75 mL, 0.562 mol) were added to a 250 mL round bottomed flask containing a magnetic stirring bar and fitted with a reflux condenser. The flask was cooled to 0°C using an ice-water bath. A catalytic amount of dichloroacetic acid (0.9 mL, 8.4 mmol, Aldrich, 99%) was

added, and the reaction was left to proceed for one hour. A second portion of dichloroacetic acid (0.33 mL, 2.83 mmol) was then added to the mixture. The flask was warmed to room temperature and stirred for five hours. A final portion of dichloroacetic acid (0.33 mL) was added, and the reaction was left to stir overnight. Excess ethyl vinyl ether was removed, the 6-chlorohexyl acetaldehyde acetal residue was stirred over anhydrous sodium carbonate and distilled under reduced pressure.

A jacketed 250 mL two-necked flask containing a magnetic stirring bar, fitted with a nitrogen inlet and a septum and cooled to -10°C using a Brinkman RM 6 circulating bath, was used for the preparation of the organolithium compound. Diethyl ether (40 mL, Aldrich, 99%) and lithium wire (0.9 g, 0.123 mol, Aldrich, 98%, cut and hammered into small pieces) were transferred to the flask. 6-Chlorohexyl acetaldehyde acetal (11.48 g, 0.055 mol) was added dropwise from a syringe over one hour. The temperature of the circulating bath was raised to 20°C , and the reaction was left to proceed overnight. Stirring was stopped to allow the LiCl precipitate to settle, and the clear supernatant was transferred using a canula to a Schlenk flask purged with nitrogen. The solution was stored at -20°C until needed. The exact activity of the 6-lithiohexyl acetaldehyde acetal solution was determined by the method of Lipton *et al.* (4). Dry THF (50 mL) and 1,3-biphenyl-2-propanone tosylhydrazone (*ca.* 328 mg, 0.85 mmol, Aldrich, 98%) were placed in a nitrogen-purged flask fitted with a septum. The solution was slowly titrated with the organolithium compound solution to the appearance of a faint orange color. The concentration (0.86 M) was calculated from the average of three determinations.

5.2.3.5. Synthesis of Linear Polystyrene with Acetal Pendant Groups

The preparation of linear polystyrene bearing acetal functional groups was performed in the glass reactor shown in Figure 5.3. Ampules containing chloromethylated polystyrene (4.0 g, 9.5 meq CH_2Cl units) and DPE (3.39 mL, 19 mmol) were prepared according to the procedure outlined in Section 5.2.1.4. The two ampules and the THF line were mounted on the reactor, which was evacuated, flamed and filled with dry nitrogen. Dry THF (400 mL) was added to the reactor, followed by the DPE solution. The solution was titrated with the 6-lithiohexyl acetaldehyde acetal solution until a persistent pale pink color was observed. An 11 mL aliquot (9.5 mmol) of the 6-lithiohexyl acetaldehyde acetal solution was then added, and left to react for 15 minutes at room temperature. The reactor was cooled to -20°C , and the chloromethylated polystyrene solution was added dropwise while stirring until the mixture became colorless. The solvent was removed on a rotary evaporator, the residue was dissolved in toluene and precipitated into methanol. An acetal group content of 23 mol% was determined by $^1\text{H-NMR}$ spectroscopy.

5.2.3.6. Synthesis of Acetal-Terminated Comb-Branched Polystyrene

The synthesis of a comb-branched (arborescent polymer generation G0) polystyrene bearing acetal functional groups at the end of the side chains was performed in the glass reactor shown in Figure 5.3. Two ampules containing chloromethylated polystyrene (1.0 g, 1.0 meq CH_2Cl groups) and DPE (0.36 mL, 2.0 mmol) were prepared according to the procedures outlined in Section 5.2.1.4. An ampule containing purified styrene monomer (22.3 g, 0.214 mol) was prepared as described in Section 5.2.1.3. The three ampules, a septum, the THF and toluene lines were mounted on the reactor that was evacuated, flamed and filled with nitrogen. Toluene (250 mL) was added, followed by two drops of styrene.

The initiator, 6-lithiohexyl acetaldehyde acetal, was added dropwise until a persistent pale yellow color was observed. The required amount of initiator solution (0.80 mL, 0.75 mmol, for a target $M_n = 30\,000$ g/mol) was then added to the reactor, followed by the remaining monomer. After 15 minutes, the reactor was cooled to -78°C and THF (100 mL) was added. The polymerization was allowed to proceed for 30 minutes. The DPE solution was added to the mixture, yielding a deep red color. After 10 minutes, a sample of the solution was removed with a syringe and terminated with degassed methanol, to characterize the polystyrene side chains. The reactor was warmed to -30°C and the chloromethylated polystyrene solution was added dropwise until a faint orange coloration was observed. Warming to room temperature led to further fading of the color. Residual living anions were terminated with degassed methanol. The polymer solution was concentrated on a rotary evaporator, precipitated into methanol, dried under vacuum, and characterized by SEC.

5.2.3.7. Fractionation and Acetal Group Hydrolysis

The graft polymers were separated from non-grafted material by precipitation fractionation in a toluene-methanol mixture. Hydrolysis of the acetal chain ends was achieved at the same time. The procedure was also used to hydrolyze the pendant acetal groups on the linear polymer. In a 1-L cone-shaped flask, 3.0 g of the raw graft polymer was dissolved in toluene (250 mL). Methanol (130 mL) and concentrated HCl (3-4 mL) were added to yield a turbid solution. The flask was then placed in a water bath at 60°C for one hour. When the solution clarified, more methanol was added again to obtain a turbid solution. The water bath was allowed to cool to room temperature overnight. The hydrolyzed polymer settled to the bottom of the flask as a clear viscous solution. The

polymer solution was removed with a syringe, diluted with toluene and precipitated in methanol. Complete removal of non-grafted (linear) polymer from the graft copolymer was confirmed by size exclusion chromatography (SEC). Hydrolysis of the acetal groups was confirmed by FT-IR spectroscopy.

5.2.4. Polydimethylsiloxane Graft Copolymers

5.2.4.1. Metal-Halogen Exchange Reaction

Arborescent polymers can contain residual chloromethyl groups, due to incomplete grafting reactions. Side reactions involving the chloromethyl groups can lead to cross-link formation during the copolymerization reaction (3). To deactivate these residual chloromethyl groups, a metal-halogen exchange reaction was performed.

The apparatus used for the metal-halogen exchange reaction is displayed in Figure 5.4. The polymer solution (2.0 g polymer dissolved in 30 mL THF) contained in an ampule was first dried by azeotropic distillation with dry THF using the procedure described in Section 5.2.1.4. The ampule was mounted on a three-necked flask, together with the dry THF line and a septum. The flask was evacuated, flamed, and filled with nitrogen. THF (250 mL) was transferred to the flask and cooled to -78°C . A large excess of *n*-butyllithium solution (20 mL, 0.05 mol, Aldrich, 2.5 M in hexanes) was added through the septum with a syringe. The polymer solution was added dropwise to the reaction mixture over 1 hour. The solution was stirred further for 1 hour, and the reaction was terminated with deionized water (10 mL). The solvent was removed on a rotary evaporator, and the polymer residue was redissolved in toluene. The organic solution was washed two times with a water/hydrochloric acid mixture (75/25) and three times with water. The polymer was

precipitated in methanol and dried overnight under vacuum. Analysis by SEC was used to confirm that there was no change in the molecular weight distribution of the product.

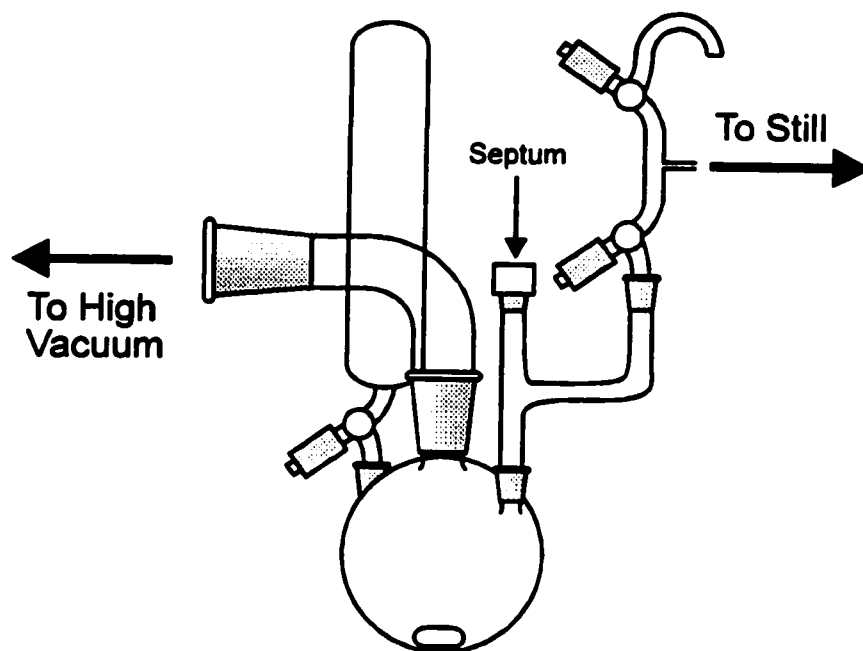


Figure 5.4. Apparatus for the metal-halogen exchange reaction

5.2.4.2. Copolymer Based on Linear Polystyrene with Pendant Hydroxyl Groups

The copolymerization using the hydroxyl-functionalized linear polystyrene substrate as a polyfunctional initiator was performed in an ampule with a PTFE stopcock. The hydroxyl-functionalized polystyrene (250 mg, 0.37 meq hydroxyl units) and Kryptofix 222 (180 mg, 0.487 mmol) were loaded into an ampule and purified by azeotropic distillation as described in Section 5.2.1.4. The ampule was left on the azeotropic drying manifold, the PTFE stopcock was removed and the solution was titrated with lithium naphthalide solution contained in a syringe until a persistent green

color was observed. The ampule was sealed, removed from the manifold, and the solution was stirred overnight at room temperature.

The ampule was mounted on the monomer purification manifold shown in Figure 5.1, and frozen in liquid nitrogen. The manifold was evacuated, flamed and filled with nitrogen. A monomer solution (15.0 mL solution, 4.00 g, 0.0179 mol D_3), purified as described in Section 5.2.1.3, was loaded in flask A. After freezing, evacuation and thawing of the flask, the monomer solution was recondensed to the ampule frozen in liquid nitrogen. When the transfer was completed the ampule was thawed, filled with nitrogen and sealed. The copolymerization reaction was left to proceed for 3 days at room temperature. The polymerization was terminated by stirring with chlorotrimethylsilane (1.0 mL, 8.0 mmol) for 24 hours.

The reaction mixture was diluted with chloroform (100 mL) and extracted with three portions of deionized water (100 mL each). The organic phase was then transferred to a round-bottomed flask and concentrated on a rotary evaporator. Solvent removal was completed under vacuum overnight. The copolymer was characterized by size exclusion chromatography (SEC), $^1\text{H-NMR}$ and FTIR spectroscopy.

5.2.4.3. Copolymer Based on Hydroxyl-Terminated Comb-Branched Polystyrene

The procedure described in Section 5.2.4.2 was used for the preparation of a polydimethylsiloxane graft copolymer using the hydroxyl-terminated comb-branched (arborescent polymer generation G0) polystyrene precursor. In this case 250 mg of the core polymer (0.01 meq hydroxyl groups), 5 mg (0.013 mmol) Kryptofix 222, and 4.0 g (15.0 mL solution, 0.0179 mol) D_3 monomer were used.

5.2.4.4. Copolymer Based on Hydroxyl-Terminated G1 Arborescent Polystyrene

A twice-grafted (G1) arborescent graft copolymer with 5 000 g/mol hydroxyl-terminated side chains was already available in the laboratory. It was synthesized using a procedure similar to the one described in Section 5.2.4.2. The reagents used in the synthesis of the copolymer were 250 mg arborescent polystyrene core (0.05 meq hydroxyl groups), 30 mg (0.078 mmol) Kryptofix 222, and 4.0 g (15.0 mL solution, 0.0179 mol) D_3 monomer. It was necessary to break down insoluble polymer aggregates by sonication of the ampule for *ca.* 20 minutes before the addition of the D_3 solution in this case.

5.2.5. Characterization

5.2.5.1. Size Exclusion Chromatography

Size exclusion chromatography (SEC) was used to characterize the arborescent polystyrene cores, linear polydimethylsiloxanes and arborescent graft copolymers. The instrument consisted of a Waters Model 510 pump, a Waters R401 differential refractometer detector and a Jordi DVB 500 mm linear mixed bed column. Tetrahydrofuran served as the mobile phase at a flow rate of 1 mL/min. A linear polystyrene standards calibration curve was established using samples with molecular weights ranging from 500 to 4.75×10^6 g/mol. A higher detector sensitivity ($\times 1/4$ attenuation) was necessary for the characterization of polymers containing PDMS than for polystyrene samples ($\times 2$ attenuation). Toluene was also used as the mobile phase for the SEC characterization of some products.

5.2.5.2. Infra-red Spectroscopy

A Bomem MB-series FT-IR spectrophotometer was used to characterize the arborescent polydimethylsiloxane copolymers and to monitor the hydrolysis of the acetal-terminated polymeric precursors. The samples were analyzed as thin films obtained by casting a solution of the polymer (20 mg) in chloroform (1 mL) onto a polished NaCl plate. Spectra were obtained from 600 to 4000 cm^{-1} in the absorbance mode with a resolution of 4 cm^{-1} . The hydrolysis for the acetal-functionalized polystyrenes was confirmed by monitoring the disappearance of the *C-O-C* bending absorption (1120 cm^{-1}).

5.2.5.3. $^1\text{H-NMR}$ Spectroscopy

Routine composition analyses of the graft copolymers, chloromethylated core polystyrenes and initiator precursors were performed using $^1\text{H-NMR}$ spectroscopy on a Bruker AM-250 nuclear magnetic resonance spectrometer. Solutions in chloroform-*d*, with a concentration of 0.5-2% (w/v) were used in the measurements, and a minimum of 32 scans were acquired.

5.3. Results and Discussion

The development of proper purification and polymerization techniques for hexamethylcyclotrisiloxane (D_3) was a prerequisite for the successful preparation of the graft copolymers. For this reason, the preparation of linear PDMS using both *n*-butyllithium and lithium *n*-butoxide as initiators will be discussed first, followed by the synthesis of the polyfunctional grafting precursors. The results of the PDMS arborescent copolymer syntheses will then be presented.

5.3.1. Synthesis of Linear Polydimethylsiloxane

5.3.1.1. *n*-Butyllithium-Initiated Anionic Polymerization

The anionic polymerization of D_3 was accomplished using a two-stage reaction at room temperature. In the first stage, a seeding solution was prepared by reacting the monomer with *n*-butyllithium in toluene. The second stage consisted of adding THF as a promoter for the reaction. The size exclusion chromatography (SEC) trace obtained for a sample of linear PDMS prepared by this technique is shown in Figure 5.5. The polymer is characterized by an apparent (polystyrene equivalent) weight-average molecular weight $M_w = 2\,600$ g/mol and a narrow molecular weight distribution ($M_w/M_n = 1.10$). This result is in good agreement with the results published by Maschke and Wagner (6), and confirms that the monomer purification and seeded initiation techniques used are appropriate.

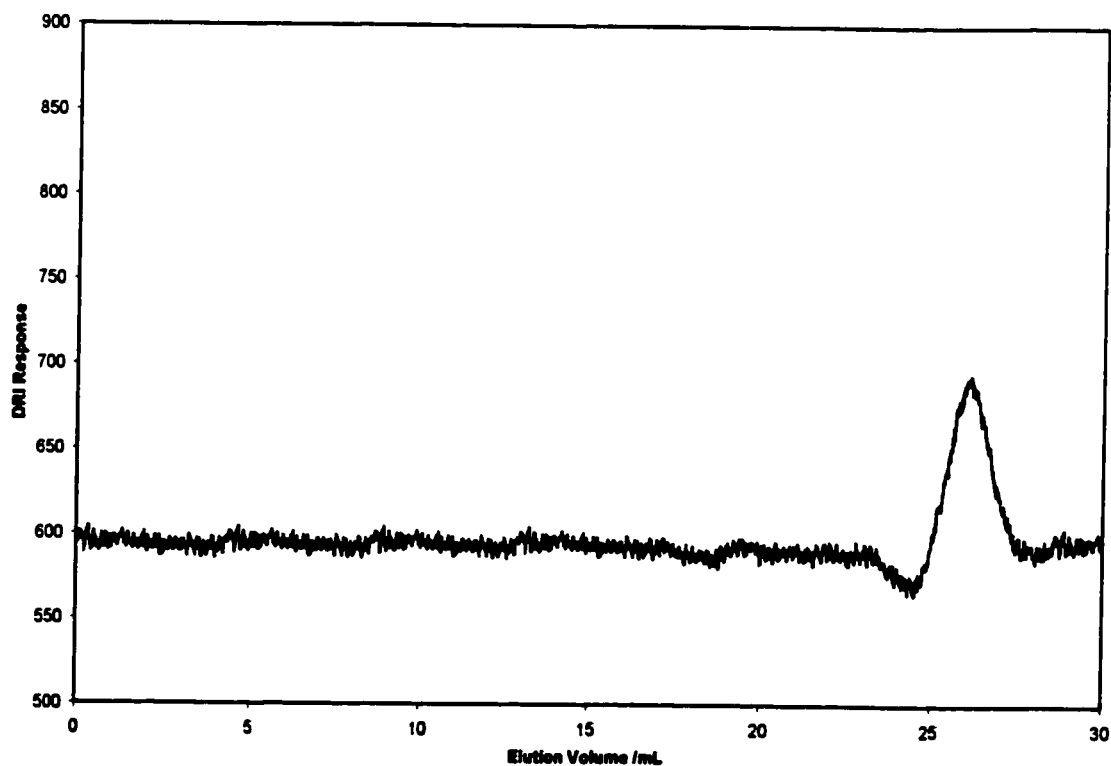


Figure 5.5. SEC trace for linear PDMS prepared using *n*-butyllithium

5.3.1.2. Lithium *n*-Butoxide-Initiated Anionic Polymerization

Two different approaches were considered for the reaction. In the first case, the seeding step was carried out in toluene and in the second case, in THF. The SEC characterization results for the products obtained by both methods are summarized in Table 5.1. A much narrower molecular weight distribution was obtained when the seeding step was carried out in toluene. This is generally considered to be the result of a fast rate of initiation relative to the rate of propagation (9), a primary requirement to achieve a narrow molecular weight distribution. A monomer conversion of 65% was attained after 48 hours. When initiation was carried out in THF, the resulting molecular weight distribution was broader, although a higher conversion of 80% was achieved after 48 hours.

Table 5.1. SEC Characterization results for linear PDMS samples prepared using lithium *n*-butoxide.

Initiation Solvent	$M_n / \text{g}\times\text{mol}^{-1}$	$M_w / \text{g}\times\text{mol}^{-1}$	M_w/M_n
Toluene	9 500	10 400	1.10
THF	18 400	26 400	1.43

5.3.2. Synthesis of Chloromethylated Polystyrene Cores

5.3.2.1. Chloromethylation of Linear Polystyrene

A sample of linear polystyrene was prepared by anionic polymerization initiated with *sec*-butyllithium. Characterization of the polymer by SEC yielded a $M_w = 21\ 000\ \text{g/mol}$ and a narrow molecular weight distribution ($M_w/M_n = 1.05$). The $^1\text{H-NMR}$ spectrum for a sample chloromethylated under the conditions described in Section 5.2.3.2 is shown in

Figure 5.6. A mole fraction $x = 28\%$ of chloromethylated units was determined by comparing the integrated peak areas corresponding to the chloromethyl protons (A, $\delta \approx 4.5$ ppm) and the aromatic protons (B, $\delta \approx 6.4$ -7.2 ppm) using the equation

$$\frac{2x}{5-x} = \frac{A}{B} \quad (5.1)$$

Analysis of the chloromethylated sample by SEC demonstrated that the molecular weight distribution remained essentially unchanged ($M_w = 21\,500$ g/mol and PDI = 1.07). This shows that no intermolecular cross-linking occurred during the chloromethylation reaction.

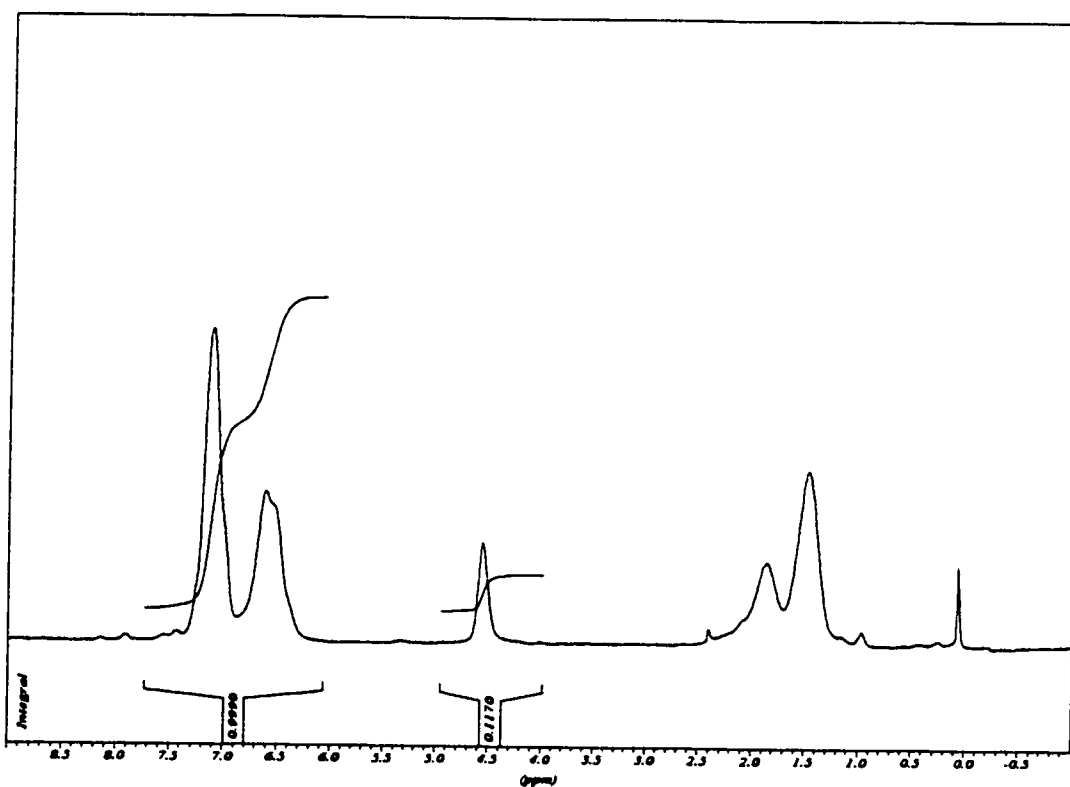


Figure 5.6. ^1H -NMR spectrum of linear Partially chloromethylated polystyrene

5.3.2.2. Living Free Radical Polymerization

The living stable free radical copolymerization technique provides three advantages when compared to the chloromethylation method for the preparation of a linear grafting substrate. A large amount of polymer can be prepared in a single reaction, the use of chloromethyl methyl ether (a known carcinogen) is avoided, and this approach is significantly less time-consuming than anionic polymerization. Furthermore, because it is a living polymerization technique, it allows control over the molecular weight, molecular weight distribution and degree of functionalization of the products in the same sense as the anionic polymerization/chloromethylation path.

Characterization of the styrene-4-chloromethylstyrene copolymer by SEC analysis yielded a $M_w = 23\ 000$ g/mol and a fairly narrow molecular weight distribution ($M_w/M_n = 1.15$). A 4-chloromethylstyrene content of 11 mol% in the copolymer was determined by $^1\text{H-NMR}$ analysis.

5.3.3. Preparation of Hydroxyl-Functionalized Core Polymers

5.3.3.1. Synthesis of Bifunctional Initiator

The steps involved in the preparation of the bifunctional initiator 6-lithiohexyl acetaldehyde acetal are described in Figure 5.7. The reaction between 6-chlorohexyl acetaldehyde acetal and metallic lithium is carried out in presence of an excess of lithium, to maximize the yield of the reaction and minimize the competing coupling reaction. The activity of the bifunctional initiator was determined using 1,3-diphenyl-2-propanone tosylhydrazone, based on a titration procedure reported in the literature (4). A concentration

of 0.86 M was determined from the average of three titrations.

5.3.3.2. Synthesis of Acetal-Functionalized Linear Polystyrene

The linear core with acetal pendant groups was prepared by coupling a linear polystyrene sample containing 28 mol% chloromethyl groups with 6-lithiohexyl acetaldehyde acetal, as outlined in Figure 5.8. The $^1\text{H-NMR}$ spectrum of the product, displayed in Figure 5.9, confirms the presence of $-\text{CH}_2-$ protons from the acetal group around 3.4 ppm. The success of the acetal groups hydrolysis reaction could also be confirmed using $^1\text{H-NMR}$ spectroscopy (Figure 5.10) from the disappearance of the characteristic acetal signals.

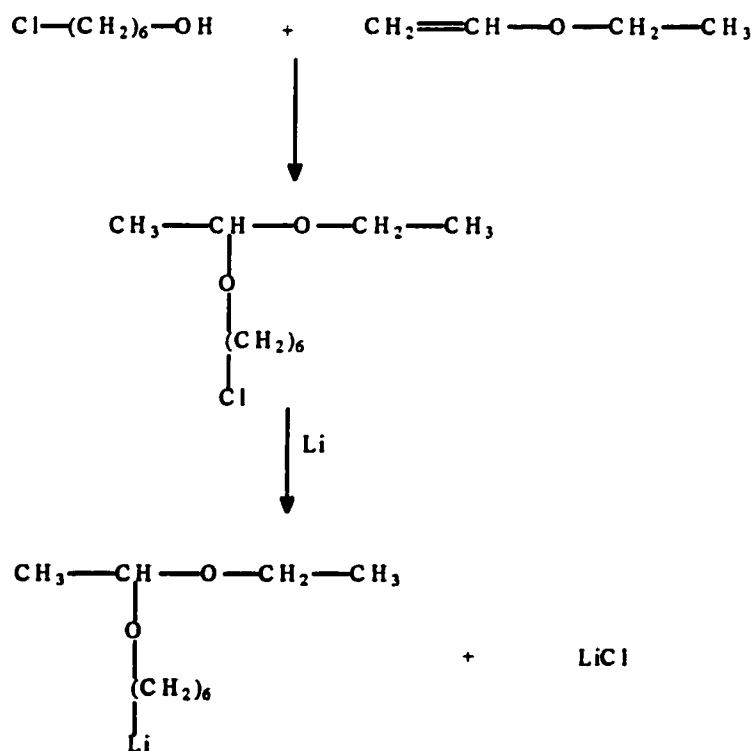


Figure 5.7. Synthesis of the bifunctional initiator 6-lithiohexyl acetaldehyde acetal

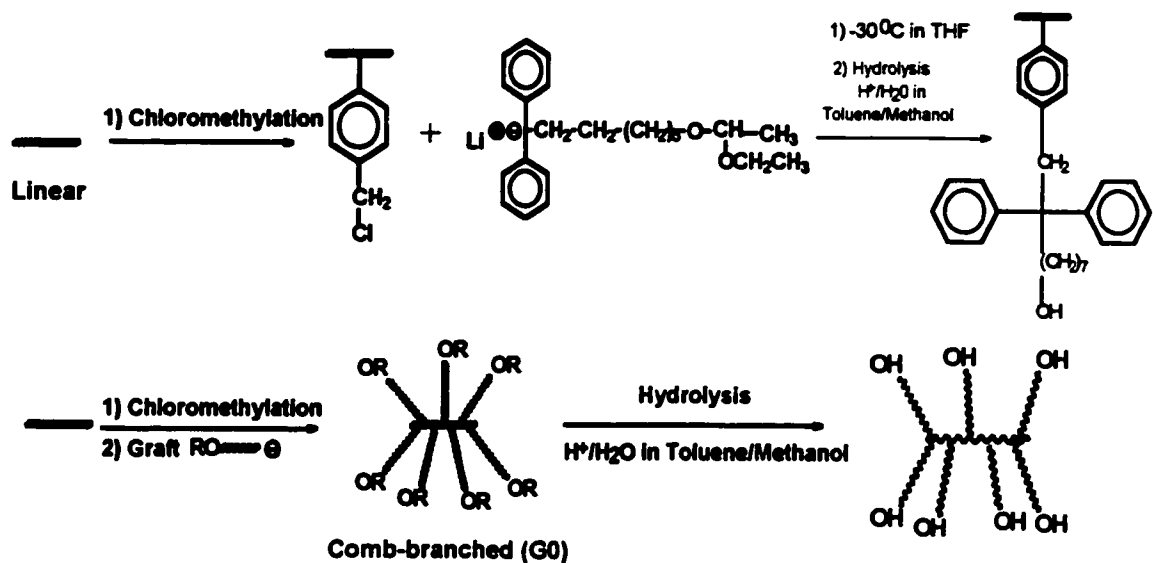


Figure 5.8. Synthesis of linear polystyrene with acetal pendant groups (top) and comb polystyrene with acetal end groups (bottom)

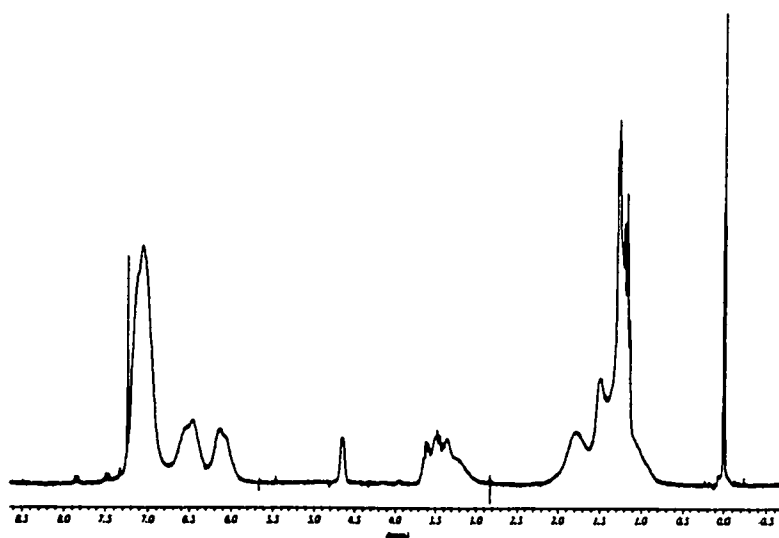


Figure 5.9. $^1\text{H-NMR}$ spectrum of acetal-functionalized linear polystyrene

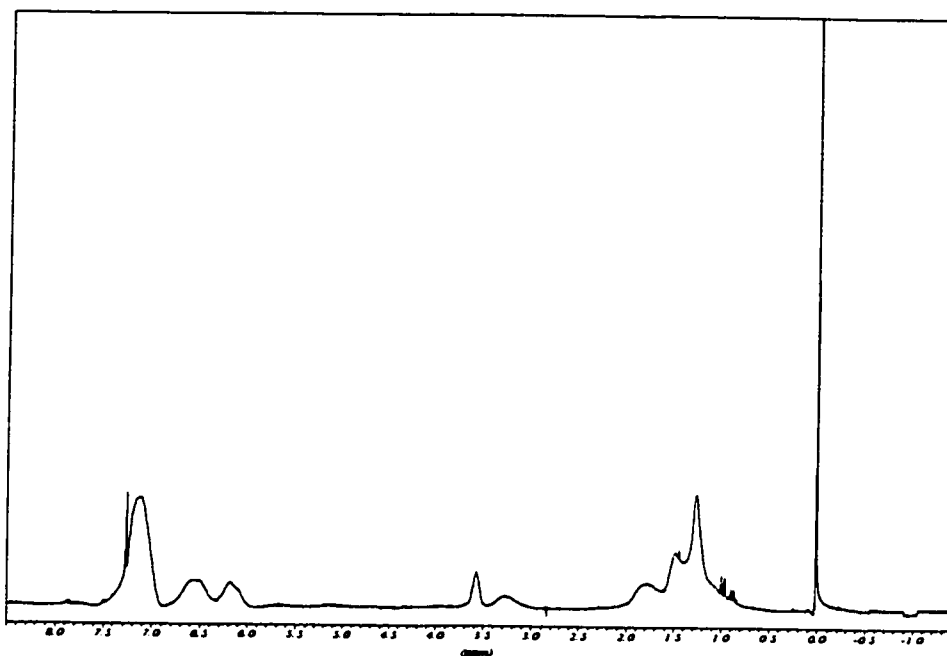


Figure 5.10. ^1H -NMR spectrum of hydroxyl-functionalized linear polystyrene

5.3.3.3. Synthesis of Acetal-Terminated Comb Polystyrene

The synthetic steps used to prepare comb polystyrenes with acetal end groups are outlined in Figure 5.8. Analysis of the crude grafting product by SEC yielded two main peaks (Figure 5.11). The high molecular weight (leftmost) peak, attributed to the graft copolymer, has an apparent $M_w = 338\ 000\ \text{g/mol}$, and $M_w/M_n = 1.2$. The second peak, at a lower molecular weight, corresponds to non-grafted linear polystyrene ($M_w = 30\ 000\ \text{g/mol}$, $M_w/M_n = 1.06$). The grafting efficiency can be determined from SEC measurements on the raw grafting product, by comparing the peak areas obtained for the graft polymer and for the non-grafted component. A prerequisite for the success of this approach is that the response of the differential refractometer (DRI) detector to each fraction in the sample must be the same. The refractive index of polymers is known to be

almost independent of molecular weight above 10^3 g/mol (10), so that the response from the DRI detector becomes only a function of the concentration of the species eluted from the SEC column and independent of molecular weight. All the polymers analyzed in this work have a molecular weight well above 10^3 g/mol. Under these conditions, the grafting efficiency can be determined from the ratio of areas for the graft polymer peak over the total peak areas for the graft polymer and the non-grafted component. The grafting efficiency determined by this method was 85 % for the acetal-terminated comb polystyrene.

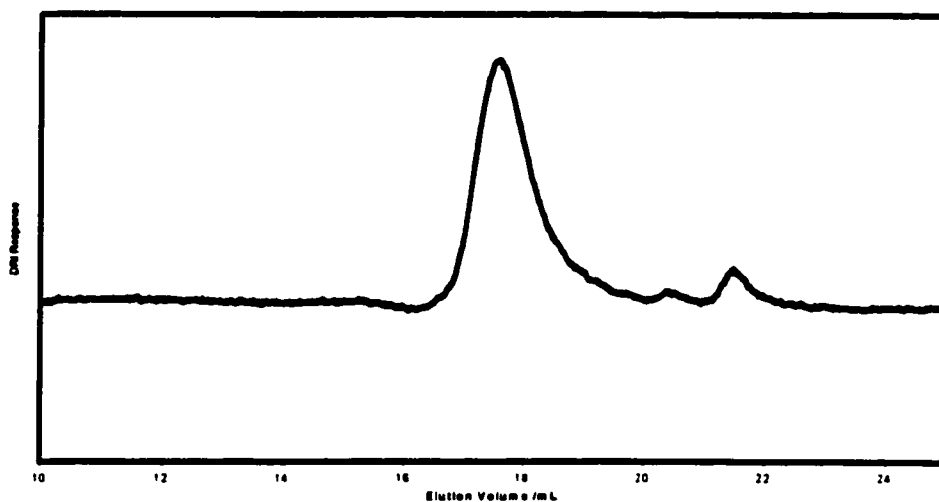


Figure 5.11. SEC trace for the crude acetal-terminated comb polystyrene synthesized

5.3.3.4. Fractionation and Hydrolysis of Acetal-Terminated Comb Polystyrene

Fractionation and hydrolysis of the acetal-terminated polystyrene cores were performed simultaneously. Successful fractionation of the crude product was confirmed by the disappearance of the peak corresponding to the non-grafted polystyrene component.

The success of the hydrolysis reaction could be monitored by IR analysis using the acetal *C-O-C* absorption at 1120 cm^{-1} . The FT-IR spectra for the acetal- and hydroxyl-terminated comb polystyrenes are compared in Figure 5.12. Hydrolysis of the acetal groups is accompanied by the disappearance of the weak absorption at 1120 cm^{-1} . While the peak at 1120 cm^{-1} is weak, due to the low concentration of acetal groups in the polymer, the peaks clearly disappears from the spectrum after the reaction. The hydrolysis of acetal end groups in the arborescent polymers could not be verified by $^1\text{H-NMR}$ spectroscopy, due their low concentration.

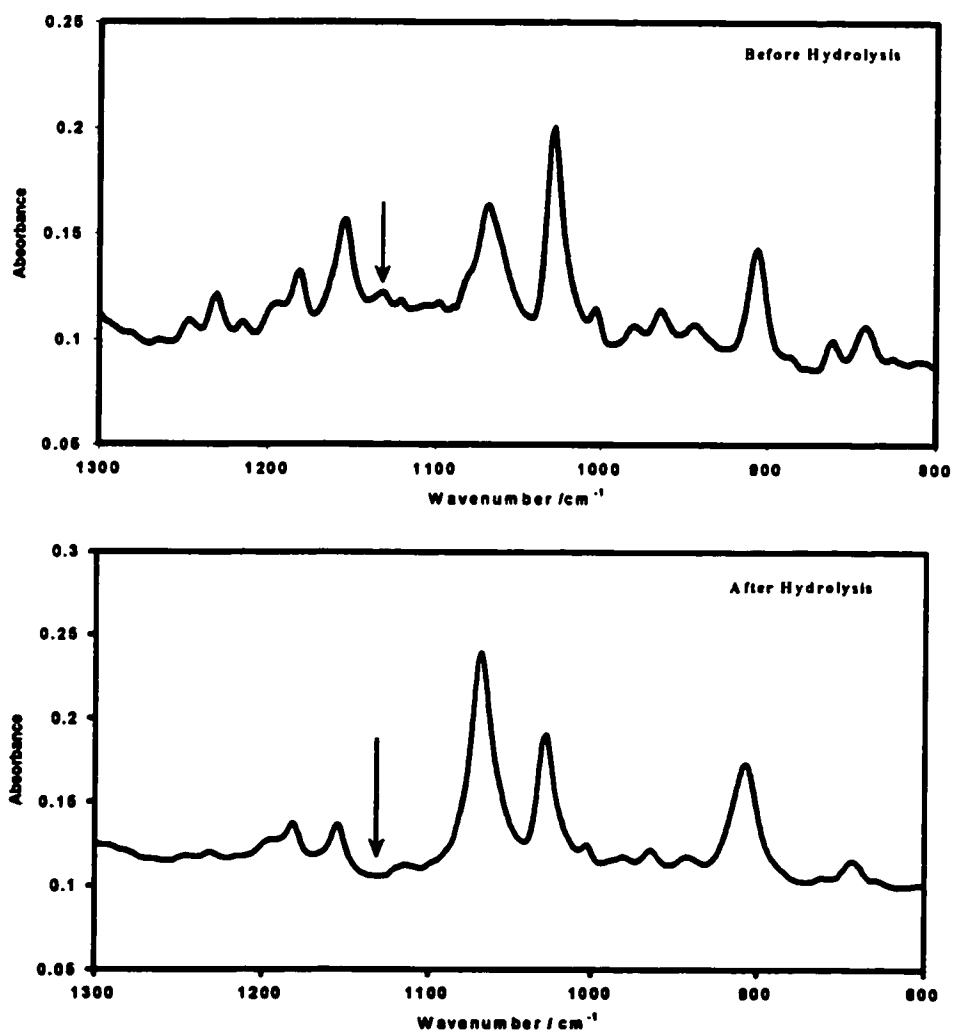


Figure 5.12. FT-IR spectra for the acetal-terminated comb PS before and after hydrolysis

5.3.3.5. Metal-Halogen Exchange Reaction

A metal-halogen exchange reaction was used to deactivate any residual chloromethyl groups that may still be present in the hydroxyl-functionalized polystyrene substrates. While no measurable amounts of residual chloromethyl groups could be detected by $^1\text{H-NMR}$ analysis of the grafting substrates, it was still considered preferable to carry out the metal-halogen exchange reaction. This is important because the presence of residual chloromethyl sites can lead to intermolecular cross-linking reactions, during the titration of the hydroxyl groups with lithium naphthalide, according to the reaction shown in Figure 5.13 (3).

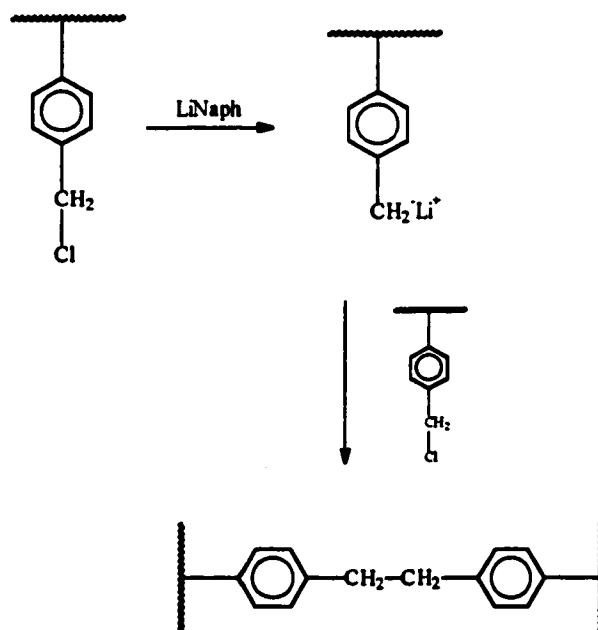


Figure 5.13. Intermolecular cross-linking reactions involving metal-halogen exchange

The exchange reaction allows the substitution of the chlorine atom with lithium. The benzyllithium species generated are subsequently converted to methyl groups upon hydrolysis with water. Since the metal-halogen exchange is an equilibrium reaction (11), a

large excess of *n*-butyllithium was used. The reaction was also carried out at low temperature (-78°C), because under these conditions the kinetics of the reaction is very fast relative to the nucleophilic coupling reaction with *n*-butyl anions (12).

The adequacy of the metal-halogen exchange reaction conditions was confirmed by comparison of SEC traces of the grafting substrate before and after the exchange reaction: No change in either the peak shape or in the apparent molecular weight could be observed.

5.3.3.6. Synthesis of G1 Hydroxyl-Terminated Polystyrene

The synthesis of a G1 hydroxyl-terminated polystyrene was carried out by Jennifer Wiebe during a fourth-year undergraduate research project (13), based on the procedure described for the preparation of a hydroxyl-functionalized comb (G0). This was done by grafting polystyryl anions with a $M_w = 5\ 100\ \text{g/mol}$ and $M_w/M_n = 1.03$, prepared using the 6-lithiohexyl acetaldehyde acetal initiator, onto a 25 mol% chloromethylated comb polymer with $M_w = 5\ 900\ \text{g/mole}$ side chains (13). A grafting efficiency of 87% was determined by comparison of the integrated peak areas in the raw product. The graft copolymer had an apparent weight-average molecular weight $M_w = 127\ 000\ \text{g/mol}$ and $M_w/M_n = 1.08$. The raw grafting product was fractionated and hydrolyzed in this project, as described in Section 5.2.3.7. The success of the fractionation procedure was verified by SEC analysis. Acetal group hydrolysis was confirmed by the disappearance of the IR absorption at $1120\ \text{cm}^{-1}$.

5.3.4. Synthesis of Arborescent PDMS Graft Copolymers

The synthetic steps leading to arborescent PDMS graft copolymers are illustrated in

Figure 5.14, using a G1 arborescent polystyrene substrate with hydroxyl end-groups as an example. Titration of the hydroxyl groups with a lithium naphthalide solution to a faint stable green coloration yields lithium alcoholate functionalities. These active centers then serve to initiate the anionic ring opening polymerization of hexamethylcyclotrisiloxane, to give arborescent copolymers with end-linked PDMS segments.

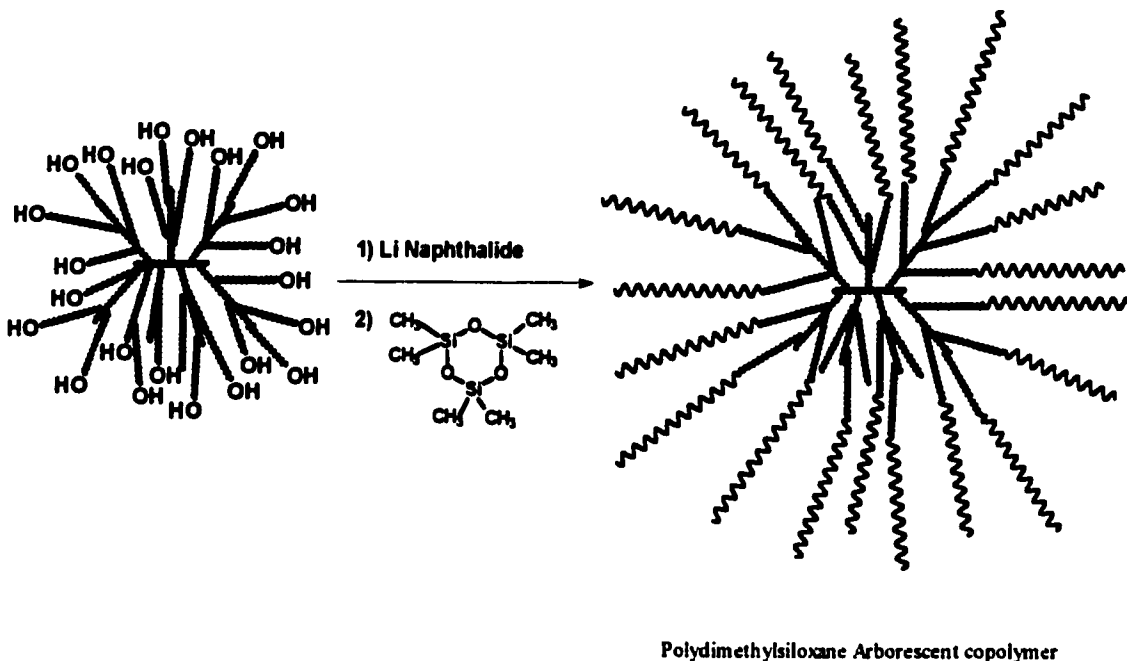


Figure 5.14. Arborescent PDMS graft copolymer synthesis by a *grafting from* method

5.3.4.1. PDMS Copolymers Based on G1 Hydroxyl-Terminated Core Polymer

The G1 arborescent polystyrene with hydroxyl end groups was used as a polyfunctional initiator in a series of grafting reactions with D_3 under different conditions. Extensive aggregation of the core polymer was observed as lithium naphthalide was added to the hydroxylated polystyrene in the core titration process. Analysis by SEC of the crude grafting product obtained in a first attempt without cryptand yielded two peaks (Figure 5.15). The high molecular weight peak, with $M_w = 255\ 000\ \text{g/mol}$ and

$M_w/M_n = 1.11$, is attributed to the PDMS graft copolymer. The second peak, at a lower molecular weight ($M_w = 24\ 000\ \text{g/mol}$, $M_w/M_n = 1.07$), corresponds to non-grafted linear PDMS. There is a significant, albeit modest increase in the apparent molecular weight of the graft copolymer relative to the core ($M_w = 127\ 000\ \text{g/mol}$, $M_w/M_n = 1.08$).

To reduce aggregate formation a cryptand, Kryptofix 222 (structure given in Figure 2.17) was incorporated in subsequent reactions. The role of the cryptand is to form a complex with the lithium counterion. This not only reduces the aggregation tendency of the propagating centers, but also increases their reactivity. The cryptand was used in excess (30 mol%) relative to the hydroxyl groups present on the grafting substrate.

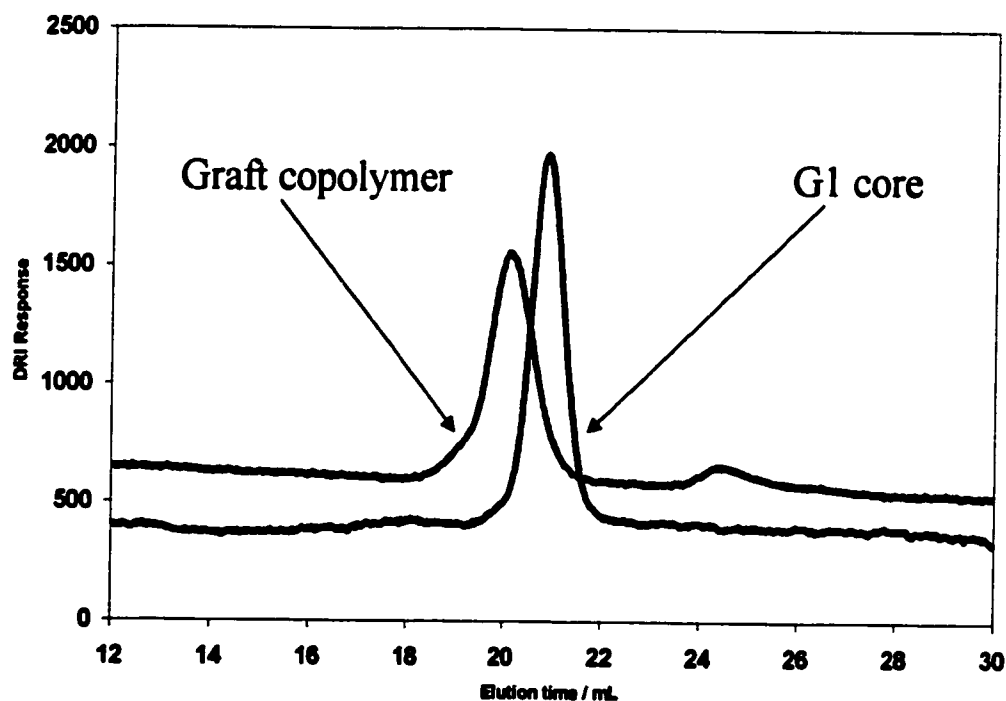


Figure 5.15. SEC traces for G1 hydroxyl-terminated core polymer and arborescent PDMS graft copolymer obtained without cryptand

The SEC traces obtained for the G1 hydroxyl-functionalized core and for the PDMS graft copolymer obtained in a first reaction attempt with cryptand are compared in Figure 5.16. The trace for the PDMS copolymer, obtained at $\frac{1}{4}$ attenuation on the DRI detector, shows a marked increase in molecular weight relative to the core. There are also two overlapping peaks present in the chromatogram. During the core titration procedure, it was noticed that some of the core polymer adhered to the wall of the ampule above the solution level, as a result of too vigorous stirring. The shoulder in the chromatogram, at an elution volume $V_e \approx 21$ mL, is likely due to the small amount of non-titrated polyfunctional core that adhered to the wall of the ampule, since it appears at the same elution volume. The DRI response for the core polymer is very large, since the detector is much more sensitive to the polystyrene component than to the PDMS component (refractive index differences $n_{PS} - n_{THF} = 0.19$ and $n_{PDMS} - n_{THF} = 0.035$).

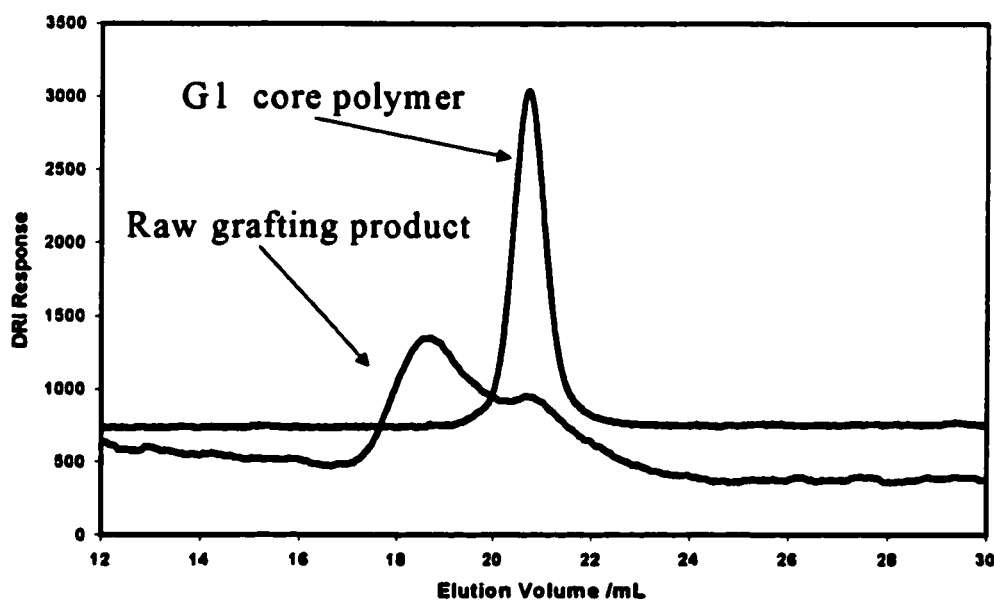


Figure 5.16. SEC traces for G1 hydroxyl-terminated core polymer and arborescent PDMS graft copolymer obtained with cryptand, first attempt

To verify this hypothesis a second copolymerization was carried out under the same conditions used in the first attempt, this time using a lower stirring rate in the core titration process, to make sure that the core polymer was completely titrated. The SEC trace for the new graft copolymer obtained under these conditions (Figure 5.17) shows one single peak corresponding to the PDMS arborescent copolymer without residual core polymer. The graft copolymer has an apparent weight-average molecular weight $M_w = 474\ 000\ \text{g/mol}$ and $M_w/M_n = 1.3$. Oligomeric siloxane species with a broad molecular weight distribution also seem to be present in the product, as indicated by a shift in the baseline of the SEC chromatogram on the right of the copolymer peak. The raw product was purified by fractionation before composition analysis by $^1\text{H-NMR}$ spectroscopy.

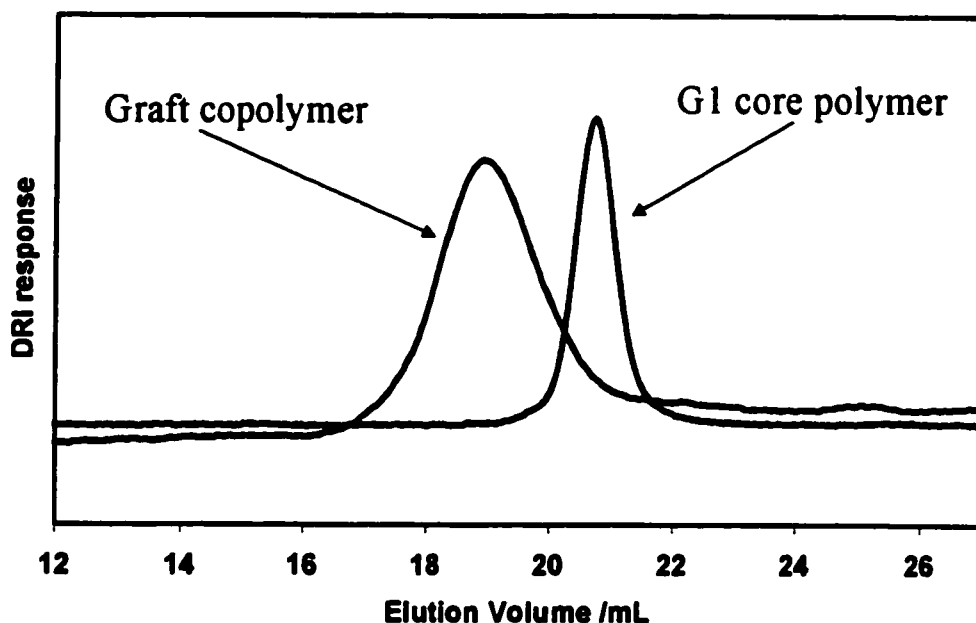


Figure 5.17. SEC traces for G1 hydroxyl-terminated core polymer and arborescent PDMS graft copolymer obtained with cryptand, second attempt

Composition analysis of the fractionated PDMS graft copolymer by $^1\text{H-NMR}$ spectroscopy (Figure 5.18) indicated a polydimethylsiloxane content of 92 % by weight. The mole fraction x of siloxane units in the copolymer was determined by comparing the integrated areas for peaks corresponding to the silicon-bound methyl protons (A, $\delta \approx 0.1$ ppm) with the area of the peaks for the aromatic protons (B, $\delta \approx 6.4-7.2$ ppm):

$$\frac{6x}{5(1-x)} = \frac{A}{B} \quad (5.1)$$

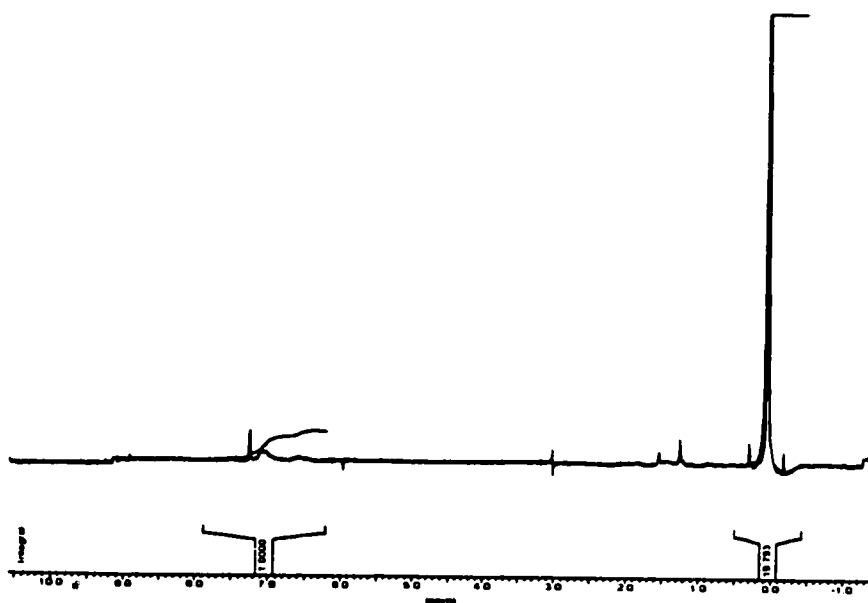


Figure 5.18. $^1\text{H-NMR}$ spectrum of fractionated arborescent PDMS graft copolymers

Based on these results, the synthesis of arborescent PDMS graft copolymers is considered to be successful. However, it cannot be excluded that a small amount of linear PDMS (less than 5% by weight) be present as a contaminant in the fractionated copolymer. It was determined experimentally that graft copolymer samples intentionally contaminated

with 5 % pure PDMS by weight yielded a detectable second peak in a SEC chromatogram at the ¼ attenuation setting on the DRI detector, normally used to analyze the copolymers.

FT-IR spectra obtained for linear PDMS, the G1 polystyrene core and the arborescent PDMS graft copolymer are compared in Figure 5.19. PDMS is characterized by a broad *Si-O-Si* absorption at 1000-1110 cm^{-1} and a *Si-CH₃* absorption at 1250 cm^{-1} . Polystyrene has three absorptions (at 1451, 1492 and 1600 cm^{-1} characteristic of aromatic carbon-carbon bonds) that do not overlap with those of PDMS. The FT-IR spectrum of the arborescent PDMS graft copolymer clearly shows the presence of absorptions characteristic of the PDMS and polystyrene components.

5.3.4.2. PDMS Copolymer Based on Comb Polystyrene Core

The synthesis of a PDMS graft copolymer based on a hydroxyl-terminated comb polystyrene core was carried out in the presence of cryptand. Analysis of the crude product by SEC, at ¼ attenuation on the DRI detector, yielded two peaks (Figure 5.20). The high molecular weight peak ($M_w = 580\,000\text{ g/mol}$, $M_w/M_n = 1.2$) is attributed to the PDMS graft copolymer. The second peak, at a lower molecular weight, corresponds to non-grafted linear PDMS ($M_w = 50\,000\text{ g/mol}$, $M_w/M_n = 1.2$). There is an increase in the apparent weight-average molecular weight of the PDMS graft copolymer relative to the core ($M_w = 338\,000\text{ g/mol}$, $M_w/M_n = 1.2$).

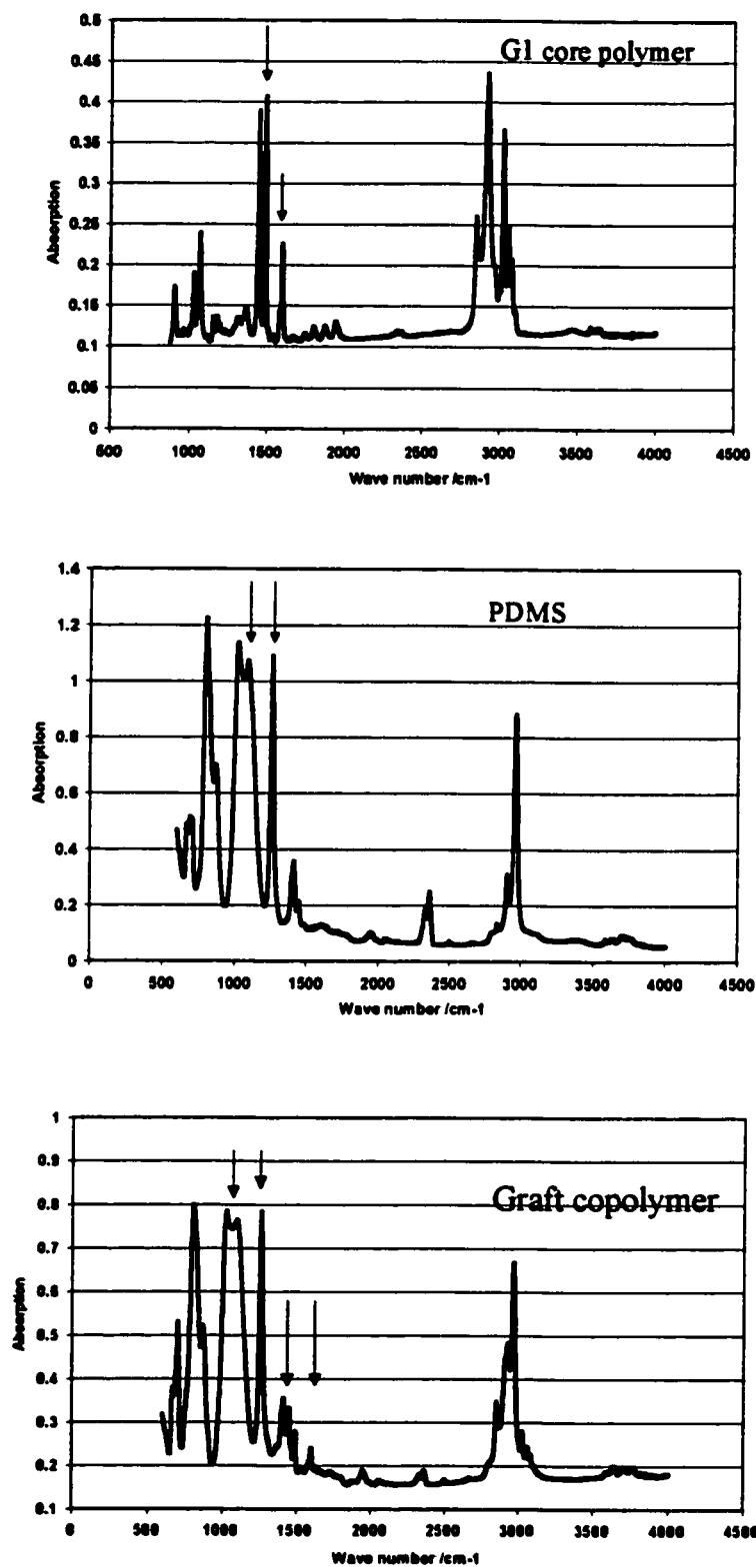


Figure 5.19. FT-IR spectra for the G1 core polymer, linear PDMS and arborescent graft copolymer

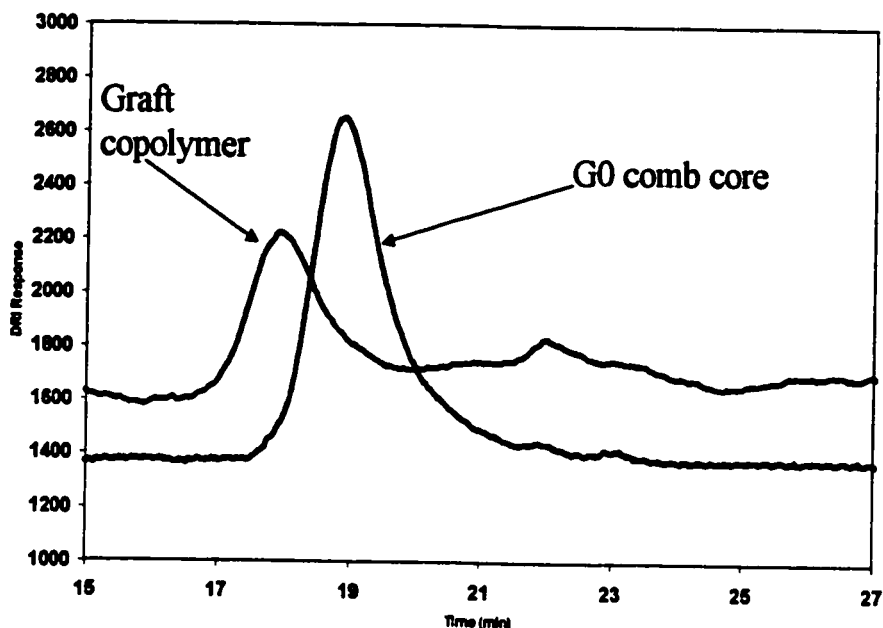


Figure 5.20. SEC traces for G0 core polymer and arborescent PDMS graft copolymer

5.3.4.3. PDMS Copolymer Based on Hydroxyl-Functionalized Linear Polystyrene Core

The synthesis of a PDMS graft copolymer based on a linear polystyrene substrate carrying hydroxyl Pendant groups was carried out in the presence of cryptand. Analysis of the PDMS graft copolymer by SEC indicated only a small increase in molecular weight ($M_w = 51\ 000\ \text{g/mol}$, $M_w/M_n = 1.3$) relative to the core ($M_w = 49\ 000\ \text{g/mol}$ and $M_w/M_n = 1.3$). It is unclear whether the small shift is due to a lower grafting efficiency in this system than in the previous reactions. The comb structure and highly flexible nature of the PDMS side chains could have coincidentally led to a small coil with a hydrodynamic volume comparable to the grafting substrate. Composition analysis of the graft copolymer by $^1\text{H-NMR}$ spectroscopy nonetheless indicated the presence of a significant polydimethylsiloxane content in the copolymer.

5.4. Conclusions

Arborescent graft copolymers incorporating over 90 % (w/w) polydimethylsiloxane (PDMS) were successfully prepared from hydroxyl-functionalized polystyrene cores using a *grafting from* procedure. The success of the approach was confirmed for linear, comb-branched and twice-grafted (G1) arborescent polystyrenes acting as polyfunctional initiators in the anionic polymerization of hexamethylcyclotrisiloxane (D_3).

An alternate method for the synthesis of arborescent PDMS graft copolymers could be based on a hydrosilylation route. In this scheme, hydrosilyl-terminated PDMS segments could be prepared by capping the living PDMS chains with chlorodimethylsilane. Coupling of the PDMS segments with an arborescent polyisoprene graft copolymer could be then achieved in the presence of chloroplatinic acid.

5.5. References

1. Gauthier, M.; Möller, M. *Macromolecules* **1991**, *24*, 4548.
2. Kee, R. A.; Gauthier, M. *Polym. Mater. Sci. Eng.* **1997**, *77*, 177.
3. Gauthier, M.; Tichagwa, L.; Downey, J. S.; Gao, S. *Macromolecules* **1996**, *29*, 519.
4. Lipton, M. F.; Sorensen, C. M.; Sadler, A. C.; Shapiro, R. H. *J. Organomet. Chem.* **1980**, *186*, 155.
5. Marvel, C. S.; Porter, P. K. *Org. Synth.* **1951**, *1*, 377.
6. Maschke, U.; Wagner, T. *Makromol. Chem.* **1992**, *193*, 2453.
7. Kazmaier, P. M.; Daimon, K.; Georges, M. K.; Hamer, G. K.; Veregin, R. P. N. *Macromolecules* **1997**, *30*, 2228.

8. Eaton, P. E.; Cooper, G.F.; Johnson, R. C.; Mueller, R. H. *J. Org. Chem.* **1972**, *37*, 1947.
9. Bywater, S.; Worsfold, D. J. *J. Phys. Chem.* **1966**, *70*, 162.
10. Huglin, M. B. In *Light Scattering From Polymer Solutions*; Huglin, M. B., Ed.; Academic: New York, 1972; Chapter 6.
11. Winkler, H. J. S.; Winkler, H. J. *Am. Chem. Soc.* **1966**, *88*, 964.
12. Gilman, H.; Langham, W.; Moore, F. W. *J. Am. Chem. Soc.* **1940**, *62*, 2327.
13. Wiebe, M. J. *Arborescent Polydimethylsiloxane Copolymers: A Synthetic Investigation*; Chem 492 Project Report, University of Waterloo: Waterloo, 1996.

Chapter 6: Arborescent Poly(ϵ -caprolactone) Graft Copolymers

6.1. Introduction

Sequential anionic polymerization has been employed for the synthesis of block copolymers based on ϵ -caprolactone (1,2). Triblock copolymers with a poly(ethylene glycol) midblock were prepared by anionic ring opening polymerization in tetrahydrofuran (THF) at room temperature. The potassium salt of poly(ethylene glycol) was first generated, and used as a macroinitiator for the polymerization of ϵ -caprolactone. The synthesis of the block copolymers is described in Figure 6.1. A high molecular weight and a high conversion were achieved in a short time (5 minutes), but the copolymer had a broad molecular weight distribution.

Polyol molecules such as erythritol, xylitol and sorbitol were also used as initiators for the ring-opening polymerization of ϵ -caprolactone to yield star-branched poly(ϵ -caprolactone)s (3). These alcohols bear 4, 5 and 6 reactive hydroxyl groups, respectively. The polymerizations were carried out in the bulk at 140^oC in the presence of stannous octoate. The molecular weight distribution of the polymers was narrow initially, but M_w/M_n increased to 1.8-1.9 at higher conversion.

The objective of this project was to demonstrate the synthesis of arborescent graft copolymers containing poly(ϵ -caprolactone) segments. These materials are expected to

have interesting properties in terms of biocompatibility, in combination with the unusual properties of branched polymer systems (4).

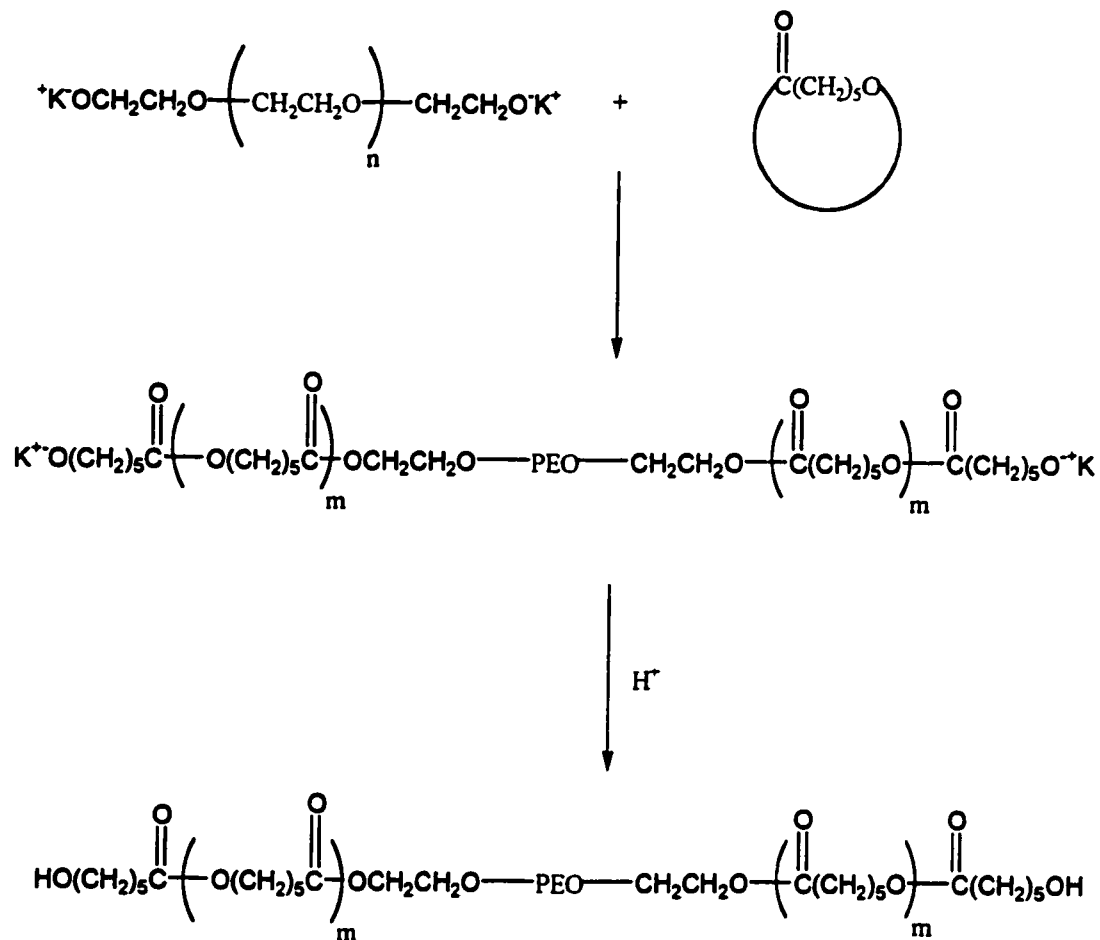


Figure 6.1. Synthetic scheme for the preparation of poly(ϵ -caprolactone)-*b*-poly(ethylene glycol)-*b*-poly(ϵ -caprolactone)

6.2. Experimental Procedures

6.2.1. Monomer and Reagent Purification

The ϵ -caprolactone monomer (Aldrich, 99%) was first purified by distillation from calcium hydride under reduced pressure and stored under nitrogen at -5°C . The monomer

was further purified over calcium hydride (2 g for 4 g monomer) immediately prior to polymerization, using the manifold shown in Figure 5.1. The monomer was degassed with three successive freeze-pump-thaw cycles under vacuum, and slowly recondensed to an ampule with a PTFE stopcock. The ampule was then filled with purified nitrogen and stored at -5°C until the polymerization.

Tetrahydrofuran (Caledon, Reagent) was dried by refluxing with sodium-benzophenone ketyl under dry nitrogen for two hours and distilled immediately prior to use. A lithium naphthalide solution in THF was prepared in a three-necked flask containing a glass-encased magnetic stirring bar. After the flask was evacuated, flamed and filled with nitrogen, dry THF (200 mL) was added followed by naphthalene (6.4 g, 50 mmol, Baker) and lithium metal (1.62 g, 42 mmol, Aldrich). After stirring overnight at room temperature, the dark green-colored solution was filtered using a Schlenk funnel and stored in a Schlenk flask at -20°C until needed. All other reagents were used as obtained from the suppliers unless otherwise indicated.

6.2.2. Anionic Polymerization of ϵ -Caprolactone Initiated with Lithium *n*-Butoxide

In order to establish satisfactory conditions for the preparation of poly(ϵ -caprolactone) using a lithium alcoholate initiator, a model polymerization initiated by lithium *n*-butoxide was performed. The reaction was carried out in a three-necked flask mounted on the high-vacuum line with an ϵ -caprolactone monomer ampule (10 g, 0.0876 mol) and the dry THF line from the still. The apparatus was evacuated, flamed and filled with nitrogen. Tetrahydrofuran (100 mL) and 1-butanol (0.2 mL, 2.0 mmol)

were added to the flask, and the alcohol was titrated a lithium naphthalide solution (0.95 M) until a persistent green color was obtained. The monomer was added to the flask and the polymerization was allowed to proceed for 10-12 minutes, before termination with a mixture of HCl and water (25/75 by volume). The polymer solution was evaporated, first on a rotary evaporator and then under vacuum, and the product was characterized by size exclusion chromatography (SEC).

6.2.3. Synthesis of Copolymers

6.2.3.1. Copolymer Based on Linear Polystyrene with Hydroxyl Pendant Groups

The synthesis of a copolymer based on a linear hydroxyl-functionalized polystyrene core was done in an ampule sealed with a PTFE stopcock. The hydroxyl-functionalized polystyrene (250 mg, 0.37 meq hydroxyl units) and a cryptand, Kryptofix 222 (180 mg, 0.487 mmol) were loaded in an ampule and purified by azeotropic distillation as described in Section 5.2.1.4. After the purification the stopcock was removed and the solution was titrated with a lithium naphthalide solution (0.95 M) until a persistent green color was observed. The ampule was filled with nitrogen, sealed and the solution left to stir overnight.

The ampule was then mounted on the monomer purification manifold shown in Figure 5.1 and immersed in liquid nitrogen. The manifold was evacuated, flamed and filled with nitrogen. The monomer (3.00 g, 0.013 mol), purified as described in Section 6.2.1, was recondensed to the ampule. When transfer of the monomer was completed the ampule was quickly thawed, filled with nitrogen and sealed. The polymerization reaction was allowed to proceed for 10-12 minutes at room temperature, and terminated with a mixture of HCl and deionized water (25/75 by volume). The solvent was removed, first on a rotary evaporator

and then under vacuum. The graft copolymer was characterized by SEC analysis.

6.2.3.2. Copolymer Based on Hydroxyl-Terminated G1 Arborescent Polystyrene

The synthesis of a poly(ϵ -caprolactone) arborescent copolymer incorporating a hydroxyl-terminated G1 arborescent polystyrene core was also carried out using the procedure described in Section 6.2.3.1. The reagents used were 250 mg arborescent polystyrene core (0.05 meq hydroxyl units), 30 mg (0.078 mmol) of cryptand and 3 g (0.013 mol) of monomer. It was necessary to break down aggregates by sonicating the ampule for *ca.* 20 minutes before addition of the monomer.

6.2.4. Characterization

Size exclusion chromatography (SEC) was used to characterize the arborescent polystyrene cores, the linear poly(ϵ -caprolactone) and the arborescent graft copolymer samples prepared. The instrument consisted of a Waters Model 510 pump, a Waters R401 differential refractometer detector and a Jordi DVB 500 mm linear mixed bed column. Tetrahydrofuran served as the mobile phase at a flow rate of 1 mL/min. A linear polystyrene standards calibration curve was established using samples with molecular weights ranging from 500 to 4.75×10^6 g/mol.

6.3. Results and Discussion

6.3.1. Synthesis of Linear Poly(ϵ -caprolactone)

The linear poly(ϵ -caprolactone) sample prepared using lithium *n*-butoxide yielded an apparent (polystyrene equivalent) $M_w = 4730$ g/mol and $M_w/M_n = 1.45$ by SEC analysis, compared to a target molecular weight of 5 000 g/mol. The SEC trace for the product is shown in Figure 6.2. The monomer conversion obtained was around 90%. The broad molecular weight distribution observed is in good agreement with the results published by Morton and Wu (5). Broadening of the molecular weight distribution was explained in Section 2.5.1 by the occurrence of intramolecular and intermolecular transesterification reactions.

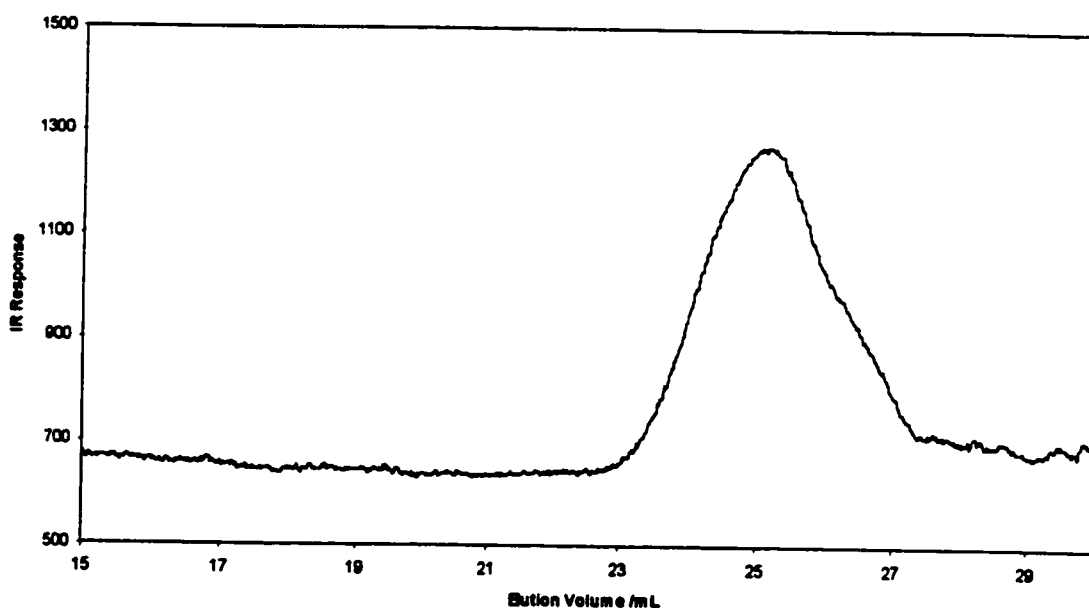


Figure 6.2. SEC trace for linear poly(ϵ -caprolactone) obtained from lithium *n*-butoxide

6.3.2. Arborescent Poly(ϵ -caprolactone) Graft Copolymers

The synthesis of arborescent poly(ϵ -caprolactone) copolymers was achieved using a *grafting from* technique. Titration of the hydroxyl groups on the polyfunctional precursor with lithium naphthalide served to generate lithium alcoholate functionalities. These active centres were subsequently used to initiate the anionic ring opening polymerization of ϵ -caprolactone to give the copolymers. A cryptand (Kryptofix 222) was incorporated in all the reactions, to decrease the strong aggregation tendency of the hydroxylated polystyrene substrates after titration with lithium naphthalide. The cryptand was used in excess (30 mol%) relative to the hydroxyl groups present on the hydroxylated polystyrenes.

6.3.2.1. Poly(ϵ -caprolactone) Copolymer Based on Linear Polystyrene with Pendant Hydroxyl Groups

The SEC traces obtained for the hydroxyl-functionalized linear polystyrene precursor and for the poly(ϵ -caprolactone) graft copolymer are compared in Figure 6.3. The grafting substrate was obtained from a coupling reaction of the bifunctional initiator 6-lithiohexyl acetaldehyde acetal with a chloromethylated linear polystyrene sample (28 mol% chloromethyl groups), as described in Section 5.2.3.5. The hydroxylated polymer is characterized by a $M_w = 49\,000$ g/mol and $M_w/M_n = 1.3$. Analysis of the crude grafting product by SEC yielded two main fractions. The high molecular weight peak at an elution volume $V_e \approx 22$ mL is attributed to the poly(ϵ -caprolactone) graft copolymer. The second fraction, consisting of multiple overlapping peaks from $V_e \approx 24$ mL, is attributed to non-grafted oligomeric and/or low molecular weight poly(ϵ -caprolactone). Unreacted monomer is not visible on the chromatogram, because its elution volume lies outside the limits of the plot ($V_e \approx 30$ -31 mL). There is a significant increase in the apparent molecular weight of the

poly(ϵ -caprolactone) graft copolymer ($M_w = 89\,000$ g/mol and $M_w/M_n = 1.45$) relative to the hydroxylated substrate ($M_w = 49\,000$ g/mol and $M_w/M_n = 1.3$).

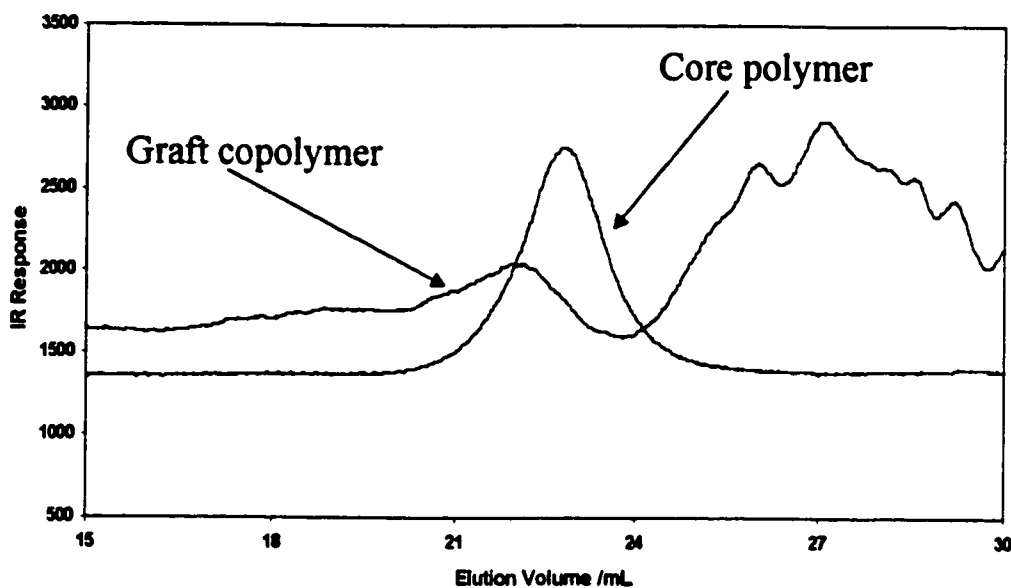


Figure 6.3. Arborescent poly(ϵ -caprolactone) prepared from linear polystyrene with hydroxyl pendant groups

The formation of oligomeric species, not observed in the model reaction using lithium *n*-butoxide as initiator, could be explained in a few different ways. The core polymer substrate may have been accidentally overtitrated with lithium naphthalide, or else contaminated by protic impurities prior to the titration. Another possibility is the enhancement of transesterification reactions of the type discussed in Section 2.5.1. In the preparation of the linear polymer, the propagating centres remain relatively far apart from each other, because of the low concentration of living ends in the reaction. In the polymeric initiators, however, each substrate molecule contains many propagating centres that lie in close proximity to each other. Under these conditions the occurrence of intramolecular

transesterification reactions (both *intrachain* and *interchain*, within the branched structure), leading to depolymerization, the elimination of cyclic oligomeric species and the cleavage of side chains should be enhanced.

The SEC trace for the graft copolymer is a lot noisier than for the precursor polymer. This is because of the high detector sensitivity ($\times 1/4$ attenuation) necessary to detect the copolymer using the differential refractometer. The DRI response for the core polymer is very large, since the refractive index difference between polystyrene and the THF mobile phase is large ($n_{\text{PS}} - n_{\text{THF}} = 0.19$) (6). For polycaprolactone in THF the refractive index difference ($n_{\text{PCL}} - n_{\text{THF}} = 0.064$) (7) is three times lower, and so is the DRI detector sensitivity. Considering the fact that a significant amount of oligomeric polycaprolactone was formed in the reaction, the amount of graft copolymer actually injected in the SEC column for the analysis is also decreased.

6.3.2.2. Poly(ϵ -caprolactone) Copolymer Based on G1 Core

The SEC traces for the G1 hydroxyl-functionalized core and the poly(ϵ -caprolactone) graft copolymer are compared in Figure 6.4. The SEC trace for the graft copolymer indicates the presence of two main fractions, as observed in the previous case. The high molecular weight peak is attributed to the arborescent poly(ϵ -caprolactone) graft copolymer. The second (multimodal) peak at a lower molecular weight is attributed to non-grafted oligomeric and/or low molecular weight poly(ϵ -caprolactone). There is a small increase in the molecular weight of the poly(ϵ -caprolactone) graft copolymer ($M_w = 137\,000$ g/mol, $M_w/M_n = 1.15$) relative to the hydroxylated substrate ($M_w = 127\,000$ g/mol, $M_w/M_n = 1.08$). The reactions based on a linear polymeric initiator substrate and a G1 branched

polyfunctional substrate are both characterized by the formation of a significant fraction of oligomers in the product. The overtitration and/or protic impurity contamination arguments raised to explain the formation of the oligomers would imply that both reactions suffered from the same problems, which seems rather unlikely. Therefore, the more plausible explanation for the formation of low molecular weight poly(ϵ -caprolactone) seems to be an increased rate of intramolecular transesterification reactions in the branched systems.

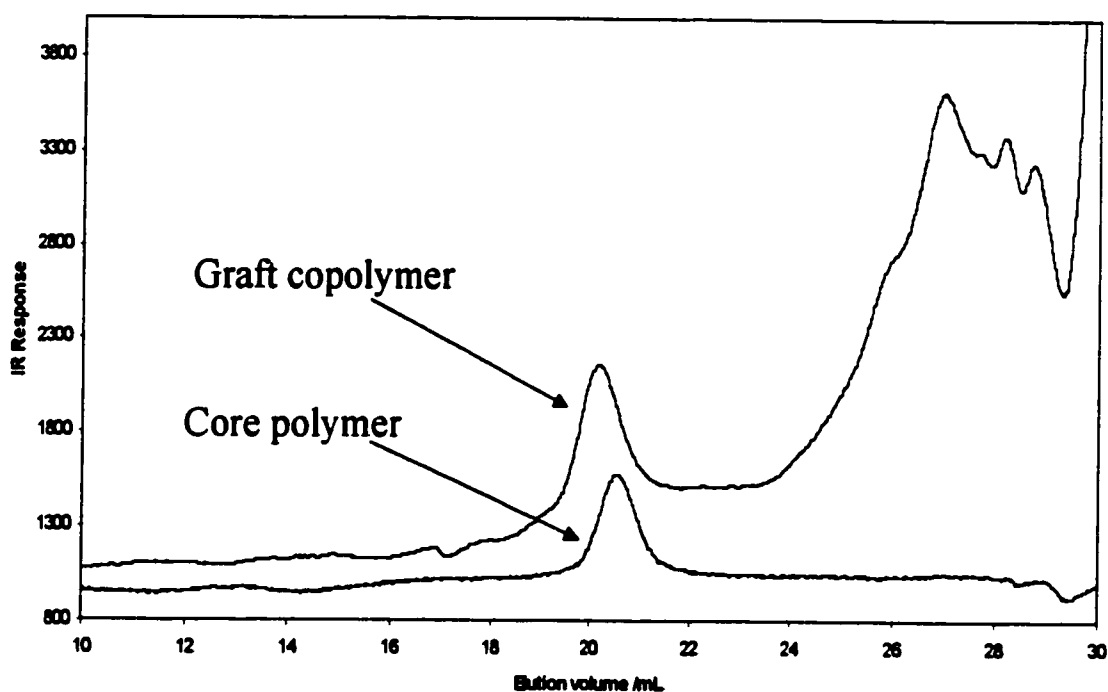


Figure 6.4. Arborescent poly(ϵ -caprolactone) prepared from a hydroxyl-terminated G1 core polymer

6.4. Conclusions

The *grafting from* method was applied to the synthesis of arborescent poly(ϵ -caprolactone) graft copolymers, and led to significant increases in molecular weight for

the graft copolymers relative to the grafting substrates. However, the raw products are contaminated with important amounts of poly(ϵ -caprolactone) oligomers. Further work is required to minimize the formation of these species. This may be possible if the lithium counterion is replaced by another counterion less prone to side reactions, such as a coordinating alkylaluminium species (3,8).

More detailed characterization of the materials prepared should be carried out, following fractionation of the crude products. It would also be interesting to investigate the influence of branching functionality and of the size of the poly(ϵ -caprolactone) side chains on the physical properties of arborescent caprolactones, to help identify applications for these materials.

6.5. References

1. Zhu, Z.; Xiong, C.; Zhang, L.; Deng, X. *J. Polym. Sci., Polym. Chem. Ed.* **1997**, *35*, 709.
2. Yamashita, Y. In *Ring Opening Polymerization: Kinetics Mechanism and Synthesis*; McGrath, J. E., Ed.; ACS Symposium Series 166; American Chemical Society: Washington, 1981; pp. 199-209.
3. Duda, A.; Florjanczyk, Z.; Hofman, A.; Slomkowski, S.; Penczek, S. *Macromolecules* **1990**, *23*, 1640.
4. Kopecek, J.; Ulbrich, K. *Progr. Polym. Sci.* **1983**, *9*, 1.
5. Morton, M.; Wu, M. In *Ring Opening Polymerization: Kinetics Mechanism and Synthesis*; McGrath, J. E., Ed.; ACS Symposium Series 286; American Chemical Society: Washington, 1985; pp 175-182.

6. Huglin, M. B. In *Polymer Handbook, 3rd Edition*, Brandrup, J. and Immergut, E. H., Eds.; Wiley: New York, 1989; p VII/409.
7. Huglin, M. B. In *Light Scattering From Polymer Solutions*; Huglin, M. B., Ed.; Academic: New York, 1972; Chapter 6.
8. Kurcok, P.; Dubois, P.; Sirkorska, W.; Jedliński, Z.; Jérôme, R. *Macromolecules* **1997**, *30*, 5591.

Chapter 7: Conclusions and Suggestions for Future Work

The results obtained in the investigation of mixtures of arborescent and linear polymers demonstrate that arborescent homopolymers and copolymers, when blended with linear polystyrene (PS) and poly(methyl methacrylate) (PMMA), can have a major influence on their melt viscosity.

The addition of arborescent polystyrenes with a low branching functionality to a linear PS matrix resulted in enhanced melt viscosity (melt strengthening) at high temperatures. The observed increase in the melt viscosity was directly related to the amount of arborescent polymer added. Arborescent polystyrenes, when blended with PMMA, led to a decrease in melt viscosity (melt thinning) over the whole temperature range studied. The decrease was independent of the arborescent polymer concentration. This result is very significant, since it shows that the addition of even small amounts of immiscible arborescent polymers is sufficient to bring about a large decrease in melt viscosity. Furthermore, the decrease was more pronounced for higher generation arborescent polystyrenes.

Arborescent polyisoprene copolymers, when blended with PS had either no effect or led to slight melt strengthening. Arborescent polyisoprene copolymers, when blended with linear PMMA, sometimes led to even larger decreases in melt viscosity. The magnitude of the decrease was strongly dependent on the molecular weight of the polyisoprene side chains in the copolymers, and most pronounced for copolymers with short side chains. Arborescent copolymers with long polyisoprene side chains led to a decrease in the melt

viscosity of PMMA at low concentrations (1 and 2.5% w/w), but at higher concentrations (5 and 10% w/w) the melt viscosity increased, due to cross-linking reactions occurring in the sample.

The results obtained in this investigation demonstrate that depending on the nature of the matrix and of the branched polymer, arborescent polymers can influence the melt viscosity in different ways and may thus be useful as melt processing additives. Melt strengthening is of interest in certain operations such as blow molding processes. Melt thinning effects such as those observed in the PMMA blends are important for processes such as injection molding or extrusion, to increase processing throughput.

Since the preparation of arborescent polymers is difficult and ultimately costly, it would be preferable to minimize the amount used for industrial applications. Consequently, future work should concentrate on examining blends with very low concentrations of arborescent polymers (less than 1% w/w). A lower additive concentration would be preferable not only in terms of lowering the cost, but also to minimize the impact of the additives on the mechanical properties of the matrix. Blends based on linear polyisoprene with PMMA and PS could be investigated for comparison with the blends of arborescent polyisoprene copolymers. The arborescent polyisoprene copolymers could also be hydrogenated before blending with linear polymers. This is of interest since hydrogenation may make it possible to avoid cross-linking reactions, specially in the case of arborescent polyisoprene copolymers with longer side chains.

Arborescent graft copolymers incorporating over 90 % (w/w) polydimethylsiloxane (PDMS) were successfully prepared from hydroxyl-functionalized polystyrene cores using a *grafting from* procedure. The synthesis of arborescent PDMS graft copolymers can be

considered successful. However, it is possible that some linear PDMS still be present in the copolymers. Characterization of arborescent PDMS copolymers by SEC could be attempted in a different solvent from THF, to allow the detection of smaller amounts of linear PDMS in the samples.

An alternate method for the synthesis of arborescent PDMS graft copolymers could be based on a *grafting onto* method using hydrosilylation. In this scheme, hydrosilyl-terminated PDMS segments could be prepared by capping living PDMS chains with chlorodimethylsilane. Coupling of the PDMS segments with an arborescent polyisoprene graft copolymer could then be achieved in presence of a chloroplatinic acid catalyst.

The *grafting from* method yielded promising results when extended to the synthesis of arborescent poly(ϵ -caprolactone) graft copolymers. However, further work on the synthesis and more detailed characterization of these materials are needed. Structural features that would be interesting to vary include the branching functionality of the polyfunctional initiator core and the size of the poly(ϵ -caprolactone) side chains. Improvement of the grafting efficiency for these materials should also be investigated. This may be possible if other counterions such as alkylaluminium species are used, since they are less susceptible to interchain transesterification reactions.